Small Airplane

Crashworthiness Design Guide

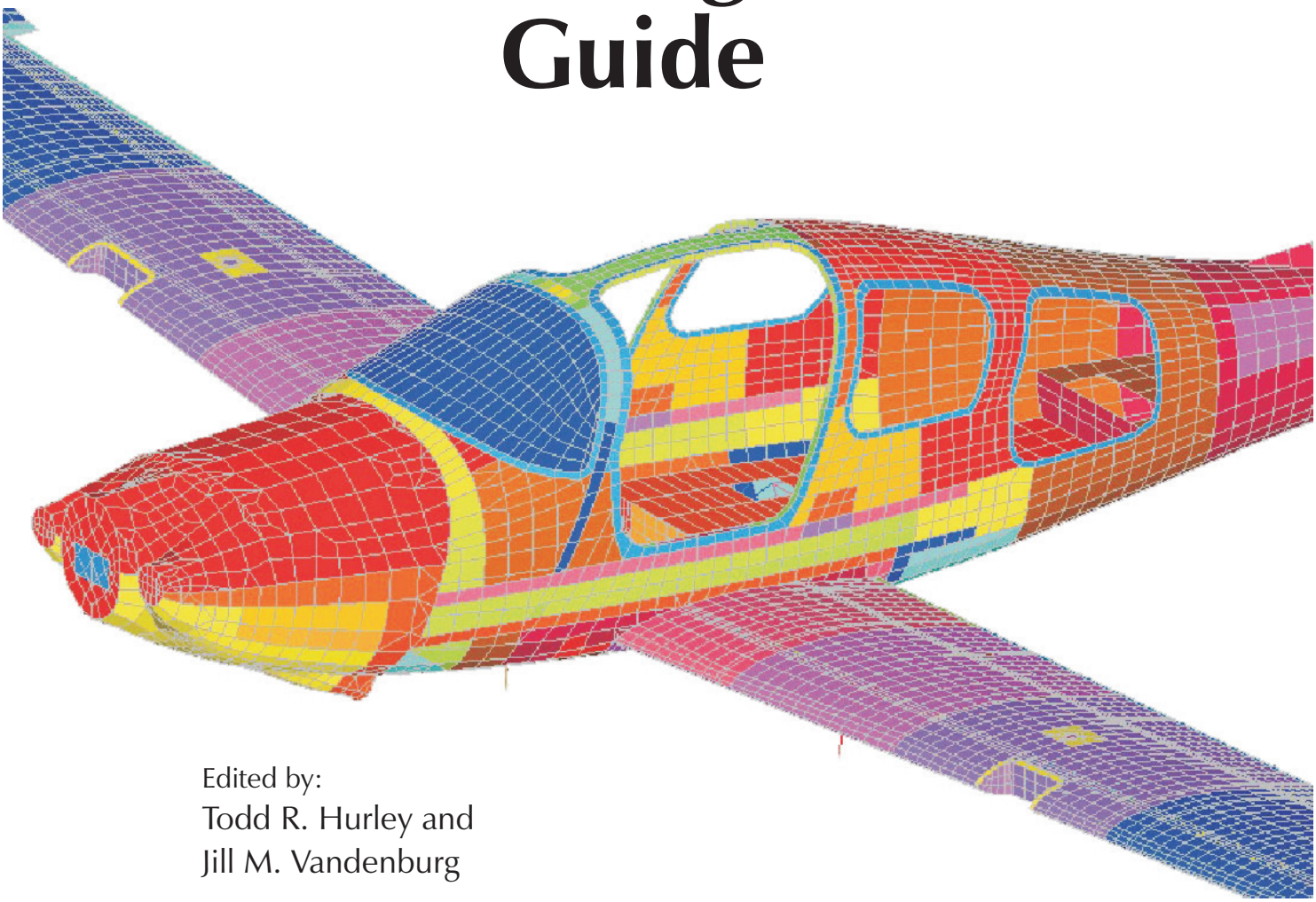

Edited by:
Todd R. Hurley and
Jill M. Vandenburg

SIMULA

AGATE
NASA INDUSTRY FAA
ADVANCED GENERAL AVIATION TRANSPORT EXPERIMENTS

Report Reference Number: AGATE-WP3.4-034043-036
Work Package Title: WBS3.0 Integrated Design and Manufacturing
Date of General Release: April 12, 2002

Small Airplane Crashworthiness Design Guide

Todd R. Hurley
Jill M. Vandenburg
editors

Prepared for:
The NASA Langley Research Center
General Aviation Program Office
Hampton, VA

and

The AGATE
Integrated Design and Manufacturing
Technical Council

Prepared by:
Simula Technologies, Inc.
10016 South 51st Street
Phoenix, AZ 85044

Simula Technologies Reference Number: TR-98099
AGATE Reference Number: AGATE-WP3.4-034043-036
Work Package Title: WBS 3.0 Integrated Design and Manufacturing (ID&M)
Release Date: April 12, 2002

SIMULA Technologies

AGATE
NASA INDUSTRY FAA
ADVANCED GENERAL AVIATION TRANSPORT EXPERIMENTS

Acknowledgements

Many people were involved over the course of writing and editing the Small Airplane Crashworthiness Design Guide. In addition to the chapter authors, credit is due to Barbara Nadolny, who is responsible for most of the illustrations and graphics, and to Mark Ayers, the copy editor.

Special thanks are extended to S. Harry Robertson and Dr. J. W. “Doc” Turnbow for their assistance and contributions to Chapters 2 and 10, and for their permission to reprint the “Fuel System Design Checklist” and “Hazard Level Rating System” papers found in Appendices C and D, respectively.

Credit is also due to the authors, companies and organizations listed in the Reference sections of each chapter, and to the authors of the many editions of the U.S. Army Aircraft Crash Survival Design Guide, for their contributions to the field.

Simula prepared the Small Airplane Crashworthiness Design Guide for the Integrated Design and Manufacturing (ID&M) Technical Council of the Advanced General Aviation Transport Experiments (AGATE) Alliance, and for the National Aeronautics and Space Administration (NASA) Langley Research Center, Hampton, Virginia, under NASA cooperative agreements NCA1-137 and NCA1-167, for Program Years 1997 through 2001. Funding was provided by the NASA AGATE Program, the NASA Aviation Safety Program, and Simula.

Table of Contents

Acknowledgements i

Foreword v

Chapter 1 - Introduction to Crashworthiness 1-1

Chapter 2 - Crash Physics 2-1

Chapter 3 - Aircraft Design Crash Impact Conditions 3-1

Chapter 4 - Biometrics 4-1

Chapter 5 - Modeling 5-1

Chapter 6 - Airframe Structural Crash Resistance 6-1

Chapter 7 - Seats 7-1

Chapter 8 - Personnel Restraint Systems 8-1

Chapter 9 - Delethalizing Aircraft Interiors 9-1

Chapter 10 - Post-Crash Factors 10-1

Appendix A - Definitions A-1

Appendix B - General Aviation Crashworthiness Design Evaluation B-1

Appendix C - Design Checklist C-1

Appendix D - Hazard level Rating System D-1

Foreword

The Small Airplane Crashworthiness Design Guide was created to assist aircraft designers in understanding the design considerations associated with the development of crashworthy General Aviation (GA) aircraft. The document was originally conceived as a condensed, single-volume version of the five-volume U.S. Army Aircraft Crash Survival Design Guide. In fact, certain sections of this work are direct excerpts from the U.S. Army Design Guide. However, the U.S. Army Design Guide focused primarily on the crashworthiness of rotorcraft and, as a result, was lacking information that related directly to the design of GA aircraft. Also, various groups, such as the Advanced Crashworthiness Group of the AGATE Alliance, have conducted many research programs on the crashworthiness of GA aircraft since the last revision of the U.S. Army Design Guide was published in 1989. Some of the information obtained from these research endeavors has been incorporated into this document along with information pertaining to the GA crashworthiness information that was missing from the U.S. Army Design Guide. The Small Airplane Crashworthiness Design Guide goes well beyond the original concept to include current state-of-the-art crashworthiness technologies applicable to civil GA aircraft.

The scope of this design guide focuses on the crashworthiness of the so-called “AGATE-class” airplane, but also covers most other light airplanes. An AGATE-class airplane was defined as an all-composite, single-engine, single-pilot, fixed-wing airplane holding 2 to 6 occupants with a maximum gross weight of 6,000 lb. While “all-composite” was part of the AGATE definition, this work also includes guidance for small airplanes constructed of other materials. The principles and guidance are also appropriate for larger airplanes up to the size covered by Part 23 of the Federal Aviation Regulations (14 CFR Part 23). The terms “small airplane” and “light airplane” are used interchangeably throughout and are meant to describe all airplanes that fit the scope of the document.

The Small Airplane Crashworthiness Design Guide is divided into 10 chapters and 4 appendices. The first five chapters lay the foundation of aircraft crashworthiness. Chapter 1 introduces the principles of crashworthiness and briefly discusses the history of occupant protection in small airplanes. Chapter 2 is a brief review of the physics involved in impact dynamics. The physical principles of deceleration distance and the absorption of kinetic energy by performing work presented in Chapter 2 are fundamental to successful crashworthy designs. Chapter 3 presents design impact conditions, both the regulatory seat test conditions and the AGATE-developed whole-airplane conditions. Chapter 4 covers the human aspects of crashworthiness design including discussions on human anthropometry, occupant motion and flail envelopes, injury tolerance criteria, and anthropometric test devices (ATD’s) or crash test dummies. Finally, Chapter 5 outlines some of the general computer modeling practices that are used to simulate the response of the occupant and aircraft structure in crash events.

The next five chapters, Chapters 6 through 10, address the crashworthiness of specific areas of the airplane. Chapter 6 covers the structural aspects of crashworthy design. The chapter begins with a description of the general requirements and considerations for structural design. The chapter then proceeds to define more detailed design considerations for strength, controlled crush, analysis, and testing of the airframe. Chapter 6 also presents a simplified analysis to estimate firewall crash loads that was used by the AGATE Advanced Crashworthiness Group in the design of a small airplane full-scale test article crash tested at NASA Langley in July of 2001. Chapter 7 provides design specifications for aircraft seating

systems, which are the last line of protection for the occupant in crashes with a severe vertical component. Chapter 8 describes conventional occupant restraints and how to design their installation into the aircraft. This chapter goes on to describe more advanced restraint concepts including inflatable systems such as air bags and air belts. Chapter 9 outlines several techniques for designing the interior of the aircraft to minimize secondary impact injuries. Finally, Chapter 10 focuses on design methodologies used to prevent post-crash fire and to facilitate occupant egress following a crash.

Appendix A provides definitions of crashworthiness and crash survival terminology. Appendix B presents a GA crashworthiness design evaluation tool first used at the AGATE Small Airplane Crashworthiness Design Seminar held in October of 2000. This evaluation can be used as a design checklist, used during design trade studies to compare one concept to another, and/or used to evaluate the crashworthiness of existing designs. Appendices C and D are reprints of papers that contain detailed evaluation checklists for the crashworthiness of fuel systems.

One major difference of this work from the U.S. Army Design Guide is the inclusion of guidance pertaining to the regulations. Where possible, this guidance comes from the real-world crashworthiness certification experience of the members of the AGATE Advanced Crashworthiness Group. While the guidance is considered to be accurate, nothing in the Small Airplane Crashworthiness Design Guide supercedes applicable laws and regulations unless a specific exemption has been obtained from the appropriate regulatory agency. For consistency, we have chosen the abbreviation 14 CFR Part 23, or sometimes just 14 CFR 23, to indicate the Code of Federal Regulations, Title 14 Part 23, "Airworthiness Standards: Normal, Utility, Acrobatic, and Commuter Category Airplanes". This is synonymous with the Federal Aviation Regulations, or FAR, Part 23. Other Federal regulations are abbreviated in the same way.

The Small Airplane Crashworthiness Design Guide is intended to be the first, best source of information on crashworthiness design of light airplanes. The information that is provided in this document represents the current knowledge for aircraft design in this field. It is our hope that this research will continue and be incorporated in future revisions of the document.

Todd R. Hurley and Jill M. Vandenburg, Editors

December 2001

Chapter 1

Introduction to Crashworthiness

Todd R. Hurley
Jill M. Vandenburg
Lance C. Labun

In a 1995 aircraft market survey, analysts discovered that safety was the primary concern among pilots and passengers of General Aviation (GA) aircraft (Reference 1-1). For pilots, the level of safety offered by the aircraft was said to be the primary decision factor when purchasing a light airplane. For potential pilots (the "latent market" for airplanes and flight services), a lack of safety was the primary reason for not piloting light airplanes. And for potential passengers, a lack of safety was the primary reason for not wanting to travel in light airplanes.

The respondents of this survey were not given a definition of the term safety; they were allowed used their own definition in formulating their response. Even though there were probably nearly as many concepts of what defines safety as there were people surveyed, safety can be broadly categorized into two areas. The first is the control and minimization of the factors that cause accidents, or accident prevention. The second area is the control and minimization of the factors that cause injury once an accident occurs, or injury mitigation. Designing for crashworthiness addresses this second category of safety.

Customer concern over the safety of GA aircraft is somewhat warranted. Although declining, the accident rate of GA aircraft remains relatively high (Table 1-1) and the average number of GA-accident-related fatalities remain significantly higher than other forms of air transportation (Table 1-2).

Table 1-1.
U.S. General Aviation safety data (References 1-2 and 1-3)

	1975	1980	1985	1990	1995	2000[c]
Total accidents[a]	3,995	3,590	2,739	2,215	2,053	1,835
Total fatal accidents	633	618	498	443	412	341
Total fatalities	1,252	1,239	956	767	734	592
Total seriously injured persons	769	681	483	402	395	N/A
Flight hours (in thousands)[b]	28,799	36,402	28,322	28,510	24,906	30,800

[a] Since April of 1995, the National Transportation Safety Board (NTSB) has been required by law to investigate all public-use accidents, thereby increasing the number of NTSB-reported GA accidents by approximately 1.75 pct.
[b] Flight hours are estimated by the Federal Aviation Administration.
[c] Data is preliminary.
N/A - not available.
Note: Not all data is available for 2000.

Table 1-2.
Average annual U.S. aviation fatalities 1990-1999 (Reference 1-2)

Mode	Fatalities	Percentage of Total
General Aviation	713	80
Commercial transport	94	11
Commuter	26	3
Air taxis	54	6
TOTAL	887	

Aviation, as a whole, has historically devoted much more energy to accident prevention. While this approach has been very effective in the commercial and business jet aviation sectors, accident prevention has not been as successful in GA. Based on the number of flight hours, GA has an accident rate approximately 20 times that of the scheduled airlines (Table 1-3, Reference 1-2).

Table 1-3.
Accidents, fatalities, and rates, 2000 preliminary statistics for U.S. Aviation (Reference 1-2)

	Accidents		Fatalities			Accidents per 100,000 Flight Hours	
	All	Fatal	Total	Aboard	Flight Hours	All	Fatal
U.S. air carriers operating under 14 CFR 121							
Scheduled	49	3	92	92	17,170,000	0.285	0.017
Nonscheduled	5	-	-	-	870,000	0.575	-
U.S. air carriers operating under 14 CFR 135							
Scheduled	12	1	5	5	550,000	2.182	0.182
Nonscheduled	80	22	71	68	2,430,000	3.29	0.91
U.S. General Aviation	1,835	341	592	582	30,800,000	5.96	1.11
U.S. civil aviation	1,975	365	748	747			

Notes: All data are preliminary.
Flight hours and departures are compiled and estimated by the Federal Aviation Administration (FAA).
Accidents and fatalities in the categories do not necessarily sum to the figures in U.S. civil aviation because of collisions involving aircraft in different categories.

If GA is to grow significantly and become the alternative to the hub and spoke air transportation system that the National Aeronautics and Space Administration (NASA) envisions, perceived and real safety must improve. The latent market (people interested in GA, but not currently using it) will not participate without a stronger perception of safety. The general public has come to expect crash safety in their cars, and will likely demand the same from light airplanes. Furthermore, crash safety at aviation velocities has been demonstrated in racecars and in small airplane and helicopter full-scale tests. While many of the improvements in overall safety should come from accident prevention through such areas as enhancements in the airspace

infrastructure, flight systems, training, etc., the automotive experience has shown that privately owned and operated vehicles will continue to crash. A zero accident rate is not likely. The automotive industry has accepted this reality and designed crashworthiness into its cars, and consequently thousands of lives are saved each year. By designing crashworthiness into light airplanes, GA can see similar results.

1.1 Principles of Crashworthiness

The concept of crashworthiness refers to those vehicle design characteristics that protect the occupant from injury or death during a crash event. Specifically, the designer strives to (1) eliminate injuries and fatalities in relatively mild impacts, (2) minimize injuries and fatalities in all severe but survivable crashes, and (3) minimize the damage to the aircraft structure in all crash events (Reference 1-4). The fundamental principles of crashworthiness can be described using the acronym CREEP (Reference 1-5):

- **C**ontainer (fuselage structure)
- **R**estraint (restraint system, seats, and attachments)
- **E**nergy Management (seats, restraints, fuselage, and engine mounts)
- **E**nvironment (items within the occupants' strike zone)
- **P**ost-crash Factors (fuel system, fire, and egress)

The most critical consideration for crashworthiness concerns the container, or the occupant compartment. A strong, enclosed container must be maintained around the occupants in order to create a survivable volume. Protection provided by the other four principles is of no value if the cabin volume is compromised.

Restraining the occupants within the container is the next-most-important consideration. The key issues in restraint design are the placement of the restraints and the attachment strength. The restraints should transfer the inertial loads from the occupants out through the body's strong skeletal structure rather than through soft tissue or vital organs. Restraints are also used to control the occupant's motion to prevent striking the interior of the airplane, or to allow interaction with secondary restraints such as airbags.

Controlling the peak decelerations and maximum forces applied during the crash is perhaps the most sophisticated and complex aspect of crashworthy design. Energy-absorbing technologies incorporated into the fuselage structure, landing gear, seats, and restraints can be used to effectively control these decelerations and forces.

Proper design of the cabin interior is required to minimize occupant injury. From an aircraft designer's perspective, the risk of injury can be reduced by understanding the types of injury mechanisms that can occur, limiting the size of the occupant's flail envelope, and eliminating, relocating, or delethalizing all potential strike hazards.

The final task is to minimize the post-crash hazards and ensure safe egress for the occupants. This requires the prevention of post-crash fire and the accessibility of functional egress pathways and exits. Fire prevention can be achieved by eliminating the spillage of flammable fluids and by controlling hazardous ignition sources. Exits should be clearly identified, accessible in a rolled and/or deformed aircraft, easy to use, and reliable.

Substantially increasing the level of crashworthiness offered by GA aircraft requires addressing all five principles as a system. Using a "systems approach" to crashworthiness design offers the maximum level of protection to the occupants. In a systems approach, the designer ensures that all of the separate safety systems in the aircraft work together to absorb the aircraft's kinetic energy and to decelerate the occupants to rest without causing injurious loading. This is

accomplished by designing individual crashworthy components and then evaluating the performance of these components as a whole system. Continual evaluation and design iteration of the components occurs until the desired level of safety performance of the whole system is achieved.

For example, the landing gear, aircraft structure, and occupant seats must all be designed to work together as a vertical-energy-management system to absorb kinetic energy and slow the occupant to rest without injuries (Reference 1-6). Figure 1-1 depicts these three contributors to energy absorption in a fixed-wing aircraft. The landing gear is capable of absorbing energy to reduce the impact velocity to the fuselage. The subfloor structure provides additional deceleration distance. The seat completes the energy-management system by helping to protect the occupant from high decelerations and absorbing energy during the crushing process. By absorbing energy with the landing gear and subfloor structure, the occupant compartment is protected from excessive loads, so that the survivable volume is maintained. The occupant compartment structure also does not have to be as heavy as it would need to be and still maintain survivable space without these energy-absorbing mechanisms. Furthermore, by optimizing the location of energy-absorbing structures in the subfloor area of composite airframes, the loads transmitted to the stroking seat, occupant, and airframe can be minimized, which helps reduce occupant injury and structural damage. This type of systems approach to crashworthy design can easily be incorporated into the design process for GA aircraft.

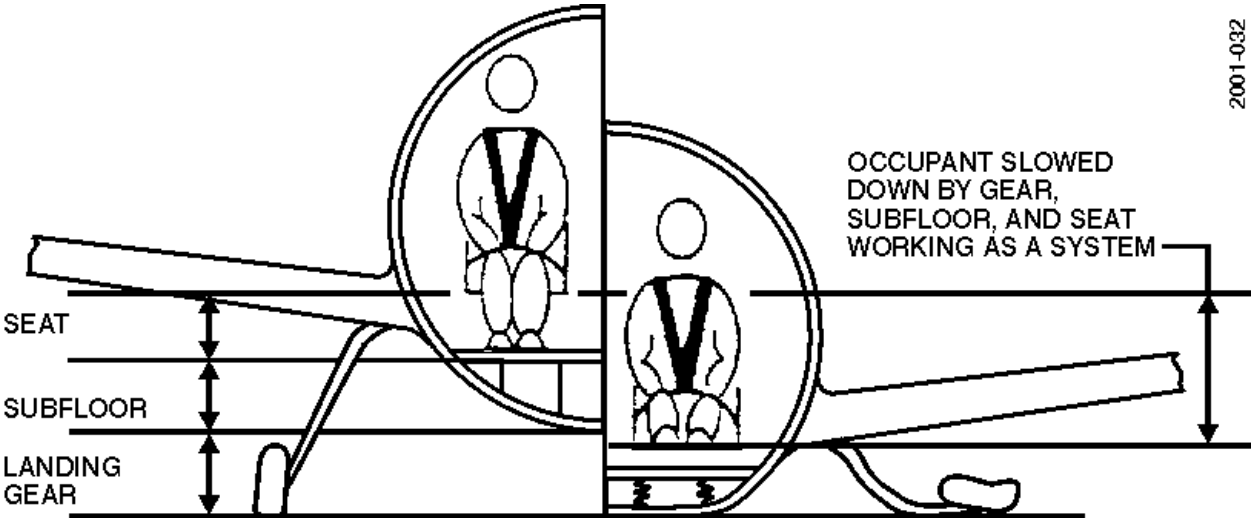

Figure 1-1.
Energy management system for a typical airplane (adapted from Reference 1-6).

It is important to note that the majority of the critical crashworthy design considerations are inherent to the general layout and structure of the aircraft. As a result, a designer must integrate crashworthiness technologies into the design from the inception of the aircraft. This Design Guide will provide the tools to achieve such a design.

1.2 Development of Light Airplane Crashworthiness

Hugh DeHaven

Some of the most significant work in the area of aviation crashworthiness and occupant survivability began in the 1920's with the research efforts of Hugh DeHaven (Reference 1-7). Deemed the "father of aviation crashworthiness," DeHaven's interest in aircraft impact survival began shortly after his own brush with death in 1917. While training to be a pilot for the Canadian Royal Flying Corps during World War I, DeHaven's aircraft was involved in a mid-air collision during a training exercise. DeHaven suffered multiple limb fractures, as well as ruptures of the spleen, liver, and pancreas. Despite his near-fatal injuries, De-Haven was the only person out of both airplanes to survive the accident.

After a 6-month recovery period, he went to work as an accident investigator with the aim of understanding how and why people were injured during traumatic events including crashes and falls. His research efforts and conclusions caught the attention of the National Research Council and the Office of Naval Research. These two organizations provided funding for DeHaven to continue his research investigations at the Cornell University Medical College. The funding allowed for the establishment of the Crash Injury Research (CIR) program, which was officially established as the Aviation Crash Injury Research (AvCIR) program in 1950.

One of DeHaven's most significant achievements was his application of freight shipping principles to aircraft crashworthiness. Recognizing that delicate cargo could be transported and delivered undamaged, DeHaven surmised that the same principles used to protect cargo could be used to protect people in aircraft. He developed the "Four Principles of Packaging for Accident Survival" and first published his theories in a 1952 Society of Automotive Engineers (SAE) paper entitled *Accident Survival – Airplane and Passenger Car* (Reference 1-8). His four principles were as follows:

1. "The package should not open up and spill its contents and should not collapse under expected conditions of force and thereby expose objects inside it to damage."
2. "The packaging structures which shield the inner container must not be made of brittle or frail materials; they should resist force by yielding and absorbing energy applied to the outer container so as to cushion and distribute impact forces and thereby protect the inner container."
3. "Articles contained in the package should be held and immobilized inside the outer structure by what packaging engineers call interior packaging. This interior packaging is an extremely important part of the overall design, for it prevents movement and resultant damage from impact against the inside of the package itself."
4. "The means for holding an object inside a shipping container must transmit the forces applied to the container to the strongest parts of the contained objects."

In this analogy, the container represents the occupant compartment, the interior packaging represents the seat and restraint system, and the objects contained in the package represent the occupants. Over the years, these fundamental crashworthiness principles have been described in many different ways. For example, one particular description, identified by the acronym CREEP, was described in Section 1.1. Although each of these definitions is slightly different, the same core principles are always represented.

Ag-1 Aircraft

In the late 1940's and early 1950's, Fred Weick at Texas A & M designed and built the first airplane using DeHaven's recommendations (Reference 1-7). The Ag-1 agricultural (crop-duster) aircraft was designed with a 40-G cockpit structure, provided a large amount of energy-absorbing structure in front of the pilot, and located the pilot as far aft as possible. The structures in front of the cockpit, specifically the engine mount and agricultural chemical hopper,

were designed to be weaker than the occupant compartment and fail progressively. The cockpit structure was composed of a tubular steel structure surrounding the pilot with a roll cage positioned above to offer extra protection in the event that the aircraft inverted during an impact. In addition to the reinforced cockpit structure, the aircraft incorporated a military-style seat belt and shoulder harness. The restraint system included inertia reels, which locked automatically under 3-G loads. Most so-called "modern," purpose-built agricultural application airplanes—the Piper Pawnee, Cessna AgWagon, Grumman AgCat, and Rockwell/Ayres Thrush, to name a few—all used the same basic layout and crashworthy design as the Ag-1 (Reference 1-9). The design appeared to have worked quite well; the only Ag-1 prototype built actually crashed and the pilot walked away with only minor injuries. In addition, a study of agricultural plane accidents by Swearingen showed that this class of airplanes generally does a good job of protecting the pilots in the event of a crash (Reference 1-10).

Beechcraft Bonanza

With the design of the Bonanza aircraft in the early 1950's, the Beechcraft Company was the first major aircraft manufacturer to integrate crashworthiness directly into the design of an aircraft (Reference 1-7). The design incorporated a long nose section to allow gradual impact deceleration of the occupants. It possessed a reinforced keel section in the fuselage, as well as a reinforced cockpit area to provide a "cocoon" around the occupants. The structure was designed not only to provide a strong, protective envelope, but the strong floor consisted of longerons (longitudinal beams) to encourage sliding over the impact surface rather than digging into it (Reference 1-11). Although very rigid, the structure was not designed to be energy absorbing. The wing design of the Bonanza was intended to attenuate energy during an impact and the seats in the aircraft were hard-mounted to the spar truss (Reference 1-7). The aircraft also incorporated a breakaway instrument panel and yoke to reduce occupant head trauma. Interestingly enough, torso restraints (in the form of three-point restraints) were offered as an option on this aircraft, but were later discontinued due to lack of customer interest (Reference 1-11). Shoulder restraints were not required by regulation in light airplanes until the late 1970's.

The Bonanza aircraft was truly ahead of its time (Reference 1-7). Beechcraft's marketing campaign highlighted the "survivability" features of the aircraft. However, in the mind of the consumer of the 1950's, advertising survivability admitted that aircraft crashes were possible. This marketing approach was a huge failure, since the GA community was not ready to hear about anything suggesting the possibility that an airplane might crash.

Helioplane Courier (HelioCourier)

In the early 1950's, another aircraft, the Helioplane Courier (HelioCourier), was designed based on the recommendations of the Crash Injury Research program (Reference 1-7). The HelioCourier incorporated a tubular-steel frame, which was designed to maintain the occupiable space around the occupants. The aircraft was also equipped with large, shock-absorbing landing gear, a 15-G floor and seat system, and lap belts and shoulder harnesses in all seats. The HelioCourier proved to be very useful in rough terrain and in jungle environments due to its ruggedness and its ability to protect its occupants.

Federal Aviation Administration

Through the 1970's and 1980's, the FAA made a series of amendments to the Federal Aviation Regulations (14 CFR Part 23, Reference 1-12) that were intended to improve the crashworthiness of light airplanes. All of the amendments focused primarily on crashworthiness afforded by restraints and seats. The first, Amendment 23-19 (1977), required shoulder harnesses for the front-row seats in newly certified light airplanes. Existing type-certified airplanes were not affected by this amendment. In 1985, Amendment 23-32 updated 23-19 by requiring shoulder harnesses in all seat positions for light airplanes of nine passengers or less

(excluding crew) manufactured one year after the effective date of the amendment. Amendment 23-32 affected all new or existing type-certified airplanes in production, but not those that had already been manufactured. The reason behind these amendments was that shoulder harnesses have repeatedly been shown to improve the survivability in airplanes that are equipped with them and when they are used (Reference 1-13).

The biggest change occurred with Amendment 23-36 (1988). This amendment added two dynamic tests of the seat and restraint system: one that represents a primarily vertical impact, and one that represents a primarily longitudinal impact. The amendment also added "pass-fail" criteria for these dynamic tests that included, for the first time, injury criteria as measured by standardized anthropomorphic test devices (ATD's). The tests and criteria were added based on a recommendation of the General Aviation Safety Panel (GASP), which was a group of aviation industry representatives convened by the FAA in the mid-1980's to look at ways to improve the crash survivability of light airplanes (Reference 1-14). This amendment affected only newly type-certified light airplanes; the retrofit of the existing fleet or of existing type-certified airplanes in production was not required. Even after being in effect for more than a decade, as of this writing only a few light airplanes have been fully certified (that is, with no exemptions) to Amendment 23-36. These airplanes—the Lancair Columbia 300, and the Cirrus Designs SR-20 and its derivative, the SR-22—have only been in production for a few years. It will be a few years more before the efficacy of the improvements imposed by Amendment 23-36 can be fully ascertained with field data.

Terry Engineering

In 1997, Terry Engineering conducted four full-scale crash tests of small composite airframes at the NASA Langley Research Center Impact Dynamics Research Facility (Reference 1-15). Two of the tests were conducted onto a concrete surface and two were onto soil. The test impact conditions used by Terry were similar to some of the earlier NASA tests of production, metallic GA aircraft (Reference 1-16). A comparison of the Terry tests with the earlier NASA tests confirmed the improvement in crashworthiness of the Terry-designed airplanes. No single feature was identified as being responsible for the improvement in crashworthiness. The combination of an energy-absorbing engine mount, an engine cowling and lower firewall designed to prevent earth scooping, a stronger cabin structure, energy-absorbing foams in the sub-floor, and the proper combination of restraints and energy-absorbing seats, limited the occupant loads to within human tolerance. The duration of the deceleration was longer, allowing more time and distance for the occupants to come to rest. The stronger cabin structure maintained the needed occupant space for survival.

While the Terry airplanes were not certified production aircraft, per se, the tests conclusively showed that small airplanes could be designed so the occupants would survive a relatively severe accident near stall speed.

AGATE Advanced Crashworthiness Group

From 1995-2001, the AGATE Advanced Crashworthiness Group (ACG) worked to substantially improve the crash safety of small airplanes (to levels seen in modern automobiles), while minimizing the cost of improvements. The charter of the ACG was to (1) develop a set of design and certification guidelines, (2) demonstrate crashworthy technologies and design processes, and (3) educate the designers and the public. This Design Guide is a product of the ACG that addressed their charter.

References

1-1. Single-Pilot GA Aircraft Market Study, conducted for NASA by Wichita State University, July 1995.

1-2. National Transportation Safety Board, http://www.ntsb.gov/aviation/Stats.htm, site accessed on December 12, 2001.

1-3. Bureau of Transportation Statistics, National Transportation Statistics 2000, http://www.bts.gov/btsprod/nts/, site accessed on September 6, 2001.

1-4. Zimmerman, R. E., and Merritt N. A., Aircraft Crash Survival Design Guide, Volume I– Design Criteria and Checklists, Simula, Inc., Phoenix, Arizona; USAAVSCOM TR 89-D-22D, Aviation Applied Technology Directorate, U.S. Army Aviation Research and Technology Activity (AVSCOM), Fort Eustis, Virginia, December 1989.

1-5. International Center for Safety Education, Crash Survival Investigation School: Basic Course Notebook, Section B-10, Course 95-2, Robertson, S. H., contributing author, Simula, Inc., Phoenix, Arizona, September 1995.

1-6. Mason-Reyes, M., "Summary of a Small Business Innovation Research Program: Thermoplastic Energy-Absorbing Subfloor Structures," Simula Government Products, Phoenix, Arizona, August 27, 1997.

1-7. Waldock, W. D., "A Brief History of Crashworthiness," Embry-Riddle Aeronautical University, no date provided.

1-8. DeHaven, H., "Accident Survival – Airplane and Passenger Car," SAE 520016, Society of Automotive Engineers, Inc., Warrendale, Pennsylvania, January 1952.

1-9. Bruggink, G. M., Barnes, A. C., and Gregg, L. W., "Injury Reduction Trends in Agricultural Aviation," Aerospace Medicine, May 1964, pp. 472-475.

1-10. Swearingen, J. J., Wallance, T. F., Blethrow, J. G., et al., "Crash Survival Analysis of 16 Agricultural Aircraft Accidents," Federal Aviation Administration Civil Aeromedical Institute, Washington, D.C., April 1972.

1-11. Snyder, R. G., "Civil Aircraft Restraint Systems: State of the Art Evaluation of Standards, Experimental Data, and Accident Experience," SAE 770154, in Aircraft Crashworthiness, PT-50, R. F. Chandler, ed., Society of Automotive Engineers, Warrendale, Pennsylvania, 1995.

1-12. "Federal Aviation Regulations, Part 23, Airworthiness Standards: Normal, Utility, Acrobatic, and Commuter Category Airplanes," 14 CFR 23, Federal Aviation Administration, Washington, D.C.

1-13. Clark, J. C., "Summary Report on the National Transportation Safety Board's General Aviation Crashworthiness Project Finding," SAE 871006, Society of Automotive Engineers, Warrendale, Pennsylvania, April 1987.

1-14. Soltis, S. J., and Olcott, J. W., "The Development of Dynamic Performance Standards for General Aviation Aircraft Seats," SAE 850853, Society of Automotive Engineers, Warrendale, Pennsylvania, April 1985.

1-15. Terry, J. E., Hooper, S. J., "Design and Test of an Improved Crashworthiness Small Composite Airframe," Phase II Report, NASA SBIR Contract NAS1-20427, October 1997.

1-16. Castle, C. B., Alfaro-Bou, E., “Crash Tests of Three Identical Low-Wing Single-Engine Airplanes,” NASA Technical Paper No. 2190, 1983.

Chapter 2
Physics

Lance C. Labun
Jill M. Vandenburg

This chapter will review the basic principles of crash physics. Descriptions of crash kinematics, as well as work-energy relationships, will be discussed. It is important to note that although this particular chapter will describe a work-energy approach to crash analysis, an impulse-momentum approach can also be used. In general, work-energy is more useful for crashworthy design, whereas impulse-momentum is more useful for accident reconstruction.

The majority of the information presented in this chapter was taken from Dr. James Turnbow's section of the International Center for Safety Education (ICSE) Crash Survival Investigation School Basic Course Notebook (Reference 2-1). Definitions and conventions for the algebraic signs of various quantities can be found in Appendix A.

2.1 KINEMATICS

A large volume of data associated with vehicle accident studies and human tolerance to decelerative loads is presented in the form of time plots of displacement, velocity, and acceleration. The following section will provide an explanation of the invariant relationships between these four quantities.

Consider an aircraft impacting a vertical wall as shown in Figure 2-1.

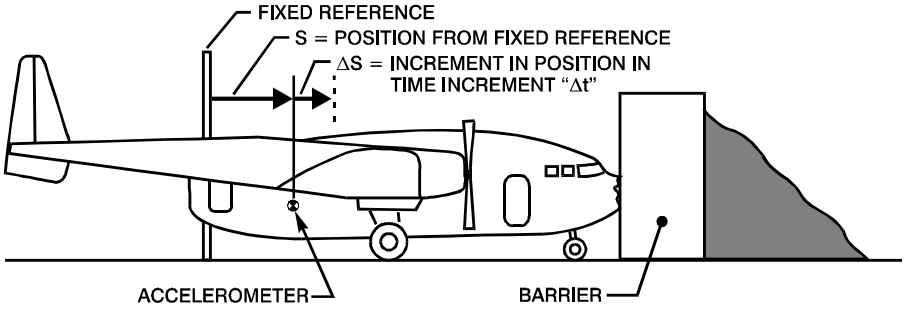

Figure 2-1.
A schematic of an aircraft impacting a vertical wall.

If ΔS is the infinitesimal displacement, which occurs in the infinitesimal time interval Δt, then we say by definition that the velocity at the beginning of the time interval is:

$$V = \frac{\Delta S}{\Delta t} \tag{1}$$

Note that the velocity is an instantaneous quantity and has the units of length per unit of time. Similarly, if ΔV is the change in velocity, which occurred in the time interval Δt, then the acceleration at the beginning of the time interval is defined by:

$$a = \frac{\Delta V}{\Delta t} \tag{2}$$

Acceleration is also an instantaneous quantity and has the unit of velocity per unit time.

Unfortunately, these mathematical expressions leave much to be desired in the practical interpretation and understanding of these basic quantities. An excellent visual aid to better understanding these quantities is the velocity-time diagram (Figure 2-2). This diagram consists of three plots: (1) acceleration versus time, (2) velocity versus time, and (3) displacement versus time.

Observation of Figure 2-2 reveals that the "a" in Equation 2 is the height of the a-t curve and $\Delta V/\Delta t$ is the slope of the V-t curve. Therefore, the height of the a-t curve is numerically equal to the slope of the V-t curve:

$$a = \frac{\Delta V}{\Delta t}$$

Height of the a-t curve = Slope of V-t Curve (3)

This is an invariant relationship and any data, whether experimental or theoretical, must meet this criterion to be valid.

Similarly, Equation 1 and Figure 2-2 illustrate that the height of the V-t curve is equal to the slope of the S-t curve:

$$V = \frac{\Delta S}{\Delta t}$$

Height of the V-t curve = Slope of the S-t curve (4)

Through basic algebraic manipulation, two additional invariant relationships can be obtained among these three curves. By rearranging Equation 2, we obtain:

$$\Sigma \Delta V = \Sigma a \bullet \Delta t \tag{5}$$

Total change in velocity = Area under the a-t curve (6)

In this expression, $\Sigma a \bullet \Delta t$ represents the area of the horizontally shaded strip in the a-t curve (see Figure 2-2). The sum of these areas in any time interval is the total area under the a-t curve in the interval. The term $\Sigma \Delta V$ is the sum of the successive changes in velocity, which is the total change in velocity in a given interval. Thus, Equation 5, which states that the total change in velocity in a given interval is equal to the area under the a-t curve in the interval, is valid for all situations.

This same condition exists between the V-t and S-t curves. By rearranging Equation (1), we obtain:

$$\Sigma \Delta S = \Sigma V \bullet \Delta t \tag{7}$$

Total change in velocity = Area under the V-t curve (8)

This expression indicates that the maximum vehicle travel, as shown on the lower curve of Figure 2-2, would have to be equal to the shaded area under the V-t curve.

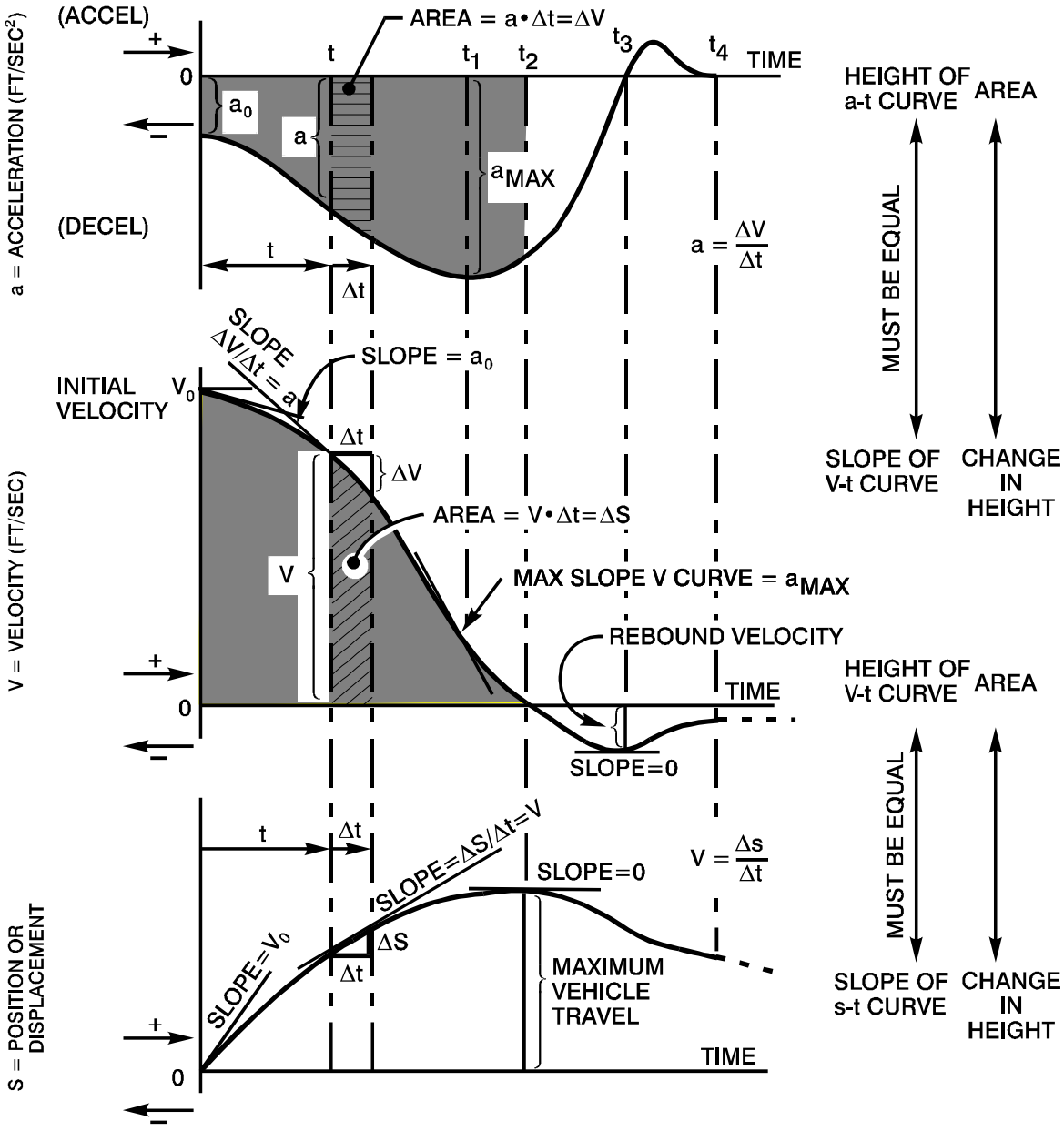

Figure 2-2.
The velocity-time diagram.

Other important relationships to note from Figure 2-2 include:

1. The areas below the t axis must be considered to be negative (deceleration), thus giving negative velocity changes or reductions in velocity. When the curve lies above the "t" axis, the area under the axis is positive (acceleration), giving an increase in velocity.
2. The velocity is changing at the most rapid rate when the acceleration (or deceleration) is maximum, time "t_1".
3. The displacement reaches a maximum when the velocity becomes zero, time "t_2".
4. The velocity need not necessarily be zero (time t_2) when the acceleration is maximum (time t_1).

5. The area under the deceleration pulse (from t_0 to t_3) is equal to the initial velocity plus the rebound velocity or the total algebraic change in velocity.
6. The area under the deceleration curve between t_2 and t_3 is equal to the rebound velocity.

These same relationships can be determined for any set of displacement, velocity, and acceleration curves.

2.2 DECELERATION PULSES

In a crash event, the acceleration pulse is usually a complex function of time. Fortunately for design engineers, the crash pulse can often be simplified into an easily managed analytic form. The following section will describe the use of basic pulse shapes, including rectangular and triangular, for calculating the key variables for different types of crash events.

2.2.1 Rectangular Deceleration Pulse

As previously mentioned, acceleration is the instantaneous change of the velocity with respect to time. Integrating the acceleration over time gives the instantaneous velocity and integrating the velocity over time gives the instantaneous distance traveled during the event. The acceleration-velocity-displacement relationships for a rectangular pulse are illustrated in Figure 2-3.

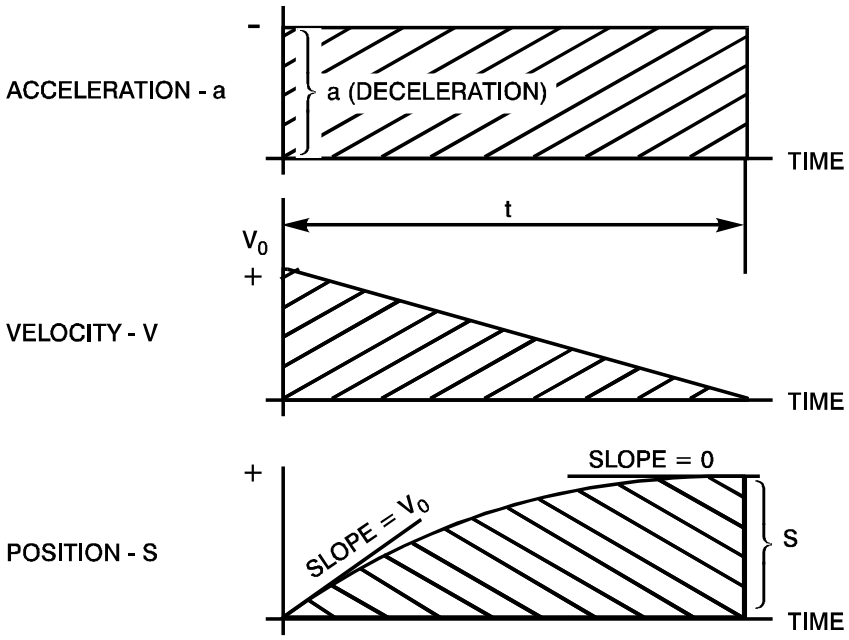

Figure 2-3.
Constant deceleration pulse (rectangular pulse).

The constant acceleration case is the simplest analytically. The integration of the acceleration and velocity curves leads to an expression for stopping distance. The stopping distance can be expressed as a function of the initial velocity by:

$$S = \frac{1}{2}\frac{V_o^2}{a} \tag{9}$$

As shown in Equation 9, a large velocity, V_0, will require a very large stopping distance. A large stopping distance will also be required if the acceleration, a, was small.

Horizontal slide out can be treated as a constant acceleration event, where the acceleration is determined by the coefficient of sliding friction. The constant-acceleration idealization is also used where energy absorption is incorporated into the design in items such as an energy-absorbing landing gear, an energy-absorbing stroking seat, or energy-absorbing structure with a uniform crush strength.

2.2.2 Symmetrical Triangular Pulse

In practice, the symmetrical triangular pulse is often used to simulate the crushing of structure. Thus, the pulse generated by an aircraft striking a barrier horizontally or vertically and crushing the fuselage would be approximated by a triangular pulse. The stopping distance for this pulse is given by:

$$S = \frac{V_o^{\,2}}{a} \tag{10}$$

The acceleration-velocity-displacement relationships for a symmetrical triangular pulse are illustrated in Figure 2-4.

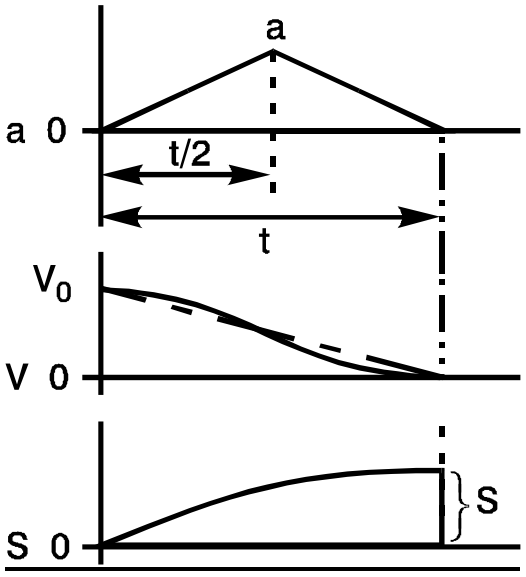

Figure 2-4.
The symmetrical triangular pulse.

2.2.3 Asymmetrical Triangular Pulses

As illustrated in Figure 2-5, asymmetrical triangular pulses can be divided into two extreme categories: zero rise time pulse and zero offset pulse. These two pulse approximations are used less often, but reviewing their behavior is useful for demonstrating the effect of shifting the peak acceleration from the midpoint of the event as in the symmetrical pulse to either earlier or later in the event. Figure 2-5 reveals that although the stopping time for the two pulses is identical, the stopping distance for the zero-offset pulse is twice the stopping distance for the zero-rise-time pulse with the symmetrical pulse midway between the two pulses. In an event

where a relatively rigid structure is presented in the crash, the peak acceleration will shift to an earlier time in the pulse. This phenomenon tends to occur in vertical water impacts, where the aircraft's belly skin fails and the water meets the relatively stiff floor structure without crushing the subfloor structure. The peak might occur late in the pulse in a case where the aircraft struck a soft surface at a small angle and began to plow up material relatively slowly, thus gradually increasing the mass to be accelerated.

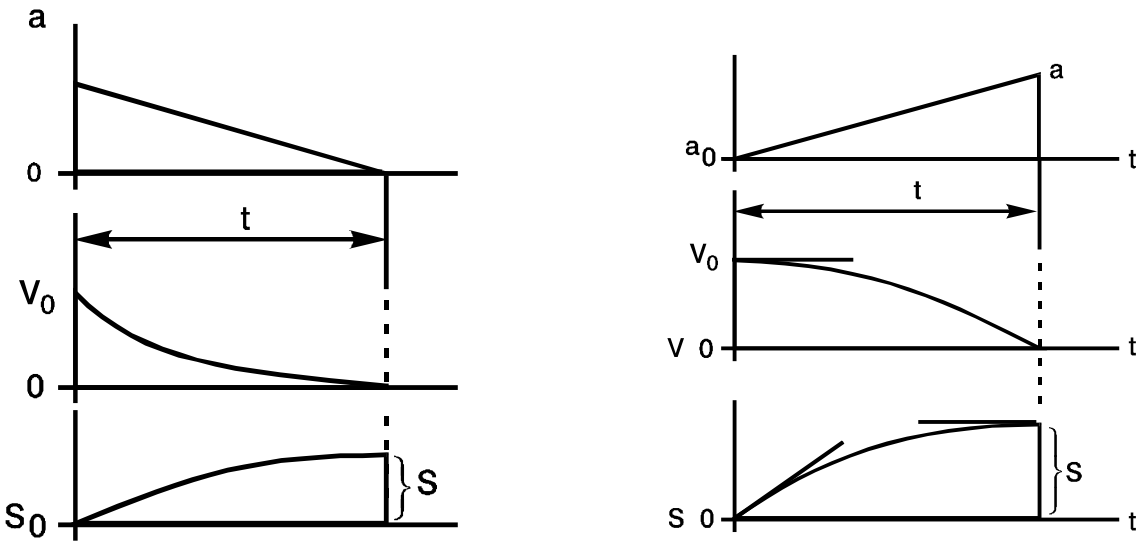

(a) **(b)**

$$S = \frac{2}{3}\frac{V_o^2}{a}$$

$$S = \frac{4}{3}\frac{V_o^2}{a}$$

Figure 2-5.
Comparison of two asymmetrical pulses: (a) zero-rise-time pulse and (b) zero-offset-time pulse.

2.2.4 Comparison of Deceleration Pulse Characteristics

Figures 2-6 and 2-7 display a summary of the pulse shapes and formulas for the four deceleration pulse types described in this chapter. As an example of the difference in magnitude of these pulses, imagine a decelerating aircraft at three different velocities: 50, 100, and 150 mph (73, 147, and 220 ft/sec) with a constant acceleration. If the stopping distance is held constant at 20 ft., then the deceleration rates are 4.25 G, 12.5 G, and 20.8 G, respectively. The deceleration rate for a 150-mph crash is almost 5 times the deceleration rate for the 50-mph crash.

The stopping time is of less significance to the designer than the stopping distance (Figure 2-7). The time to stop for the three triangular pulses is equal; however, the stopping distances are most emphatically not equal. The shortest stopping distance is achieved with the constant acceleration pulse. Thus, constant acceleration is the preferred pulse to achieve the maximum velocity change in the least distance for a given acceleration level.

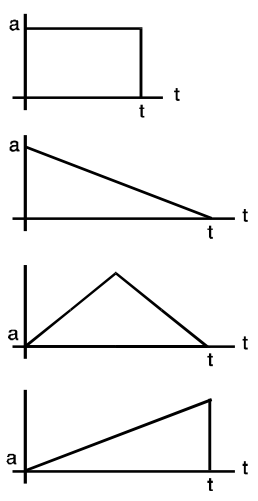

$$S = \frac{V_o^2}{2a}, \qquad t = \frac{V_o}{a}$$

$$S = \frac{2}{3}\frac{V_o^2}{a}, \qquad t = \frac{2V_o}{a}$$

$$S = 1.000\frac{V_o^2}{a}, \qquad t = \frac{2V_o}{a}$$

$$S = \frac{4}{3}\frac{V_o^2}{a}, \qquad t = \frac{2V_o}{a}$$

Figure 2-6.
Summary of stopping distance and stopping time equations for various crash pulses where $V_f = 0$.

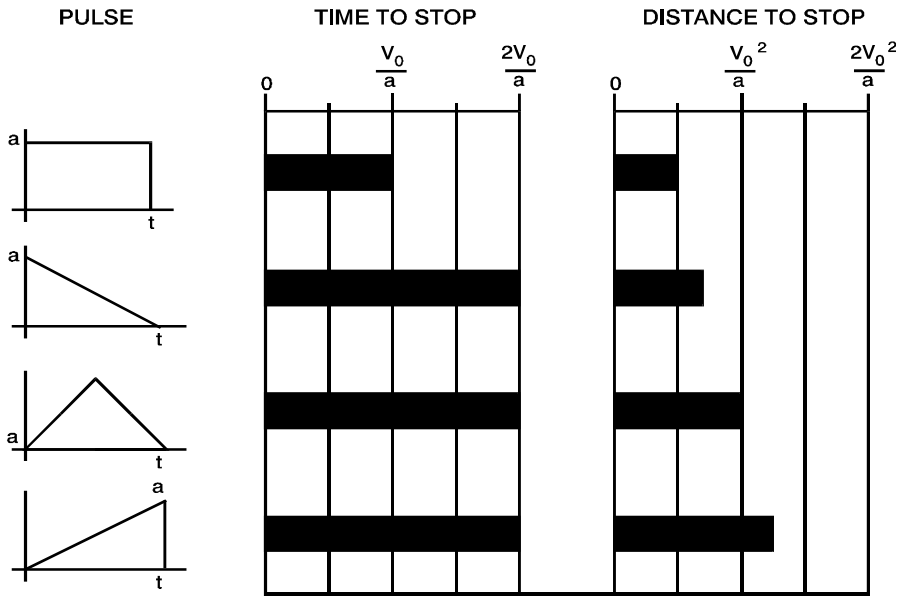

Figure 2-7.
Relative times and stopping distances for various deceleration pulses.

2.3 WORK-ENERGY RELATIONSHIP

Designing crashworthy aircraft involves finding ways to absorb the kinetic crash energy within tolerable acceleration levels. Applications include seats, restraint systems, landing gear, and in the aircraft structure itself. As a result, aircraft designers need a thorough understanding of the concepts of energy and energy-absorbing principles. This section will briefly discuss some of the key principles related to work and energy in crash scenarios.

The concept of energy arises in the work-energy principle, which is derived from Newton's Second Law. If the resultant force applied to the mass is "F", as shown in Figure 2-8, then the force, the mass, and the acceleration are related by Equation 11.

$$F = ma = m\frac{\Delta V}{\Delta t} = m\frac{\Delta V}{\Delta t} \bullet \frac{\Delta S}{\Delta S} = mV \bullet \frac{\Delta V}{\Delta S} \tag{11}$$

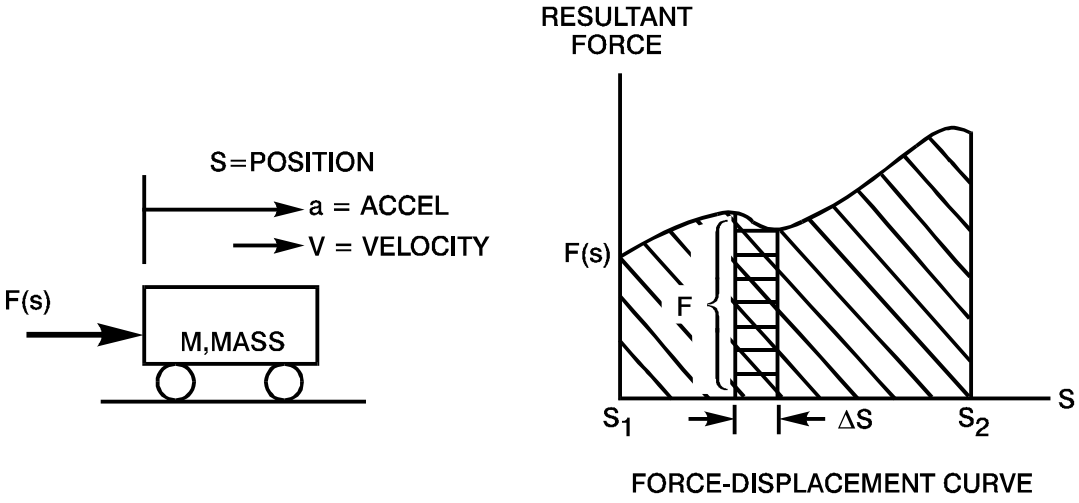

Figure 2-8.
The work-energy principle.

Further manipulation of Equation 10 yields an expression for the area under the F-S curve in Figure 2-8. The area under the F-S curve is referred to as the system's kinetic energy and is expressed as:

$$\Delta KE = \frac{1}{2}mV_2^{\,2} - \frac{1}{2}mV_1^{\,2} \tag{12}$$

The square dependence in Equation 12 is a very powerful consideration in designing for crashworthiness. It indicates that doubling the velocity of a mass quadruples its kinetic energy. But, more subtly, the square dependence indicates that the increase in kinetic energy that is due to an incremental change in velocity depends very strongly on the original velocity to which the increment is added.

The change in kinetic energy, as described by Equation 13, is equivalent to the amount of work done on the mass.

$$Work = \Delta KE \tag{13}$$

Work can also be expressed as:

$$W = \Sigma F \bullet \Delta S = area\ under\ F - S\ curve \tag{14}$$

2.4 ENERGY ABSORPTION

The area under the F-S curve in Figure 2-8 represents the amount of energy absorbed. Equations 13 and 14 indicate that the only way in which energy can be removed from a body (i.e., reducing a body's velocity) is to hold a force on the body as the body moves (Figure 2-9a). This can be accomplished by the use of a crushable structure or material that maintains a constant force as the mass travels through a certain distance (Figure 2-9b). A device or system that achieves this objective is referred to as an energy absorber.

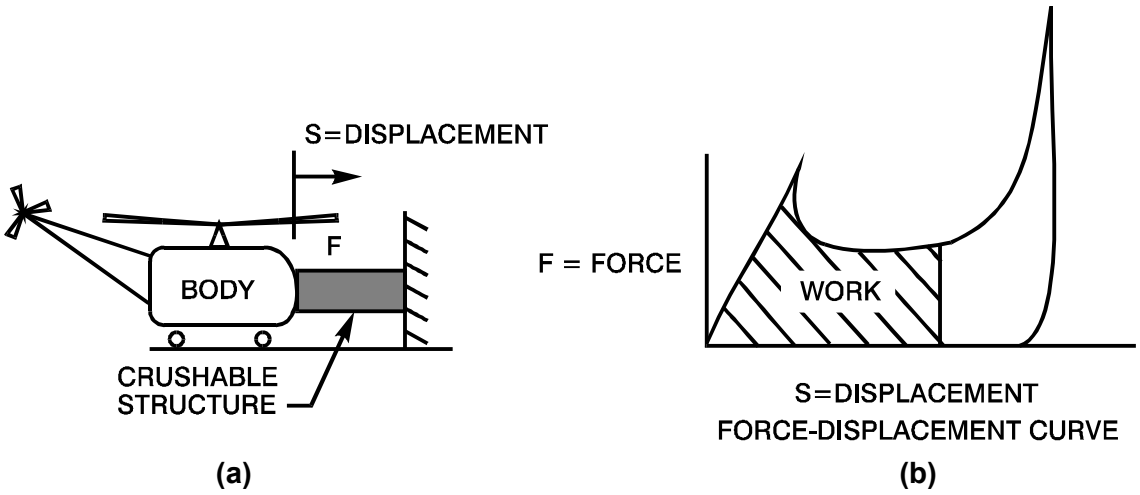

Figure 2-9.
Use of an energy absorber.

The generation of an "ideal energy absorber" is shown in Figures 2-10 and 2-11. As shown in Figure 2-10, if "a" is constant, the F=ma is also constant. The F-S curve for the energy absorber is represented by Figure 2-11. Certain foamed materials and honeycomb materials approach this ideal force-displacement curve to the extent shown in Figure 2-12.

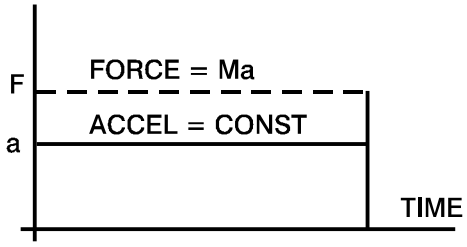

Figure 2-10.
Relationship between constant acceleration and constant force.

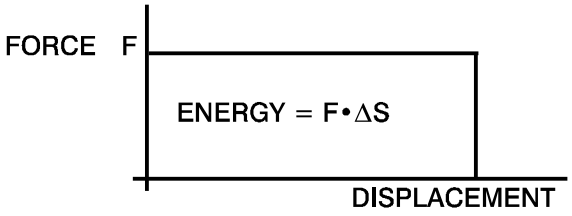

Figure 2-11.
Ideal energy absorber.

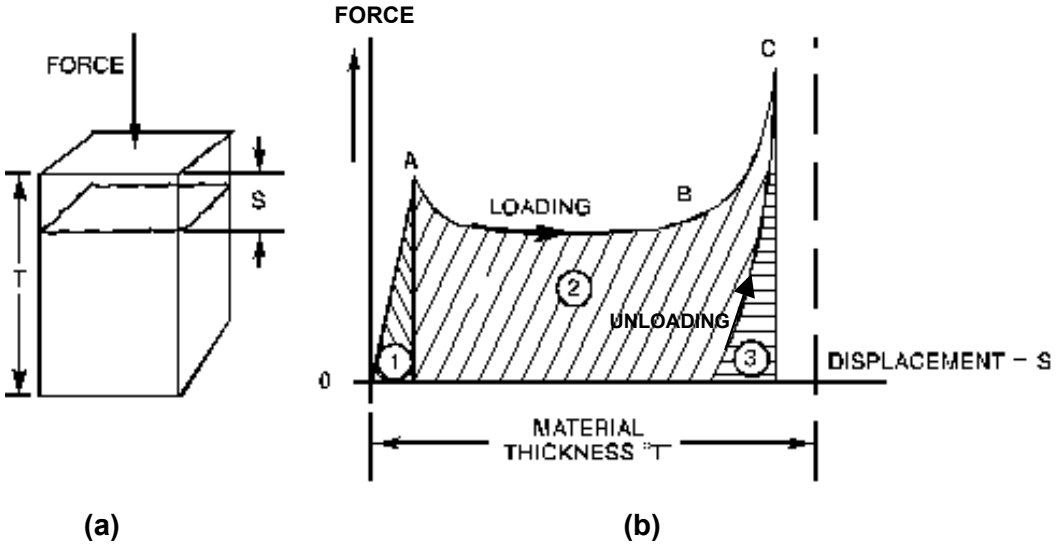

Figure 2-12.
Force-displacement curve for honeycomb materials.

As previously mentioned, the area under the force-displacement curve (Figure 2-12b) represents the amount of energy absorbed. This area can be divided into three separate regions: elastic, plastic, and rebound. If loading increases only up to Point A in Figure 2-12b, then unloading generally occurs along the elastic curve 0A, and the energy indicated by Area "1" is given back, in the same manner as a spring gives back its energy when it is unloaded. Area "2" represents plastic energy absorption. If loading reaches Point C in the figure, the energy corresponding to Areas "1" and "2" plus Area "3" is absorbed. However, as unloading occurs, the energy of Area "3" is given back in the form of rebound. Loading in the region from B to C in the figure is often referred to as "bottoming out," a condition wherein the deforming structure or material has become completely compacted and the load increases rapidly with very little increased deformation.

2.5 EXAMPLE SCENARIO

The following is an example of the calculations required to design the stroking force for a seat intended to stroke under the decelerative load imposed by a 50th-percentile male occupant (adapted from Reference 2-2). The stroking load is calculated using the equation

$$L_{Stroke} = G_L W_{Eff} \tag{15}$$

where:

L_{Stroke} = stroking load of the seat (lb)

G_L = limit load (G)

W_{Eff} = effective weight of the 50th-percentile occupant (lb)

Based on Equation 15, two parameters need to be determined in order to calculate the stroking load: the limit load, G_L, and the effective weight of the 50th-percentile occupant, W_{Eff}. Assuming that the limit load is approximately 12 G, Table 2-1 can be used to determine the effective occupant weight, W_{Eff} using the equation

$$\begin{aligned} W_{Eff} &= W_{50eff} + W_{Ceff} + W_{Beff} \\ W_{Eff} &= 136\ lbs + 2.4\ lbs + 2\ lbs \\ W_{Eff} &= 140.4\ lbs \end{aligned} \tag{16}$$

Table 2-1.
Weight parameters

Parameter	Actual Weight (lb)	Effective Weight (lb)	Symbol
Nude weight of the 50th-percentile male occupant	170	136	W_{50eff}
Weight of clothes (less shoes)	3	2.4	W_{Ceff}
Seat stroking weight (weight of seat bucket)	2	--	W_B
*Effective weight in the vertical direction represents 80 pct of the actual weight, since the occupant's lower extremities are partially supported by the floor of the aircraft.			

Using this information, the stroking load can be calculated as:

$$\begin{aligned} L_{Stroke} &= G_L W_{Eff} \\ L_{Stroke} &= (12\ G)(140.4\ lbs) \\ L_{Stroke} &= 1684.8\ lbs \end{aligned} \tag{16}$$

References

2-1. International Center for Safety Education, Aircraft Crash Survival Investigation Basic Course Manual, Course 99-3, Turnbow, J. W., contributing author, Simula, Inc., Phoenix, Arizona, September 1999, Section B-15.

2-2. Desjardins, S. P., Zimmermann, R. E., Bolukbasi, A. O., et al., Aircraft Crash Survival Design Guide, Volume IV, Aircraft Seats, Restraints, Litters, and Cockpit/Cabin Delethatlization, TR- 87442, Simula Inc., Tempe, Arizona; USARTL TR-89-D-22D, Applied Technology Laboratory, U.S. Army Research and Technology Laboratories, (AVRADCOM), Fort Eustis, Virginia, December 1989.

Chapter 3

Design Crash Impact Conditions

Todd R. Hurley
Darrel Noland

This chapter presents the impact conditions that should be used in the design of AGATE-class airplanes. The first section of this chapter presents the regulatory impact conditions of FAR Part 23 (14 CFR Part 23, Reference 3-1). The second section presents the AGATE-developed, whole-airplane impact conditions that, if used for design, may provide a higher level of occupant protection than provided by the current regulations. The third section presents background information that may be useful to the reader who wants to understand where the impact conditions originated.

The focus of this chapter is only on the impact conditions and impact-related load factors used in design. The purpose this focus is two-fold: (1) to provide an easily referenced location for impact information that is used in the design of the protection systems covered in this book; and (2) to illustrate the differences between the regulatory and AGATE impact conditions. The other requirements needed in the design of occupant protection systems are more completely presented in subsequent chapters.

3.1 CURRENT FAA IMPACT CONDITIONS

The current requirements for the impact conditions used to design aircraft occupant protection systems are located in 14 CFR Part 23, Subpart C - Structure; specifically, in Section 23.561 “General” and in Section 23.562 “Emergency Landing Dynamic Conditions.” The regulations mainly address the strength and performance of seat/restraint systems, although some consideration is given to the occupant’s immediate surroundings and to the strength of the fuselage.

The impact conditions in the regulations are based on crash research and accident investigation studies conducted by the FAA, NASA, and the NTSB from as far back as the 1950’s. In the mid-1980’s, the General Aviation Safety Panel (GASP) distilled this impact information into a recommendation that later became the basis for the dynamic test conditions that are cited in Section 23.562. Designers should note that, except for adjustments in the static loads and vertical dynamic test conditions for airplanes with stall speeds greater than 61 kts, the static and dynamic regulatory impact conditions assume that all airplanes respond similarly in a crash. In other words, the current regulations presume all airplanes crash such that the loads, accelerations, and velocity changes are the same. This assumption is clearly a simplification and emphasizes that the CFR’s are minimum performance standards.

3.1.1 14 CFR 23.561 “General”

This regulatory section states that each occupant must be protected in an emergency landing, and that the structure must be designed to provide each occupant with a reasonable chance of escaping serious injury. The 23.561 section also presents the ultimate load factors that must be

designed into the seat, restraint, and aircraft structure. The section further states that the occupant will experience static inertia forces corresponding to these stated loads if proper seats, safety belts, and shoulder harnesses are provided by the designer and used by the occupants. The ultimate load factors that must met for restraining items of mass and cargo are also presented. The load factors specified in 23.561 are shown in Table 3-1.

Table 3-1.
Load factors specified in 14 CFR 23.561

Load Direction	Category		
	Normal, Utility, and Commuter Airplanes (G)	Acrobatic Airplanes (G)	Items of Mass (G)
Upward	3.0	4.5	3.0
Forward	9.0	9.0	18.0
Sideward	1.5	1.5	4.5
Downward	6.0	6.0	N/A

The designer must increase these load factors by a formula found in Paragraph 23.562(d) of the regulation if the stall speed of the airplane at maximum take-off weight (MTOW) is greater than 61 kts.

Section 23.561 also specifies design forces and loads to be used when considering gear-up landings by aircraft equipped with retractable gear. This type of airplane is to be designed to protect each occupant during such a landing. The structure must also be designed to protect the occupants if the aircraft is likely to turn over during an emergency landing. The details of these requirements are found in Paragraphs 23.561(c) and (d). These are the only requirements in Part 23 that explicitly address airframe crashworthiness.

3.1.2 14 CFR 23.562 "Emergency Landing Dynamic Conditions"

Section 14 CFR 23.562 in the FAR specifies the impact conditions that are to be used for the design and test of the seat and restraint system. The conditions and test procedures laid out in this section are to be used to demonstrate that the occupant will be protected during an emergency landing. Human injury tolerance criteria are given that must not be exceeded during these tests. The dynamic tests are conducted with anthropomorphic test devices (ATDs) to simulate the occupant and to measure injury data.

Two tests are required. The first, found in Paragraph (b)(1), and commonly referred to as "Test 1," is a dynamic test that simulates an emergency landing with a primarily vertical impact. The seat/restraint system and occupant are oriented in their normal position with respect to the airplane, and then rotated on the test apparatus so the aircraft coordinates are 30-deg nose-down with respect to the vertical impact vector. This test may appear to simulate a nose-down accident, but is actually devised to simulate an essentially flat, high sink-rate impact onto a surface that has a 0.5 coefficient of friction. The test orientation of the aircraft coordinates depends on the test apparatus: 30-deg nose-down on a drop tower (vertical impact vector) or 60-deg nose-up on a sled (horizontal impact vector). Consequently, this test condition is also referred to as the 30-deg down test or the 60-deg pitch-up test, depending on the test facility. Like the static load factors in 23.561, the crash pulse of Test 1 is modified by 23.562(d) for airplanes with a V_{so} of more that 61 kts at MTOW.

The second test, described in Paragraph (b)(2), and commonly referred to as "Test 2," simulates an emergency landing with a primarily horizontal impact. The seat/restraint system and occupant are again oriented in their normal position with respect to the airplane, and rotated with a 10-deg yaw, but no pitch, relative to the horizontal impact vector. This test condition simulates an accident with a large longitudinal component (relative to the airplane) such as a nose-down impact into dirt, or a flat, sliding impact in which the aircraft hits an obstacle such as a berm or tree. The 10-deg yaw is supposed to be oriented to produce the greatest load in the shoulder harness, but is often oriented to produce the highest likelihood of headstrike. Floor warpage must be taken into account in Test 2 by pitching one of the floor mounting rails 10 deg out of alignment with the other floor mounting rail. In addition, one of the rails must be rolled 10 deg. The crash pulse of Test 2 is not modified by 23.562(d) for airplanes with a V_{so} greater than 61 kts. The designer should always reference the appropriate FAA regulations and guidance when designing an aircraft or seating/restraint system. Both the Test 1 and Test 2 impact conditions are shown in Table 3-2.

Table 3-2.
FAA crash impact design standards

	14 CFR 23.562(b)(1) "Test 1"		**14 CFR 23.562(b)(2) "Test 2"**	
	Front Row	**All Other Rows**	**Front Row**	**All Other Rows**
Velocity Change (ft/sec)	NLT 31	NLT 31	NLT 42	NLT 42
Rise Time to Peak (sec)	0.05	0.06	0.05	0.06
Peak Acceleration (G)	19	15	26	21
Seat/Restraint Position	60-deg Pitch Up No Yaw	60-deg Pitch Up No Yaw	10-deg yaw No Pitch Floor Warpage	10-deg yaw No Pitch Floor warpage

One aspect of the regulations unique to light airplanes is that the magnitude and rise time of the pulse used to test the front row seat/restraint system differs from the pulse used for all seats behind the front row. Justification for this difference came from the NASA full-scale crash test data of 1970's-era metal monocoque light airplanes that showed the magnitude of the deceleration pulse decreased and the duration of the deceleration increased the further aft the measurement was taken (Reference 3-2). This was due to load attenuation by local deformation of the airframe and cabin structure. In other words, the front seat occupants had a shorter distance to decelerate than did the occupants in the rear. Different crew-versus-passenger-seat test pulses are not found in the regulations for any other aircraft category (i.e., Part 25, Transport Category Airplanes, and Parts 27 and 29, Rotorcraft).

More recent NASA full-scale tests of composite light airplanes that are designed to be crashworthy show little difference between the pulses measured at the pilot position versus the pulses at the passenger positions (Reference 3-3). Crashworthy airframes are designed so that the majority of deformation and energy attenuation occurs outside of the occupant compartment. This design strategy reduces the attenuation that occurs within the cabin area and, therefore, little difference is observed in the acceleration pulses between the different cabin positions. Composite airframe structures also tend to be stiffer than metal airframe structures, even when they are not designed for crashworthiness. Moving the deformation and energy-absorption zones outside of the cabin has other effects. In the 30-deg nose-down tests done

onto a hard surface, the rear-seat position actually saw higher vertical acceleration pulses due to a rapid whole-airplane rotation and a secondary impact referred to as “tail slap.” The engine mount, rather than the cabin structure, absorbed the impact energy; thus, the ground reaction load occurs further forward from the aircraft's center of gravity, causing the rapid rotation.

The regulations also allow the front and rear seat/restraint systems to be dynamically tested with different pulses. In real-world practice, the airplane designer needs to decide if the additional testing is justified in terms of cost and airframe response. Often, the front and rear seat/restraint systems are designed to use the same or virtually the same structure, cushions, energy absorbers, and restraints to reduce the cost of design and manufacturing. In systems with a great deal of commonality between the crew and passenger seats, one seat/restraint system (either the crew or passenger, depending on a rational justification of which is worst-case) can be tested to the front seat conditions and then the other positions certified by similarity. This approach has the potential to halve the number of tests and test articles required. For airframes designed to be crashworthy, the authors of this Design Guide recommend that all the seat/restraint systems for that aircraft be designed and tested to the front-row conditions, regardless of seat commonality, for the reasons described above. This recommendation is also appropriate for many composite airframes, due to their stiffness.

3.2 AGATE IMPACT CONDITIONS

The Advanced Crashworthiness Group (ACG) was a subset of the Integrated Design and Manufacturing (ID&M) Work Package in the AGATE Alliance whose task was to develop guidelines and standards to substantially improve the crashworthiness of light airplanes while minimizing the additional cost of these improvements. Like all of AGATE, the members of the ACG represented a broad cross-section of the GA industry and university researchers, in partnership with members from the FAA and NASA. One thrust of the ACG was to develop a simple design and certification methodology for whole-airplane crashworthiness focusing on airframe energy absorption and occupant compartment integrity. While the ACG had not come to a consensus on simplified occupant compartment load factors or the airframe certification methodology by the end of the AGATE program in 2001, they had agreed on the research design approach, the design features of the test airplane, and the design and test impact conditions. These impact conditions are presented here in Table 3-3 and Figure 3-1, and were used in the design of a crashworthy test airplane and in the full-scale crash test of that airplane conducted by the AGATE ACG in the summer of 2001 (References 3-4 and 3-5).

Table 3-3.
AGATE-determined impact conditions

Impact Velocity	V_{so}
Impact Angle	-30 deg (down)
Attitude	-30-deg pitch (nose down)
Weight	MTOW consisting of: • A 170-lb occupant in each seat • Fuel up to MTOW or capacity • Baggage up to MTOW, if fuel is at capacity (Other scenarios may be used if they can be justified, e.g., seats designed with restricted occupant weight should be tested at the maximum restricted weight)
Impact Surfaces	Hard (concrete) Soil (Defining parameters TBD)

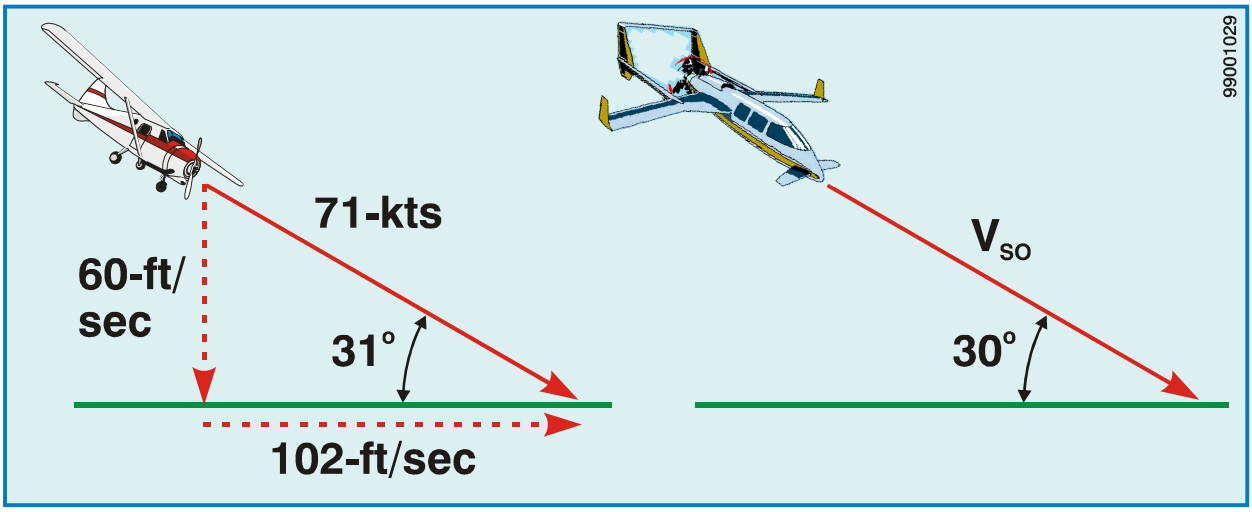

Figure 3-1.
AGATE-determined impact conditions.

It should be noted that the AGATE impact conditions are for the whole airplane and take into account the stall speed (that is, the vehicle's minimum operating speed) and weight of the airplane. These whole-airplane conditions acknowledge that different airplane designs will have different initial crash conditions based on the performance and size of the airplane. These conditions also do not presume the structural response of the airplane; the structural response is defined by the crashworthiness of the design and the ingenuity of the designer. The two different impact surfaces specified recognize that the impact surface also influences the airplane response. At 30 deg nose down, the hard-surface impact typically produces sliding impact with deformation in the lower nose structure and sometimes the front-seat footwells, a whole-airplane pitch-up rotation that aligns the airplane with the impact surface, and a higher vertical (relative to the airplane) component of acceleration. The hard-surface condition forces the designer to address energy absorption primarily in the subfloor structures and also, to a certain extent, in the nose of the airplane; the designer is also induced to address the strength of the lower forward occupant compartment, and the bending strength of the fuselage. An impact on soil at 30 deg nose down produces a very different response. For airplanes that are not designed to be crashworthy, the airplane structure will typically dig into the soil, stopping abruptly, thereby producing a very high longitudinal (relative to the airplane) deceleration. The soil-impact condition forces the designer to address energy absorption primarily in the nose or engine mount, the longitudinal strength of the occupant compartment and firewall, and the use of anti-plowing features. Properly designed, a crashworthy airplane will tend to pitch up out of the crater and thus extend the stopping distance many times over compared to an airplane that digs in (Reference 3-3). The properties of the impact test soil had not been determined by the ACG by the end of the AGATE program in 2001.

3.2.1 Justification

Members of the ACG examined the research discussed in Section 3.4 during an AGATE study of accident impact conditions to determine the design and test impact conditions. Based on the data compiled during the AGATE study, the average impact velocity and the angle at which at least one occupant survived and at least one occupant was fatally injured was 71 kts and 31 deg (Reference 3-6). Comparing the results from the AGATE study to the design pulses

recommended in the 1967 Crash Survival Design Guide (Reference 3-7) required calculating the longitudinal and vertical changes in velocities from the average impact conditions of 71 kts and 31 deg. Four accidents from the database that had very similar impact velocities and angles to the AGATE study average were selected for further analysis. After accounting for slide-out and a range of surface coefficients of friction, the average change in velocity in the longitudinal direction from the AGATE study was shown to be 58 to 69 ft/sec, which correlates well with the 60 ft/sec change in velocity recommended in the Crash Survival Design Guide. The average vertical velocity change from the study was approximately 61 ft/sec, which is larger than the 42-ft/sec change in velocity recommended in the Crash Survival Design Guide. The actual change in vertical velocity in the AGATE study is probably conservative, since the assessment assumed no airframe crushing or ground compaction.

The velocity changes in the AGATE study also compared well with those determined in the NTSB studies of survivable GA accidents. The NTSB studies suggested that longitudinal velocity changes of 60 to 70 ft/sec (with accelerations of 30 to 35 G) were survivable (Reference 3-8). The survivable vertical velocity changes were calculated to be 50 to 60 ft/sec (with 25 to 30 G). The NTSB studies also developed a "survivable envelope" that plotted impact velocity versus impact angle. The impact velocity of the NTSB survivable envelope at 30 deg is approximately 70 kts, which is almost the same as the AGATE study impact conditions. The findings of these studies and the FAA seat test pulse are summarized in Table 3-4.

Table 3-4.
A comparison of industry standards and past studies
(Adapted from Reference 3-6)

	Crash Survival Design Guide 1967 (Reference 3-7)	**NTSB Study 1985 (Reference 3-8)**	**GASP 1984 FAA 1988: Amendment 23-36 (References 3-9 & 3-2)**	**AGATE Study Findings 1999 (Reference 3-6)**
Velocity Change	**Vertical:** 42 ft/sec **Longitudinal:** 60 ft/sec	**Vertical:** 50-60 ft/sec **Longitudinal:** 60-70 ft/sec	**Vertical:** 31 ft/sec **Longitudinal:** 42 ft/sec	**Vertical:** 60 ft/sec **Longitudinal:** 58-69 ft/sec
Acceleration Load	**Vertical:** 48 G **Longitudinal:** 34 G	**Vertical:** 25-30 G **Longitudinal:** 30-35 G	**Vertical:** 19 G (15 G*) **Longitudinal:** 26 G (21 G*)	Data was inconclusive. Insufficient data to determine the acceleration loads.

*Peak G for seats behind the front row.

The FAA and GASP conditions are intended for evaluating the performance of airplane seats and restraint systems. These conditions take into account aircraft deformation, based on metal alloy aircraft, which absorbs energy and reduces the loads that are transmitted to the seats and occupants during a crash. At present, the majority of aircraft are constructed out of light metal alloys; however, as more composite aircraft enter the market, the energy-absorbing characteristics of the population of aircraft will change. Evidence of differences in energy-absorbing characteristics has already been demonstrated and was seen in the Terry Engineering and, later, in the AGATE ACG full-scale crash tests (References 3-3 and 3-5).

A comparison of the accelerations at the seat locations between the AGATE study and the FAA and GASP conditions was not possible because the data did not provide enough information on seat floor and cabin deformation to conduct a proper crash analysis. However, the initial impact

conditions in some of the full-scale tests on which the FAA and GASP condition were based were approximately 50 kts and 30 deg (References 3-2 and 3-10). The initial impact conditions are less severe than the findings from the AGATE study, the NTSB recommendations, and the Crash Survival Design Guide recommendations.

The determination of an "average" survivable impact condition of 71 kts and 31 deg is an artificial simplification, as airplanes can crash at any angle and attitude and at a wide range of speeds. In fact, the AGATE study contained accidents that met the study criteria of at least one fatality and at least one survivor that had impact velocities ranging from less than 15 kts to greater than 120 kts. However, designing for all orientations and velocities would be very difficult, so some simplification is justified. In addition, having some minimum performance standard tends to improve survivability across a wide range of accidents. For example, the automobile industry primarily uses a few crash tests to demonstrate their crashworthiness performance [Federal Motor Vehicle Safety Standards (FMVSS) 208 and 214, and the New Car Assessment Program (NCAP), References 3-11, 3-12, and 3-13]. The frontal crash tests are conducted into a rigid barrier at 30 and 35 mph, and the side-impact tests are conducted with a movable barrier at 33.5 and 38.5 mph. These are minimum standards, but the field data indicate improved survivability in cars at accident speeds and crash angles much different than those that just replicate the tests.

For the following reasons, several ACG members believed that 71 kts was too high for a design and test impact condition. One member thought was that the range assigned for each of the impact velocity "check boxes" on the NTSB accident investigation report form could have skewed the average velocity of the accident studies. These ranges are smaller (15 kts range) at impact speeds below 90 kts and larger (30 kts) above. Also, the ACG was developing a minimum standard—that is, a condition at which there is a high probability of survival—whereas the AGATE study average represented a velocity at which the airplanes apparently failed to protect roughly half their occupants. Another concern was that the NASA Langley Research Center Impact Dynamics Research Facility (IDRF), the location the ACG crash test was to take place, could not reach that impact velocity without augmentation. Finally, there was a precedence of using stall speed to modify the test condition already in the regulations (14 CFR 23.562(d)). Several members of the ACG re-evaluated some of the original AGATE study database and noted that the impact speed range checked in the NTSB accident report contained or was just above the airplane's published stall speed. As a consequence, the ACG chose V_{so} (stall speed) at the MTOW.

The MTOW was selected simply to produce the maximum loads on the cabin structure. The order in which weight is added to meet the MTOW—occupants first, then fuel, then baggage—reflects the group's emphasis on cabin integrity and occupant safety.

The ACG generally supported the 30-deg impact angle with a 30-deg nose-down attitude as an appropriate choice. The two surface conditions produce essentially two different loading cases on the occupant compartment. Many other tests had also been conducted at the IDRF at this angle and attitude (References 3-3 and 3-10), thus providing a generous supply of data for comparison.

By choosing whole-airplane impact conditions, members of the ACG were not advocating widespread, full-scale crash testing of airplanes as a means of certification. The ACG recognized that full-scale testing, at current light-airplane production volumes, would be an undue economic burden to the industry. Instead, the ACG needed the crash-impact conditions and full-scale testing in order to develop a simplified means of designing and demonstrating occupant compartment integrity and airframe energy absorption.

3.3 CRASH CONDITION BACKGROUND

Crash data for GA has been collected and analyzed in studies going back over 30 years. A brief review of the previous studies is discussed below. Much of this section comes directly from Reference 3-6.

3.3.1 1967 Crash Survival Design Guide

Early experimental data collected from full-scale crashes of light fixed-wing aircraft and helicopters were organized and presented in the U.S. Army's 1967 Crash Survival Design Guide (Reference 3-7). The information in the 1967 Design Guide has been used as a reference in many airplane and helicopter designs, and has been revised a number of times, most recently in 1989. The experimental data were presented as triangular design crash pulses corresponding to the 95th-percentile accident for light fixed-wing aircraft and helicopters. The values for the light fixed-wing pulses are shown in Table 3-4.

3.3.2 NTSB Three Phase Study

Several years later, from 1981 to 1985, the NTSB conducted a three-phase study on GA crashworthiness and occupant protection (References 3-8, 3-14, 3-15, and 3-16). In part, the NTSB performed very detailed accident reconstructions to determine the accelerations and changes in velocity for what were to be considered "survivable" accidents. These survivable crash pulse ranges are shown in Table 3-4. The NTSB noted that even though the vertical accelerations were survivable, the loads were likely to produce crippling injuries to the back and neck. According to the study findings, the then-current FAA static seat requirements of 9 G longitudinal and 3 to 6 G downward were insufficient (dynamic tests of the seat/restraint system were not required at that time). The NTSB recommended torso harnesses (shoulder belts) and vertical energy-attenuating seats as the two changes that would be most effective to protect the occupants.

3.3.3 GASP FAA Study

During the same period as the NTSB studies, the FAA requested that an independent panel be formed to recommend ways in which the FAA could promote GA safety. The General Aviation Safety Panel (GASP) was composed of a partnership of various representatives from the GA community. The panel reviewed and analyzed NTSB, NACA, and NASA accident and full-scale test data for both light airplanes and helicopters, as well as dynamic seat test data conducted by the FAA, to determine realistic dynamic performance standards for GA seat/restraint systems. The panel made its recommendation for dynamic seat testing for GA airplanes to the FAA in May 1984 (References 3-2 and 3-9). The recommendation described a dynamic seat test standard that would result in a high-strength seat that would provide occupant protection in severe, but survivable, crashes. The test conditions are described more thoroughly in Section 3.1.2 and summarized in Table 3-4. The panel also recommended including upper-torso restraint systems as mandatory equipment in all newly manufactured GA aircraft and

promoted the installation of shoulder harness on all older GA aircraft. The GASP panel reported that the use of upper-torso restraints could provide the most effective method of reducing fatal and serious injuries in GA accidents.

The FAA incorporated the GASP recommendations in two amendments to 14 CFR Part 23: Amendment 23-32 required shoulder belts for all passengers in light airplanes manufactured after December 12, 1985 (Reference 3-17); and Amendment 23-36 adopted dynamic seat/restraint system testing for airplanes certified after September 14, 1988 (Reference 3-2).

3.3.4 AGATE Crash Conditions Study

To design a crashworthy aircraft, criteria had to be selected to produce the most crashworthy airplane while taking into consideration other constraints such as costs, manufacturing, availability of materials, and public acceptance. The test criteria called out by the FAA to certify the seat/restraint system is not necessarily the impact criteria that will afford the most occupant protection. To determine the most effective criteria, three members of the AGATE ACG conducted a study of real-world accident data in 1996 and 1997 (Reference 3-6).

The purpose of the research was two-fold:

1. Provide a crash condition or multiple crash conditions representative of "real-world" GA accidents that could then be used in the design and testing of crashworthiness systems in AGATE aircraft.
2. Identify the injuries and the injury mechanisms that occur in "real-world" GA accidents so the best combination of crashworthiness technologies could be selected for AGATE aircraft.

The study focused on current GA aircraft that are representative of what will be the AGATE aircraft. The AGATE-class airplane was defined as an all-composite, single-engine, single-pilot, fixed-wing airplane holding 2 to 6 occupants with a maximum gross weight of 6,000 lb. Only a few current GA airplanes are constructed from composites, with the majority of aircraft constructed from lightweight metals. Since the accident database for the composite aircraft is so small, aircraft constructed from all materials were included, in order to obtain a significant sample size for the database. The current fleet of airplanes is likely to represent the same pre-impact conditions as composite aircraft. However, it is likely that the composite aircraft will respond differently to an impact as compared to metal aircraft.

Cases that met the criteria of at least one fatality and at least one survivor were selected in order to avoid reviewing data that involved minor accidents and data involving catastrophic accidents that are outside the limit of survivability. From this database, the results were compared to the limits of survivability that are discussed in John Clark's NTSB report (Reference 3-8) to see if there were any significant differences between the database results and previous GA crash studies (specifically, the GASP recommendations and the NTSB crashworthiness reports). Also, the study was conducted to find out if the previous studies were still valid with the current fleet and with AGATE-class airplanes.

This approach does not include accident data for single-occupant crashes. However, the information in the database still provided insight into the limits of survivable airplane accidents. The database selected only a sub-set of all aircraft accidents. The intent of the selected database was to be an accurate representation of aircraft accidents pertaining to AGATE-class aircraft.

The results from the AGATE study were compared to previous GA crashworthiness studies and shown to be similar. The more pertinent results of the AGATE study were presented in Section 3.3.1.

References

3-1. Federal Aviation Regulations, Part 23, Airworthiness Standards: Normal, Utility, Acrobatic, and Commuter Category Airplanes, 14 CFR 23, Federal Aviation Administration, Washington, D.C.

3-2. 14 CFR Part 23, Amendment 23-36, "Small Airplane Crashworthiness Review Program, Amendment 1," Published in 53 FR 30802, August 15, 1988.

3-3. Terry, J. E., Hooper, S. J., and Nicholson, M., "Design and Test of an Improved Crashworthiness Small Composite Airframe," Phase II Report, Terry Engineering, Andover, Kansas; NAS1-20427, NASA Langley Research Center, Hampton, Virginia. October 1997.

3-4. Hooper, S. J., Henderson, M. J., and Seneviratne, W. P., "Design and Construction of a Crashworthy Composite Airframe," National Institute for Aviation Research - Wichita State University, Wichita, Kansas, August 9, 2001.

3-5. Henderson, M. J. and Hooper, S. J., "AGATE Composite Airframe Impact Test Results," National Institute for Aviation Research - Wichita State University, Wichita, Kansas, October 31, 2001.

3-6. Grace, G. B., Hurley, T. R., and Labun, L., "General Aviation Crash Safety Analysis and Crash Test Conditions: A Study of Accident Data from 1988 to 1995," TR-98002, Simula Technologies, Inc., Phoenix, Arizona, February 15, 1998.

3-7. Turnbow, J. W., Carroll, D. F., et al., Crash Survival Design Guide, Aviation Safety Engineering and Research, July 1967 (Revised January 1969).

3-8. Clark, J. C., "Summary Report on the National Transportation Safety Board's General Aviation Crashworthiness Project Finding," SAE 871006, Society of Automotive Engineers, Warrendale, Pennsylvania, April 1987.

3-9. Soltis, S. J., and Olcott, J. W., "The Development of Dynamic Performance Standards for General Aviation Aircraft Seats," SAE 850853, Society of Automotive Engineers, Warrendale, Pennsylvania, April 1985.

3-10. Castle, C. B., and Alfaro-bou, E., "Crash Tests of Three Identical Low-Wing Single-Engine Airplanes," NASA Technical Paper 2190, NASA Langley Research Center, Hampton, Virginia, 1983.

3-11. 49 CFR Part 571, Federal Motor Vehicle Safety Standards, Subpart 208, Occupant Crash Protection, National Highway Traffic Safety Administration, Department of Transportation, Washington, D.C., October 1, 2001.

3-12. 49 CFR Part 571, Federal Motor Vehicle Safety Standards, Subpart 214, Side Impact Protection, National Highway Traffic Safety Administration, Department of Transportation, Washington, D.C., October 1, 2001.

3-13. National Highway Traffic Safety Administration web site, http://www.nhtsa.gov, site accessed December 14, 2001.

3-14. "General Aviation Crashworthiness Project, Phase One," NTSB/SR-83/01, National Transportation Safety Board, Washington, D.C., June 27, 1983.

3-15. "General Aviation Crashworthiness Project, Phase Two – Impact Severity and Potential Injury Prevention in General Aviation Accidents," NTSB/SR-85/01, National Transportation Safety Board, Washington, D.C., March 5, 1985.

3-16. "General Aviation Crashworthiness Project, Phase Three – Acceleration Loads and Velocity Changes of Survivable General Aviation Accidents," NTSB/SR-85/02, National Transportation Safety Board, Washington, D.C., September 4, 1985.

3-17. 14 CFR Part 23, Amendment 23-32, "Shoulder Harnesses in Normal, Utility, and Acrobatic Category Airplanes," Published in 50 FR 46872, November 13, 1985.

Chapter 4
Biometrics

Jill M. Vandenburg
Anita E. Grierson

The primary objectives of crashworthy aircraft design are to prevent occupant fatalities and minimize injury during crash scenarios. To meet these objectives, aircraft designers need to have an understanding of the human body and how it responds to trauma. General knowledge of human anthropometry (Section 4.1), occupant flail envelopes (Section 4.2), and human injury tolerance (Section 4.3) will prove to be a tremendous asset to the aircraft designer during the design process. In addition, aircraft designers should also have an understanding of the types of anthropometric test devices (ATDs) that can be used to represent the human body during the design, testing, and certification of aircraft safety systems and components (Section 4.4).

4.1 HUMAN BODY ANTHROPOMETRY AND ITS APPLICATION TO AIRCRAFT DESIGN

The discipline of anthropometry is concerned with the measurement of the human body and its biomechanical characteristics. Scientific measurement techniques are used to measure body dimensions, mass properties, and joint range of motion of human volunteer subjects within a particular population. In the design of General Aviation (GA) aircraft, anthropometric measurements are used to create a comfortable, safe, and functional environment for the pilots, passengers, and crew of the aircraft. Specifically, anthropometric measurements define the dimensions of those aircraft components that directly interact with the human body, including:

- **Crew stations** - Functional reach, instrument panel design, location of primary flight controls, crew seat dimensions and comfort, seatback height, seat pan and seat cushion length and width, seat adjustment range, seat restraint system anchor locations, design eye view, etc.
- **Passenger seats** - Functional reach, seatback height, seat pan and seat cushion length and width, view of exterior, seat adjustment range, restraint system anchor locations, comfort, seat pitch, egress issues, etc.

These measurements are also used to design human and ATD computer models for aircraft simulation and analysis purposes. In addition, the anthropometric measurements are used to assess the accessibility and functionality of components related to the maintenance, repair, and overhaul of the aircraft.

Overall, the discipline of anthropometry enables aircraft designers to accommodate the wide variability in demographics that exists within the GA population of pilots, passengers, and crew. Across this population, individuals may vary in terms of age, gender, ethnicity, and health, as well as body size, shape, mass, and joint range of motion. Proper accommodation for these variable characteristics in aircraft design is imperative to enhancing the aircraft's comfort, safety, and functionality. Inadequacies in the physical dimensions of the aircraft design can lead to discomfort, fatigue, and human error.

This section of the Design Guide will further define the role of anthropometry in GA aircraft design by discussing the:

- Structure and motion of the human body
- Sources of anthropometric differentiation
- Types of anthropometric measurements
- Presentation of anthropometric data
- Anthropometric data resources and databases.

4.1.1 Describing the Structure and Motion of the Human Body

In anthropometry, the human body is described by referencing three primary anatomical planes, several different anatomical orientations and landmarks, and the joint ranges of motion (Reference 4-1). These common references help to standardize the terminology that is used during anthropometric surveys. Figure 4-1 illustrates the three primary anatomical planes that are defined for the human body, which include:

1. Sagittal plane: partitions the body into right and left halves.
2. Coronal plane: partitions the body into front and back halves.
3. Transverse plane: partitions the body into upper and lower halves.

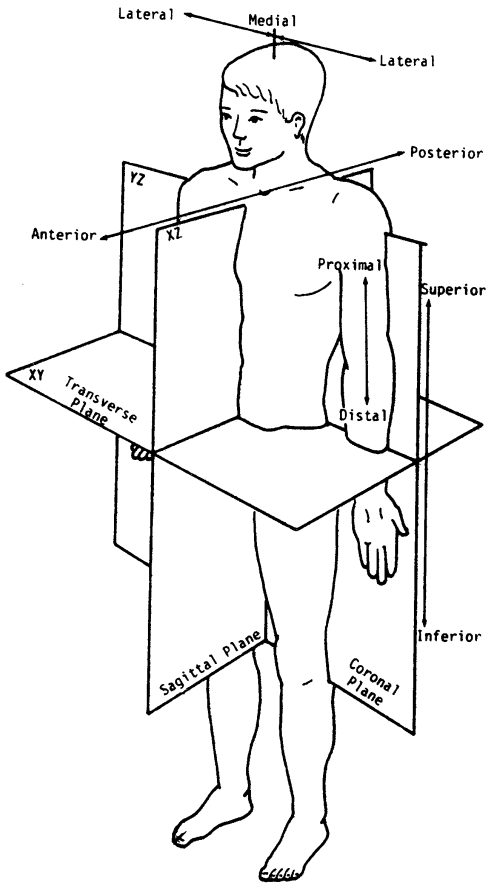

Figure 4-1.
Anatomical planes and orientations of the human body (Reference 4-1).

Figure 4-1 also displays several common anatomical orientations for the human body that are described using directional arrows. For example, the directional arrow labeled *anterior* refers to the front side of the body, whereas the directional arrow labeled *posterior* refers to the backside of the body.

Figures 4-2 and 4-3 illustrate several common anatomical landmarks that are used to define various anthropometric measurements. For example, Figure 4-3 includes the phalange and metacarpal bones of the human hand. These bones form the metacarpal-phalangeal joints of the fingers. In order to measure the breadth of the human hand, as shown in Figure 4-4, standard anthropometric procedures state that the hand breadth should be measured between the metacarpal-phalangeal joints of the second and fifth fingers. The metacarpal-phalangeal joints of these two fingers serve as anatomical landmarks for this particular type of anthropometric measurement.

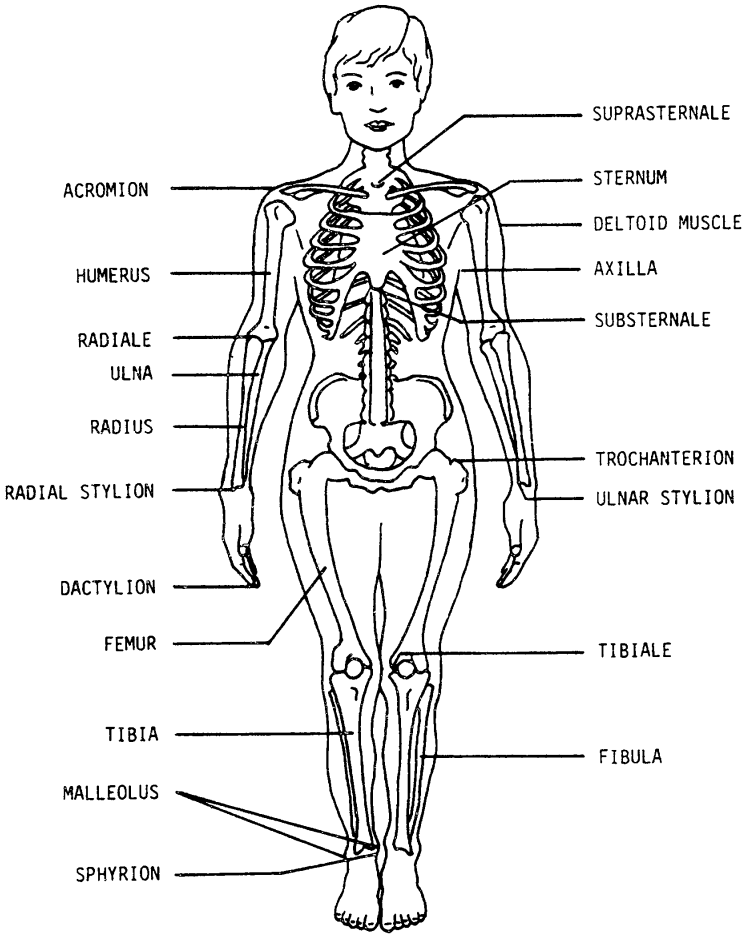

Figure 4-2.
Selected anthropometric landmarks of the human body – anterior view (Reference 4-1).

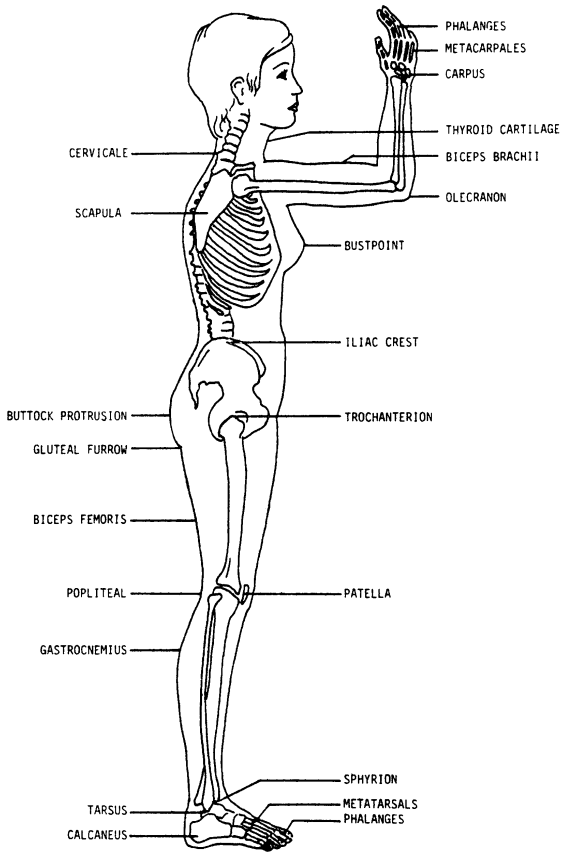

Figure 4-3.
Selected anthropometric landmarks of the human body – lateral view (Reference 4-1).

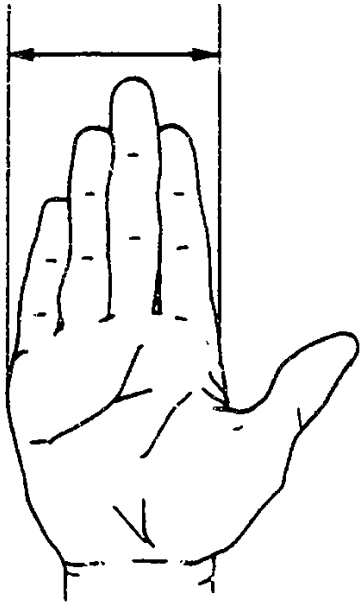

Figure 4-4.
Anthropometric measurement of the breadth of the hand (Reference 4-1).

Finally, Figure 4-5 and Table 4-1 describe the range of motion for several different human body joints. Understanding the range of motion for all major joints in the human body is essential in the assessment of body mobility within any given environment.

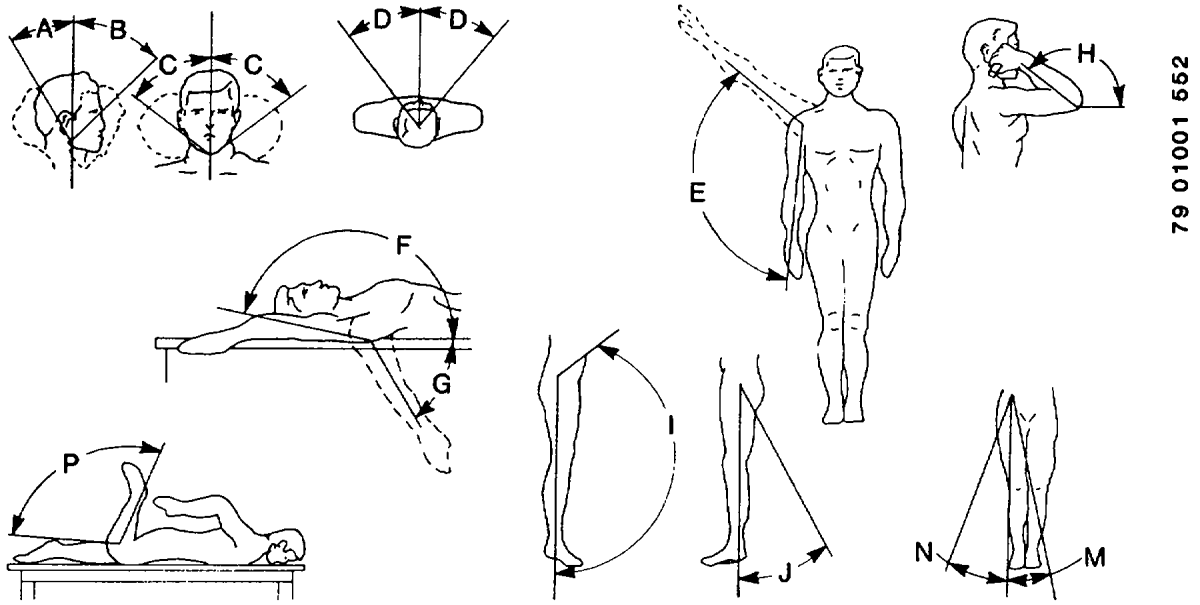

Figure 4-5.
Joint ranges of motion for various joints on the human body (Reference 4-2).

Table 4-1.
Joint ranges of motion for the human body (Reference 4-2)

Body Component Motion	Figure 4-5 Symbol	Joint Motion Description	Measured Voluntary Rotation (Deg)	Measured Forced Rotation (Deg)
Head with respect to the torso	A	Dorsiflexion	61	77
	B	Ventriflexion	60	76
	C	Lateral flexion	41	63
	D	Rotation	78	83
Upper arm at the shoulder	E	Abduction (coronal plane)	130	137
	F	Flexion	180	185
	G	Hyperextension	58	69
Forearm at the elbow	H	Flexion	141	146
Thigh at the hip	I	Flexion	102	112
	J	Hyperextension	45	54
	M	Adduction	--	--
	N	Abduction	71	79
Lower leg at the knee	P	Flexion	125	138

4.1.2 Sources of Anthropometric Differentiation

Numerous factors contribute to the anthropometric variability within a given population. As shown in Figure 4-6, these factors can be classified into three separate categories: biological factors, environmental factors, and procedural factors (Reference 4-3). Biological factors are considered to be intrinsic to the individual and are typically genetic in nature, whereas environmental factors are considered to be extrinsic to the individual. Procedural factors involve the methods used to acquire and analyze the anthropometric data.

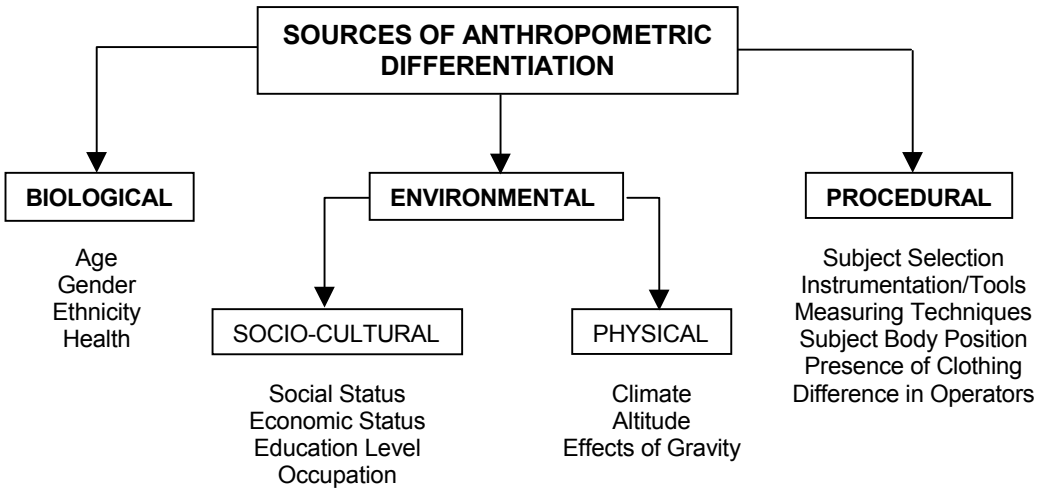

Figure 4-6.
Sources of anthropometric differentiation (Reference 4-3).

Each of the examples listed under the category headings can have a significant effect on the anthropometric characteristics of any individual within a population (Reference 4-3). For example, gender is listed as a biological factor. In the United States, on average, men are typically slightly taller and heavier than women, and generally have larger absolute body segment measurements. Common exceptions include hip breadth and circumference measurements, as well as thigh circumference measurements, which are typically larger in women. Body segment proportions also vary according to gender. For example, on average, males' arms and legs are longer than females' limbs. In addition, male arms and legs are longer in relation to stature and sitting height. Aircraft designers should recognize that these sources of anthropometric differentiation exist within any given population. As a result, it is essential for designers to be able to identify these factors and understand how they affect the population of interest. This task is accomplished by conducting an anthropometric survey of the population or using data from existing surveys.

In an anthropometric survey, a random sample of individuals is selected from the population of interest. In most cases, the selection process is not completely randomized, since the human test subjects must volunteer to participate in the study. Researchers identify potential sources of anthropometric differentiation by recording a series of pre-defined anthropometric measurements for each individual within the sample population. The measurements are selected based on the overall objectives of the anthropometric study.

4.1.3 Types of Anthropometric Measurements

There are two different types of measurements that can be recorded during an anthropometric survey of a particular population: static measurements and dynamic measurements (Reference 4-3). Static anthropometric data consists of passive measurements of the human body including heights, lengths, circumferences, breadths, and depths. These measurements are traditionally recorded while the subject is in either a seated or standing position. For example, Figure 4-7 illustrates the conventional static measurements recorded for an individual in a seated position. Static anthropometric measurements are used to determine size and spacing requirements for the design of equipment, vehicles, aircraft, workspace layout, clothing, and computer models of the human body (Reference 4-1). Dynamic anthropometric measurements are used to describe human body movement (Reference 4-3), and measure muscular strength, joint range of motion, inertial properties of body segments, and the speed and accuracy of segment motion.

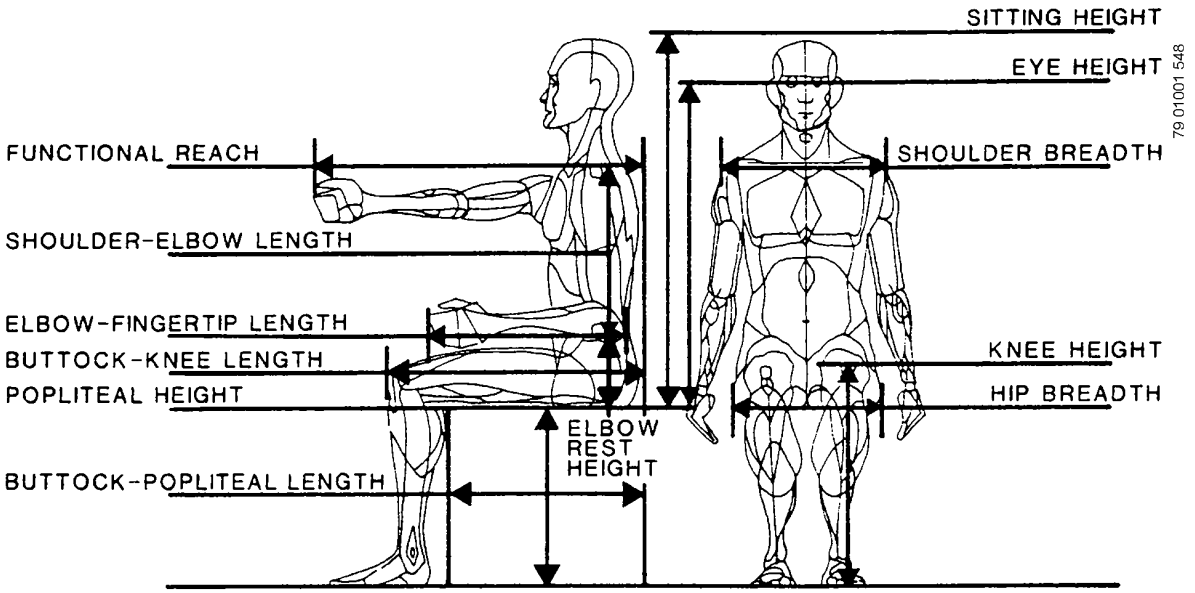

Figure 4-7.
Conventional seated anthropometric measurements (Reference 4-2).

The dynamic anthropomorphic measurements may be defined in the following manner:

- Muscular Strength Measurements: These are used to predict the ability of a human operator to perform dynamic strength tasks (Reference 4-4).
- Joint Range of Motion Measurements: Understanding the range, speed, and accuracy of motion for all major joints and segments in the human body is essential in the assessment of body mobility (Reference 4-5).
- Measurement of Inertial Properties: Inertial properties, including segment mass, volume, center of mass, and moment of inertia aid in the assessment of body mobility (Reference 4-6).

All static and dynamic anthropometric measurements are selected based on the overall objectives of the anthropometric survey.

4.1.4 Presentation of Anthropometric Data

Anthropometric data are generally analyzed in the form of a statistical distribution. The normal, or Gaussian distribution (bell-shaped curve) is the most frequently used distribution for approximating anthropometric data such as stature, body weight, sitting height, design eye height, etc. Descriptive statistics, including mean and standard deviations, are used to further describe the distribution of anthropometric data.

Current anthropometric databases and literature references typically describe anthropometric dimensions in terms of percentiles; i.e., 5th-percentile, 50th-percentile, 95th-percentile, etc. The definition of percentile states, "A percentile value of an anthropometric dimension represents the percentage of the population with a body dimension of a certain size or smaller (Reference 4-8)." The following example illustrates the use of percentiles in presenting anthropometric data.

Example:

An aircraft designer is designing the pilot seat for an aircraft. One of the most important occupant dimensions needed for the design of the seat is the eye height of the pilot. The designer's objective is to design a seat that will accommodate a range of different design eye heights to allow different-sized pilots to efficiently fly the aircraft. To obtain this dimension, the aircraft designer locates a current anthropometric data reference or database that contains a distribution for pilot eye height. The eye height data values should be based on measurements recorded for a population that is representative of the GA population of pilots.

Figure 4-8 displays the format of the data that would be provided in a standard anthropometric reference text (Reference 4-9). As shown, the eye height measurements are presented in terms of a range of percentiles. For example, the 25th-percentile mark indicates that approximately 25 pct of the sample population of male pilots have an eye height less than or equal 76.88 cm (30.27 in). On the other hand, the 25th-percentile mark also indicates that approximately 75 pct of the sample population of male pilots have an eye height greater than or equal to 76.88 cm (30.27 in). It would appear desirable to design aircraft or other vehicles to accommodate the extremes of a population (1st- and 100th-percentile occupants). Unfortunately, due to space constraints and cost issues, this can become a tremendous design challenge. As a result, most engineers elect to use the 5th- and 95th-percentiles to define the range of design dimensions. This percentile range ensures that at least 90 pct of the population will be accommodated by the design.

In this example, the use of percentiles for the presentation of anthropometric data allows aircraft designers to select an appropriate range for design eye height that will effectively accommodate the population of pilots that will fly the aircraft. This same methodology can be applied for all required anthropometric dimensions.

4.1.5 Anthropometric Data Resources and Databases

Anthropometric data can be obtained from a variety of sources. Resource texts and computer databases may serve as a quick and simple reference for aircraft designers. In those situations where the current anthropometric literature or databases do not provide the information required for the design, the aircraft designer can conduct his/her own anthropometric survey. The designer can also hire an outside company or organization to conduct a survey.

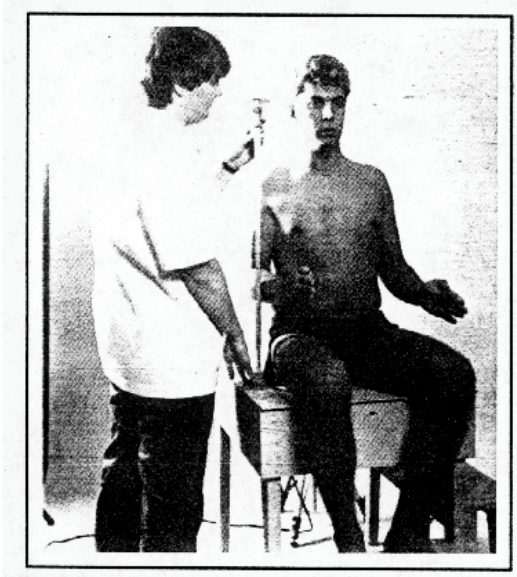

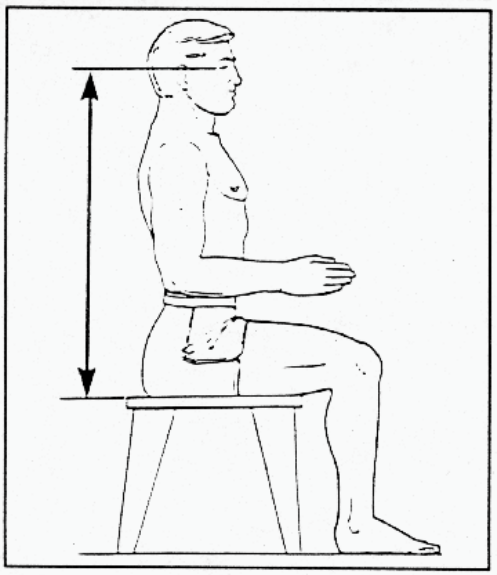

THE PERCENTILES

FEMALES			MALES	
CM	INCHES		CM	INCHES
66.40	26.14	1ST	71.18	28.02
67.21	26.46	2ND	72.11	28.39
67.74	26.67	3RD	72.70	28.62
68.46	26.95	5TH	73.50	28.94
69.60	27.40	10TH	74.76	29.43
70.38	27.71	15TH	75.61	29.77
71.01	27.96	20TH	76.29	30.04
71.56	28.17	25TH	76.88	30.27
72.06	28.37	30TH	77.40	30.47
72.52	28.55	35TH	77.88	30.66
72.96	28.72	40TH	78.34	30.84
73.39	28.89	45TH	78.79	31.02
73.82	29.06	50TH	79.23	31.19
74.25	29.23	55TH	79.66	31.36
74.68	29.40	60TH	80.10	31.54
75.13	29.58	65TH	80.56	31.72
75.61	29.77	70TH	81.04	31.90
76.13	29.97	75TH	81.55	32.11
76.71	30.20	80TH	82.13	32.33
77.37	30.46	85TH	82.78	32.59
78.21	30.79	90TH	83.61	32.92
79.43	31.27	95TH	84.80	33.39
80.20	31.57	97TH	85.56	33.68
80.75	31.79	98TH	86.10	33.90
81.59	32.12	99TH	86.93	34.23

Figure 4-8.
Design eye height for male and female U.S. Army personnel (Reference 4-9).

When searching for anthropometric data, it is important to remember to obtain the most recent data available. The more recent the data, the more accurate it will be in defining the proper dimensions for the product. The majority of the currently available anthropometric data was recorded prior to the 1980's. As a result, the data that is currently available in anthropometric literature may not be exactly representative of the United States civilian and/or military populations of today. Anthropometric data that is used for the design of newly developed GA aircraft should take into account the changes in population anthropometry.

Anthropometric surveys frequently record measurements that are required for use in a specific application (Reference 4-1). As a result, aircraft designers should verify that the selected population and the anthropometric measurements taken for the survey are applicable to their

design needs. In addition, anthropometric data should be extracted from those surveys that have standardized and/or clearly defined the subject selection criteria and measuring techniques used during the survey. Standardization allows the anthropometric data to be compared effectively from survey to survey. This is especially true for designers who utilize CAD and CAM programs that provide anthropometric models for use in design and analysis. If the anthropometric model is not based on published anthropometric data, then the final CAD or CAM design may be inadequate for the selected population. The designer should know the source dimensions, mass properties, and joint range of motion of the CAD or CAM anthropometric model, and the model should be based on published anthropometric data that has been clearly defined for a particular population.

While there are several sources for civilian anthropometry available, the most detailed data pertains to the anthropometry of military personnel. Table 4-2 lists several useful anthropometric references for both civilian and military populations. It is important to recognize that Table 4-2 is not a complete listing of anthropometric resources, and that numerous other resource texts and computer databases are available for use in aircraft design applications.

In an effort to expand on the currently available anthropometric data, researchers at the Computerized Anthropometric Research and Design (CARD) Laboratory at Wright-Patterson Air Force Base in Dayton, Ohio, in cooperation with NATO and numerous industrial partners, are conducting a large-scale anthropometric survey of civilian populations worldwide (References 4-10 - 4-12). The anthropometric data collected from this survey will be included in a state-of-the-art database called the Civilian American and European Surface Anthropometric Resource, or CAESAR.

The primary objective of this initiative is to document the anthropometric variability of American and European adult civilians (Reference 4-11). Three-dimensional digital surface anthropometry technology will be used to measure the three-dimensional size and shape of approximately 4,000 American and 4,000 European males and females of various weights and ranging in age from 18 to 65. Using a Cyberware WB4 Whole Body Scanner, researchers will be able to generate high-resolution data of the human body's surface (Reference 4-12). The anthropometric data acquired from these 3-D whole-body digital images will be easily transferred to CAD or CAM tools to be used for applications involving the design of industrial workstation layouts, automobiles, aircraft, apparel, and protective equipment.

The three populations (United States, Italy, and the Netherlands) were selected for the large-scale anthropometric survey based on their unique anthropometric characteristics (Reference 4-11):

- The United States represents the NATO nation with the largest population.
- Italy represents the NATO nation with the shortest population.
- The Netherlands represents the NATO nations with the tallest populations.

The sample populations that are selected from the three larger populations will be comprised of individuals representing a wide variety of ethnic groups, socio-economic classes, and geographic regions. The data collection methods will be standardized in order to continually update the database with the data recorded from future anthropometric surveys. Future surveys plan to target additional age groups and populations in other European countries. The project was scheduled to be completed by the end of 2000 (Reference 4-1).

Table 4-2.
Examples of anthropometric data references

YEAR	AUTHOR(S) AND AFFILIATION	TITLE AND DESCRIPTION	REF NO.
1991	Donelson, S. M., and Gordon, C. C., U.S. Army Natick Research, Development, and Engineering Center	**1988 Anthropometric Survey of U.S. Army Personnel: Pilot Summary Statistics**	4-9
1993	Tilley, A. R., Henry Dreyfuss Associates	**The Measure of Man and Woman, Human Factors in Design** Data for children through elderly; contains 1st- through 99.5th-percentile dimensions	4-13
1990	Griener, T. M., and Gordon, C. C., U.S. Army Natick Research, Development, and Engineering Center	**An Assessment of Long-term Changes in Anthropometric Dimensions: Secular Trends of U.S. Army Males**	4-14
1989	Gordon, C. C., Bradtmiller, B., and Churchill, T., et al., U.S. Army Natick Research, Development, and Engineering Center	**1988 Anthropometric Survey of U.S. Army Personnel: Methods and Summary Statistics** Data for U.S. Army men and women; contains 1st- through 99th-percentile dimensions for both females and males	4-15
1988	Robinette, K., Fowler, J., Wright-Patterson Air Force Base	**An Annotated Bibliography of the United States Air Force Engineering Anthropometry, 1946-1988**	4-16
1987	Harry G. Armstrong Aerospace Medical Research Laboratory at Wright-Patterson AFB	**Anthropometry and Mass Distribution for Human Analogues, Vol. 1: Male Military Aviators**	4-17
1987	Salvendy, G.	**Handbook of Human Factors** Fundamentals of human factors and design	4-18
1983	Young, J. W., Chandler, R. F., and Snow, C. C., Civil Aeromedical Institute	**Anthropometric and Mass Distribution Characteristics of the Adult Female**	4-19
1983	Reynolds, H. M., and Leung, S. C., Aerospace Medical Research Laboratory at Wright-Patterson Air Force Base	**A Foundation for Systems Anthropometry: Lumbar/Pelvic Kinematics**	4-20
1983	Schneider, L. W., et al., University of Michigan	**Development of Anthropometrically Based Design Specifications for an Advanced Adult Anthropomorphic Dummy Family, Volume 1** Data for adult ATDs used to test automobiles and aircraft	4-21
1982	Easterby, R., Kroemer, K. H. E., Chaffin, D. B.	**Anthropometry and Biomechanics: Theory and Application** Collection and application of anthropometric principles	4-22
1982	Reynolds, H. M., Snow, C. C., and Young, J. W., Civil Aeromedical Institute	**Spatial Geometry of the Human Pelvis**	4-23
1982	Vaughn, C. L., Andrews, J. G., and Hay, J. G.	**Selection of Body Segment Parameters by Optimization**	4-24
1981	Chandler, R. F., and Young, J., Civil Aeromedical Institute	**Uniform Mass Distribution Properties and Body Size Appropriate for the 50 Percentile Male Aircrewmember During 1980-1990**	4-25
1981	Gregoire, H. G., and Slobodnik, B., Naval Air Test Center	**The 1981 Naval and Marine Corps Aviation Anthropometric Survey**	4-26
1980	McConville, J. T., et al., AFAMRL	**Anthropometric Relationships of Body and Body Segment Moments of Inertia** Volume, center of volume, and principal moments of inertia for 31 male subjects	4-27

Table 4-2. (continued)
Examples of anthropometric data references

YEAR	AUTHOR(S)	TITLE/DESCRIPTION	REF NO.
1978	Laubach, L. L., McConville, J. T., and Tebbetts, I., Webb Associates	**Anthropometric Source Book, Volumes 1, 2, And 3** Comprehensive handbook of anthropometric data and applications of the data; also provides an annotated bibliography of 236 references covering topics in physical anthropology, anthropometry, and applications of anthropometric data in sizing and design	4-28
1977	Churchill, E., et al.	**Anthropometry of Women in the U.S. Army**	4-29
1977	Snyder, R. G., Schneider, L. W., and Owings, C. L.	**Anthropometry of Infants, Children, and Youths to Age 18 for Product Safety Design** Data for 2-18 year-olds	4-30
1976	Atkins, E. R., Dauber, R. L., Karas, J. N., and Pfaff, T. A., Vought Corporation	**Study to Determine the Impact of Aircrew Anthropometry on Airframe Configuration**	4-31
1975	Chandler, R. F., et al.	I**nvestigation of Inertial Properties of the Human Body** Moments of inertia with respect to six axes for fourteen segments of six cadavers; principal moments of inertia	4-32
1975	Reynolds, H. M., Clauser, C. E., and McConville, J.	**Mass Distribution Properties of the Male Cadaver**	4-33
1974	Kroemer, K. H. E., Aerospace Medical Research Laboratory at Wright-Patterson, Air Force Base	**Designing for the Muscular Strength of Various Populations**	4-34
1973	Walker, L. B., Harris, E. H., and Pointius, U. R.	**Mass, Volume, Center of Mass, and Moment of Inertia of Head and Head and Neck of the Human Body** Male cadaver data	4-35
1972	Becker, E. B.	**Measurement of Mass Distribution Parameters of Anatomical Segments**	4-36
1972	Clauser, C. E., et al., Wright-Patterson Air Force Base	**Anthropometry of Air Force Women**	4-37
1971	Churchill, E., et al., U.S. Army Natick Laboratories	**Anthropometry of U.S. Army Aviators - 1970** U.S. Army male aviators	4-38
1971	White, R. M., and Churchill, E., U.S. Army Natick Laboratories	**The Body Size of Soldiers – U.S. Army Anthropometry – 1966** U.S. Army male non-aviators	4-39
1970	Kroemer, K. H. E., Aerospace Medical Research Laboratory at Wright-Patterson, Air Force Base	**Human Strength: Terminology, Measurement, and Interpretation of Data**	4-40
1969	Clauser, C. E., McConville, J. T., and Young, J. W.	**Weight, Volume, and Center of Mass of Segments of the Human Body** Center of mass locations for cadaver body segments; developed regression equations	4-41
1969	Laubach, L. L., Aerospace Medical Research Laboratory at Wright-Patterson Air Force Base	**Body Composition in Relation to Muscle Strength and Range of Joint Motion**	4-42
1968	Singley and Haley	**Models and Analogues for the Evaluation of Human Biodynamic Response, Performance, and Protection** Segment mass, center of mass, and skeletal joint locations for a 50th-percentile U.S. Army male aviator	4-43
1967	Dempster, W. T., Wright Air Development Center	**Space Requirements for the Seat Operator** Moments of inertia, mass, and center of mass locations measured on cadaver body segments; link lengths between effective joint centers for major body parts	4-44

Table 4-2. (continued)
Examples of anthropometric data references

YEAR	AUTHOR(S)	TITLE/DESCRIPTION	REF NO.
1967, 1955	Dempster, W. T., and Gaughran, G. R. L.	**Properties of Body Segments Based on Size And Weights** Moments of inertia, mass, and center of mass locations measured on cadaver body segments; link lengths between effective joint centers for major body parts	4-45
1966	Laubach, L. L., Aerospace Medical Research Laboratory at Wright-Patterson Air Force Base	**Muscle Strength, Flexibility, and Body Size of Adult Males**	4-46
1965	Gifford, E. C., Provost, J. R., and Lazo, J., Aerospace Crew Equipment Lab, Department of the Navy	**Anthropometry of Naval Aviators – 1964**	4-47
1963	Santschi, W. R., DuBois, J., and Ornoto, C.	**Moments of Inertia and Centers of Gravity of the Living Human Body** Moments of inertia of live human subjects in a seated position	4-48
1962	Swearingen, J. J., Civil Aeromedical Research Institute	**Determination of Centers of Gravity of Man** Centers of gravity for adult males	4-49
1959	Buck, C. A., et al.	**Study of Normal Range of Motion in the Neck Utilizing a Bubble Goniometer** Range of motion of the head-neck complex	4-50
1937	Glanville, A. D., and Kreezer, G.	**The Maximum Amplitude and Velocity of Joint Movements in Normal Male Human Adults** Joint angles of motion for the movements illustrated in Figure 4-5	4-51

4.2 OCCUPANT FLAIL ENVELOPES

The available flail volume surrounding the occupant in an aircraft is typically referred to as the occupant's flail envelope. The occupant flail envelope can vary significantly depending on several factors, including, but not limited to, the type of torso restraint, the restraint anchorage points, the magnitude and direction of the crash deceleration, the initial slack and initial position of the restraint webbing on the occupant, the amount of webbing stored on the inertia reel spool, the occupant's size/weight, the deformation of the cabin interior, etc. Because of these variables, it is not possible to fully predict the occupant flail envelope in an actual crash, or even to predict the ATD response during seat qualification testing. Therefore, the flail envelopes provided in this section are recommended for use only for the initial design trade studies. Detailed computer simulation and/or dynamic testing will ultimately be required to fully define the occupant flail envelope for each unique aircraft/restraint configuration.
Figures 4-9 through 4-11 illustrate occupant flail envelopes for a 95th-percentile male ATD with a five-point restraint (Reference 4-52). The restraint consists of a lap belt, lap belt tie-down strap, and two shoulder straps. The motions shown are based on test data obtained during a 30-G forward impact test pulse with a velocity change of 50 ft/sec. Even though this test pulse is more severe than the current GA test requirements, it is recommended that all aircraft interior components within the extremity flail envelopes shown be designed to minimize impact injuries.

The flail envelope of the head is the primary concern when designing an aircraft's interior. If at all possible, there should be no aircraft components within the occupant's head flail envelope. Therefore, the aircraft designer must have information on the anticipated head flail envelope early in the design process.

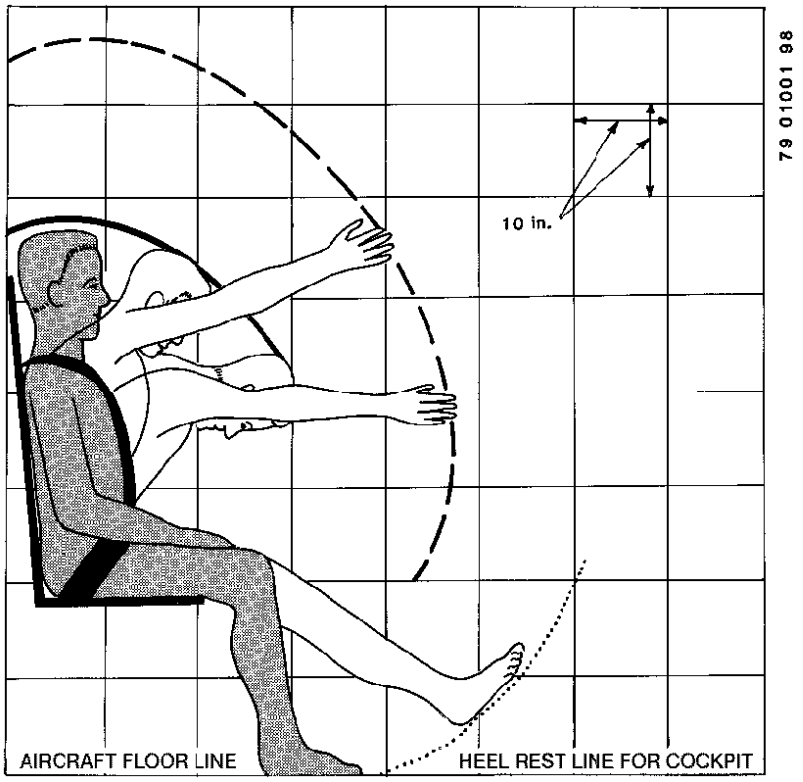

Figure 4-9.
Flail envelope for the 95th-percentile ATD wearing a five-point restraint - side view.

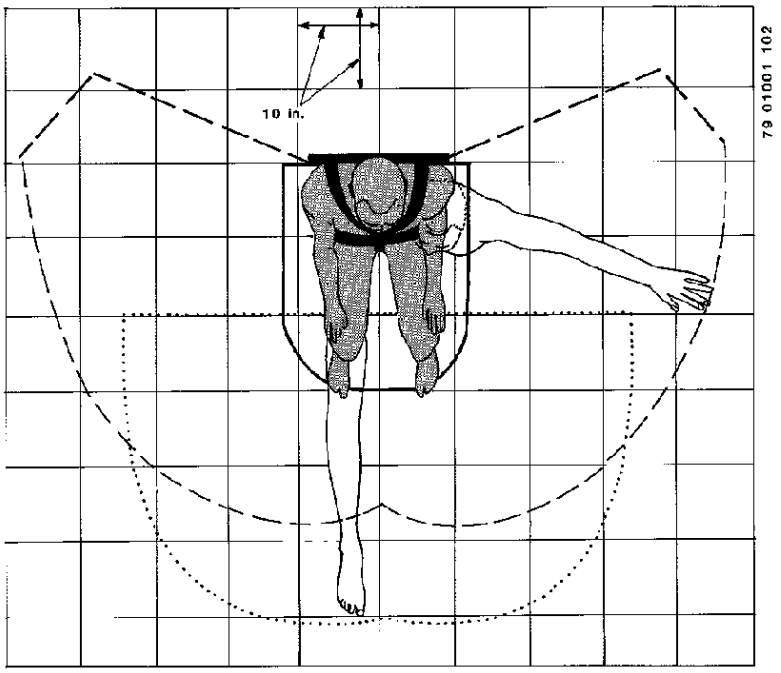

Figure 4-10.
Flail envelope for the 95th-percentile ATD wearing a five-point restraint - top view.

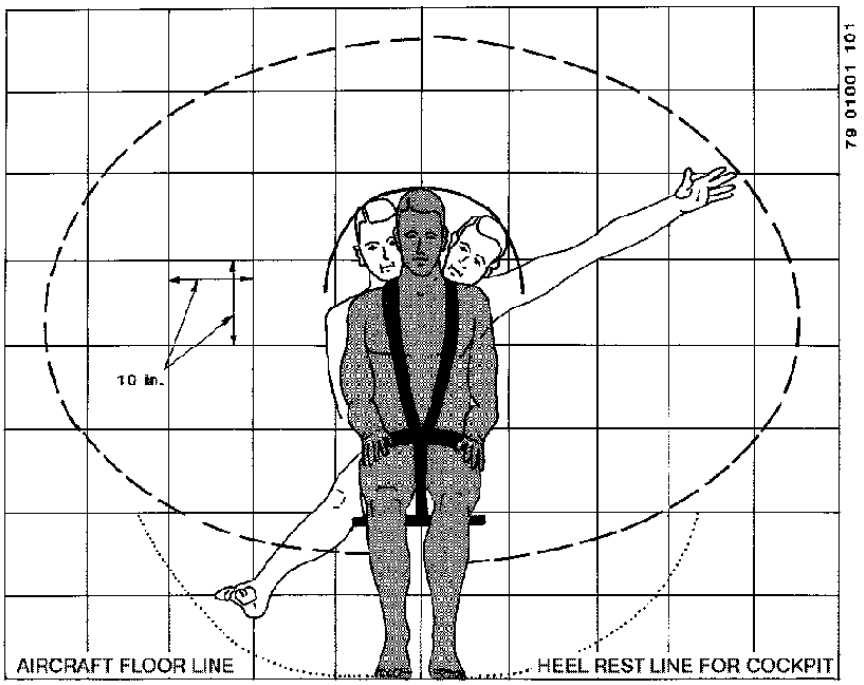

Figure 4-11.
Flail envelope for the 95th-percentile ATD wearing a five-point restraint - front view.

As previously mentioned, the occupant's flail envelope can be influenced by a number of factors, but the most influential factor is the type of occupant restraint used. To show some of the effects of restraint configuration, a series of sled tests were recently conducted to evaluate alternative restraint types for use in AGATE aircraft (References 4-53 and 4-54).

Four restraint types were evaluated using the standard FAA forward-impact test pulse (a nominal 26-G triangle pulse with a 42-ft/sec velocity change), except there was no yaw angle. A 50th-percentile male ATD was utilized. The restraint types evaluated were a conventional three-point harness (baseline), a three-point harness with a shoulder belt pre-tensioner, a three-point harness with a buckle pre-tensioner, and the three-point Inflatable Tubular Torso Restraint (ITTR™) currently in development at Simula Inc. The seat back recline angle was 20 deg from vertical.

Figures 4-12 and 4-13 show the trajectories of the ATD head center of gravity (c.g.) from the initial head position. Markers are shown at 10-msec intervals for reference. The ITTR provided significant improvement over the baseline restraint in terms of peak head excursion. The shoulder belt pre-tensioner also reduced the forward displacement, and the buckle pre-tensioner reduced the vertical displacement. More details and other benefits of the alternate restraints are discussed in Chapter 8.

™ITTR is a registered trademark of Simula, Inc.

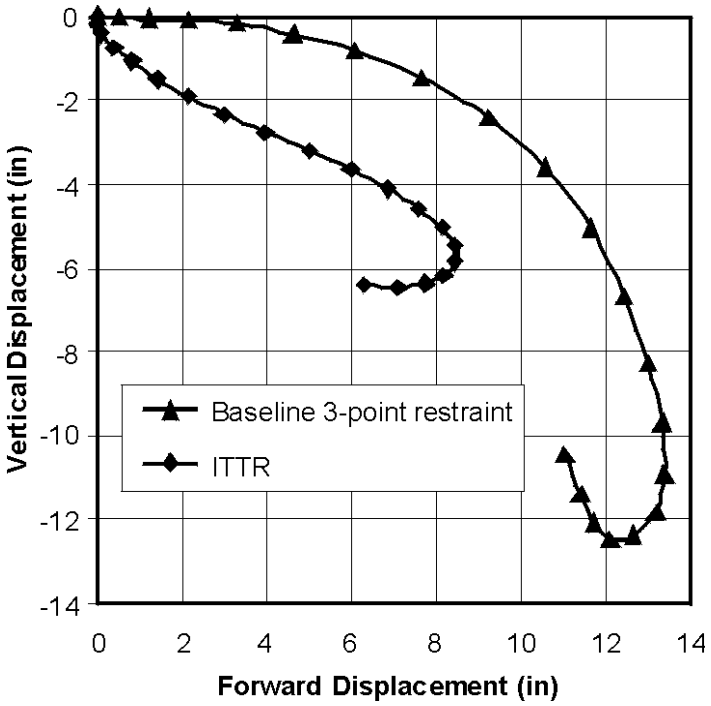

Figure 4-12.
Relative head displacement for the 50th-percentile ATD; three-point restraint and ITTR.

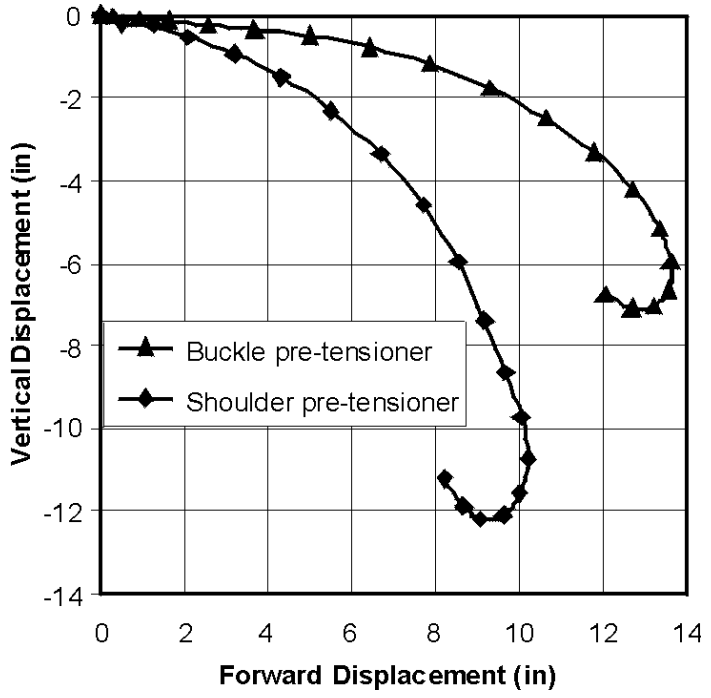

Figure 4-13.
Relative head displacement for the 50th-percentile ATD; three-point restraint with buckle pre-tensioner and shoulder belt pre-tensioner.

Figure 4-17.
Headward accelerative forces.

The skeletal configuration and mass distribution of the body are such that vertical loads cannot be distributed over as large an area as can loads applied forward or aft (G_X). These vertical loads, therefore, result in greater stress per unit area than do sternumward or spineward loads. Finally, along the direction of the long axis, the body configuration allows for greater displacement of the viscera within the body cavity. Forces applied parallel to the long axis of the body, headward or tailward (G_Z), place greater stain on the suspension system of the viscera than do forces applied sternumward or spineward (G_X), thereby increasing the susceptibility of the viscera to injuries.

As in the case of the longitudinal direction (Figure 4-16), rate of onset also affects the tolerance to vertical accelerative loads; however, insufficient data were available to establish the limits. Figure 4-18 presents one set of available data.

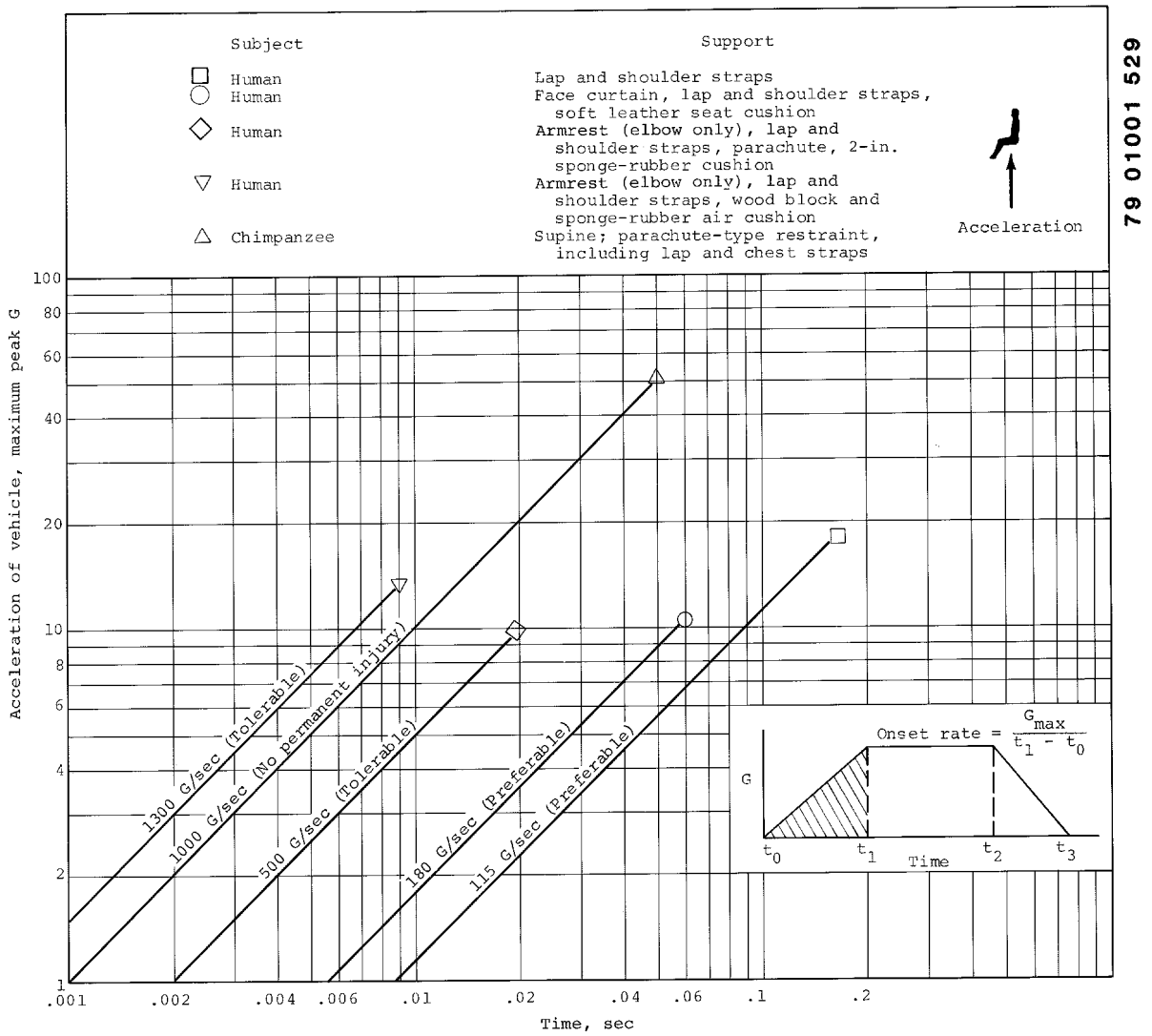

Figure 4-18.
Headward accelerative forces.

"HIC time interval." It is standard practice to define the minimum duration for the HIC time interval as 1 msec. The maximum duration is usually defined within the occupant protection regulations for each transportation industry (see Section 4.3.4.2.2.3).

As a result of Versace's work, NHTSA repealed the SI and adopted the HIC in March of 1972 (References 4-64, 4-65, 4-70). The new standard required the HIC to be calculated for contact and non-contact cases over the entire duration of the crash. In terms of Pass/Fail criteria for the standard, the original boundary value of 1,000, taken from Gadd's straight-line approximation of the WSTC, was defined as the maximum acceptable HIC value. As illustrated in Figures 4-21 and 4-22, it was later determined that the maximum HIC value represents a 16-pct risk of serious head injury (References 4-71 and 4-72). In 1986, the automotive industry revised the HIC calculation by restricting the HIC time interval (t_2-t_1) to a maximum duration of 36 msec (References 4-72 and 4-73). The 36-msec time interval corresponds to the maximum HIC tolerance value of 1,000 at a constant head acceleration of 60 G's (Reference 4-70). The 60-G acceleration limit was defined by the creators of the WSTC as a reasonable threshold for head injury.

4.3.4.2.2 Issues Surrounding the Interpretation and Application of the HIC

Following the introduction and adoption of the HIC, further research revealed that there were still numerous limitations to the WSTC, the SI, and the HIC (Reference 4-74). For example, none of these criteria are able to distinguish between skull fracture and brain injury. In addition, these three criteria do not account for the location and direction of head impact forces. As a result, several issues surround the interpretation and application of the HIC as a predictor of head injury potential. In an effort to delineate some of these issues, three of them will be addressed in the following sections. These three issues are:

- The use of the WSTC in the development of the HIC,
- The interpretation of HIC in contact-versus-non-contact impact scenarios,
- The selection of an appropriate HIC time interval.

4.3.4.2.2.1 Use of the WSTC in the Development of the HIC

As discussed in Section 4.3.4.1, the origin of the HIC was based on the development of the WSTC. However, many current researchers question the methods and procedures employed during the development of the WSTC (Reference 4-65). They point out that the curve was created using data from a variety of completely different experimental procedures. For example, data was collected from frontal-impact cadaver tests, exposed animal brains subjected to bursts of air, and human volunteers subjected to non-injurious decelerations. The researchers at WSU also made two assumptions during the analysis of the test data. They assumed that the data from these different experimental procedures could be analyzed as a single dataset. In using this combined dataset, the WSU researchers also assumed that the different test subjects all possessed the same tolerance to head injury. Finally, current researchers have proposed that the effective acceleration used in the plots was poorly defined, and a portion of the original data was not plotted correctly, while other data points were completely omitted from the acceleration-time curve.

Overall, these complex issues have led current researchers to question the validity of the WSTC and the subsequent development of the HIC. As a result, the general consensus in the industry is that the HIC does not serve as a complete measure of head injury risk.

4.3.4.2.2.2 Interpretation of the HIC in Contact Versus Non-contact Impact Scenarios

Another issue surrounding the HIC concerns whether it can be used to interpret both contact and non-contact impact scenarios (Reference 4-71). Since the HIC's conception, researchers have applied the HIC to contact and non-contact impact scenarios as an indicator of both skull fracture and brain injury. However, as noted previously, the HIC was formulated based on the WSTC, which represented a tolerance to skull fracture, and not brain injury. In addition, the HIC assumes that head injury potential can be measured by evaluating only the translational acceleration of the head. Contrary to this argument, recent head trauma research has demonstrated that rotational acceleration plays a major role in producing brain injuries, thereby suggesting that the HIC is not an appropriate measure of head injury in non-contact impact scenarios (Reference 4-75).

4.3.4.2.2.3 Selection of an Appropriate HIC Time Interval

As mentioned in Section 4.3.4.2.1, the time interval associated with the maximum HIC value is referred to as the HIC time interval. Most transportation regulations define a minimum and maximum length for the HIC time interval. It is standard practice to define the minimum duration for the HIC time interval as 1 msec. The maximum duration is usually defined within the occupant protection regulations for each transportation industry. The GA industry defines the HIC time interval as "the time duration of the major head impact, expressed in seconds" (Reference 4-76).

4.3.5 Facial Impact Tolerance

Presently, the FAA has not specified any requirements for facial impact tolerance in FAR Part 23. However, in the design of a crashworthy aircraft, it is still important to understand the anatomy of the human facial structure and what types of injuries can result from facial impacts.

The anatomy of the human face is extremely complex. The facial structure is composed of numerous bones that possess unique biomechanical properties, varying in size, shape, thickness, rigidity, and composition. These facial bones are covered by thin layers of soft tissue that provide little protection during impact. Figures 4-21 and 4-22 illustrate the anterior and lateral views of the facial bones in the human skull.

The fracture patterns generated by an impact to the skull are a function of the magnitude and direction of the applied load on the bone as well as the resistance to the load produced by the bone (Reference 4-77). Injuries can occur to both the soft and hard facial tissues that may result in permanent facial deformity, disability, and/or brain injury.

Within the general population, facial fractures typically result from motor vehicle accidents, impacts incurred while participating in athletics, and interpersonal violence (Reference 4-64). Little research has been conducted to determine the forces that cause facial bones to fracture. The facial bones receiving the most attention by researchers are the mandible, maxilla, zygoma, and nasion. Through a limited number of experiments using human cadavers, the fracture tolerance of these facial bones has been determined. It is important to recognize the non-uniformity of the test conditions defined in these experiments. Variable factors included impactor size, velocity, and mass, sample size, and the number of impacts applied per test subject. Table 4-3 displays the fracture forces of various facial bones with respect to sample size and impactor area. The following summary describes some of the results listed in the table.

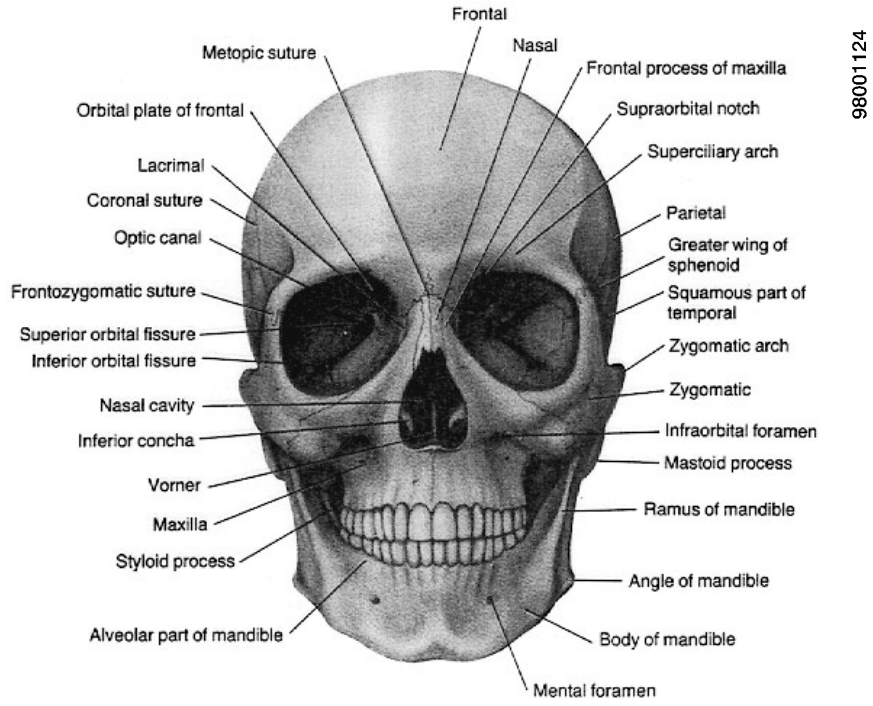

Figure 4-21.
Anterior view of the skull (Reference 4-64).

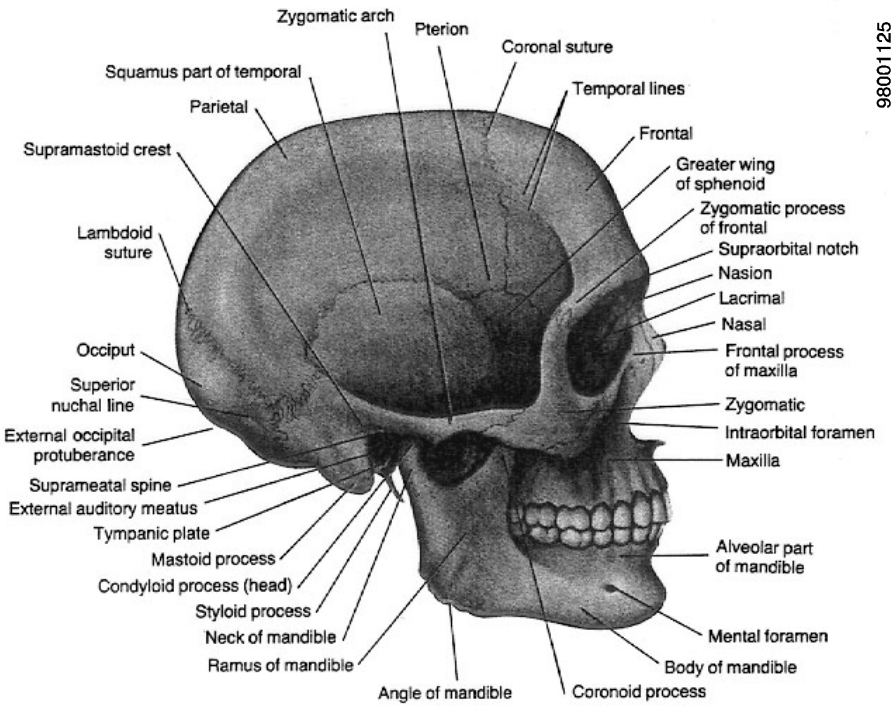

Figure 4-22.
Lateral view of the skull (Reference 4-64).

Table 4-3.
Fracture Force of Facial Bones (Reference 4-64)

Bone	Force - Range (N)	Force - Mean (N)	Sample Size	Impactor Area (cm^2)	Author (Reference)
Mandible					
Midsymphysis	1,890-4,110	2,840	6	6.5	Schneider (32)
Lateral	818-2,600	1,570	6	25.8	Schneider (32)
Maxilla	623-1,980	1,150	11	6.5	Schneider (32)
Maxilla	1,100-1,1800	1,350	6	20-mm-dia bar	Allsop (20)
Maxilla	788	788	1	25-mm-dia bar	Welbourne (36)
Zygoma	970-2,850	1,680	6	6.5	Schneider (32)
Zygoma	910-3,470	1,770	18	6.5	Nahum (31)
Zygoma[a]	1,120-1,660	1,360	4	6.5	Hodgson (28)
Zygoma[a]	1,600-3,360	2,320	6	33.2	Hodgson (28)
Zygoma[b]	2,010-3,890	3,065	4	25-mm-dia bar	Nyquist (19)
Zygoma[b]	900-2,400	1,740	8	20-mm-dia bar	Allsop (20)
Zygoma	1,499-4,604	2,390	13	Approx. 25-mm-dia bar (steering wheel)	Yoganandan (34)
Nasion	1,875-3,760	2,630	5	25-mm-dia bar	Welbourne (36)
Full face[c]	--	>6,300	5	181.0	Melvin (41)

[a]Multiple impacts prior to fracture.
[b]Both zygomas below the suborbital ridges.
[c]Greater than 6300 N for fractures other than nasal.

Hodgson is credited with performing the majority of the early research regarding the examination of facial fracture forces. Using a multiple impact technique, he discovered that the fracture force was proportional to the impactor surface area. In other words, as the impactor surface area increased, the force required to produce a fracture also increased (Reference 4-78).

Schneider and Nahum investigated the fracture forces of the maxilla and mandible. They used their data to suggest minimal fracture forces for these regions of the face, including 670 N for the maxilla, 1,780 N for the anterior-posterior mandible, and 890 N for the lateral mandible (Reference 4-79).

Yoganandan investigated the fracture forces of the zygoma during impact. He recorded forces in the range of 1,499 - 4,604 N with an average force of 2,390 N. In addition, he investigated the relationships between fracture strength, bone mineral content, and HIC. Results of his tests indicate that both mineral content and HIC do not correlate with fracture strength (References 4-80 and 4-81).

Welbourne investigated the fracture forces of the maxilla and nasion. During tests conducted on the maxilla, a range of 516 - 1,362 N was applied. Only one fracture occurred in the region of the subnasal maxilla at 788 N. These results led Welbourne to conclude that impact energy was not an effective indicator of fracture potential in this region of the face. In the tests performed to the nasion, Welbourne observed that fracture severity increased with an increase in the maximum applied force (Reference 4-82).

Melvin and Shee examined the fracture forces of the entire facial structure. Using a flat plate to impact the face, only nasal fractures were observed at forces less than 6.3 kN. They used their results to propose a force-time corridor for a full-facial rigid impact. This response corridor, illustrated in Figure 4-23, was used in the design of their deformable Hybrid III ATD face (Reference 4-83).

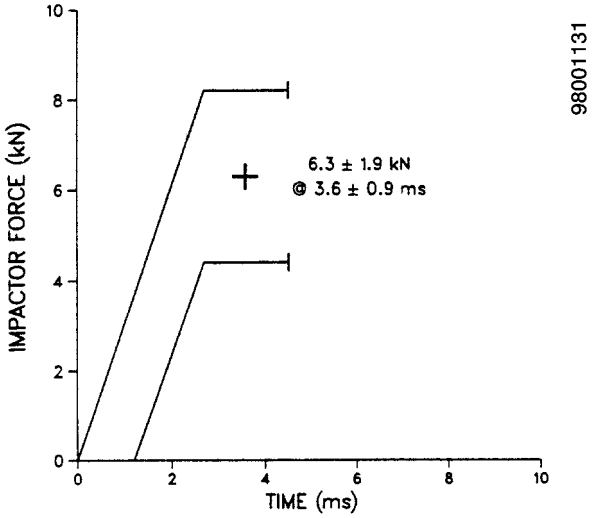

Figure 4-23.
Preliminary force-time response corridor at 6.7 msec for full-face rigid impact (Reference 4-64).

4.3.6 Neck Impact Tolerance

Currently, the FAA has not specified any requirements for neck impact tolerance in FAR Part 23. However, there is a great deal of interest in defining neck impact tolerances for transport category aircraft. The NHTSA recently added neck injury criteria to the Federal Motor Vehicle Safety Standard (FMVSS) (Reference 4-84). Initially, the NHTSA established injury tolerance criteria for the neck by conducting impact experiments using the Hybrid III ATD. The following neck injury tolerance values were adopted into the FMVSS 208 in 1998:

Neck Flexion Moment	190 Nm (SAE Class 600 filter)
Neck Extension Moment	57 Nm (SAE Class 600 filter)
Neck Axial Tension	3,300 N peak (SAE Class 1,000 filter)
Neck Axial Compression	4,000 N peak (SAE Class 1,000 filter)
Neck Fore-Aft Shear	3,100 N peak (SAE Class 1,000 filter)

In October 2000, the NHTSA adopted the N_{ij} criterion into FMVSS 208. The N_{ij} criterion evaluates the axial forces and fore/aft bending moments applied to the occupant's head and neck. The criterion defines four classifications of combined neck loading modes: tension-extension, tension-flexion, compression-extension, and compression-flexion. These modes are referred to as "N_{ij}" or N_{TE}, N_{TF}, N_{CE}, and N_{CF}, where the first index represents the axial load, while the second index represents the bending moment within the sagittal plane. A linear combination of the axial loads and fore/aft bending moments is determined using the equation:

$$Nij = \left(\frac{F_z}{F_{\text{int}}} \right) + \left(\frac{M_y}{M_{\text{int}}} \right) \quad (3)$$

where: F_z = axial force
F_{int} = critical axial force intercept value
M_y = fore/aft bending moment
M_{int} = critical fore/aft bending moment intercept value.

An Nij equal to 1.0 is equivalent to a 22-pct risk of an AIS-3 neck injury.

If similar tolerance specifications are eventually added to FAR Part 25, it is possible that the specifications may also be added to FAR Part 23. Therefore, it is important to understand the anatomy of the human neck structure as well as the neck injury mechanisms and injuries that can result from an impact scenario.

The internal structure of the human neck is composed of seven vertebrae and their surrounding soft tissues. Figure 4-24 illustrates the arrangement of these vertebrae. Injury to the neck can occur from direct contact and inertial loading, and may occur at any location along the cervical spine, affecting the hard and/or soft tissue.

4.3.6.1 Injury Mechanisms

Traditionally, neck injuries are categorized by the primary direction of loading (Reference 4-64). The five basic engineering descriptions of neck loading (bending, compression, tension, torque, and shear) are shown in Figure 4-25. The neck loading mechanisms can be further defined by describing the head motion that occurs under a load with respect to a fixed location. However, the general motion of the head does not necessarily represent the actual loading mechanisms that occur at the vertebral level. The head motions illustrated in Figure 4-26 occur about the craniocervical junction.

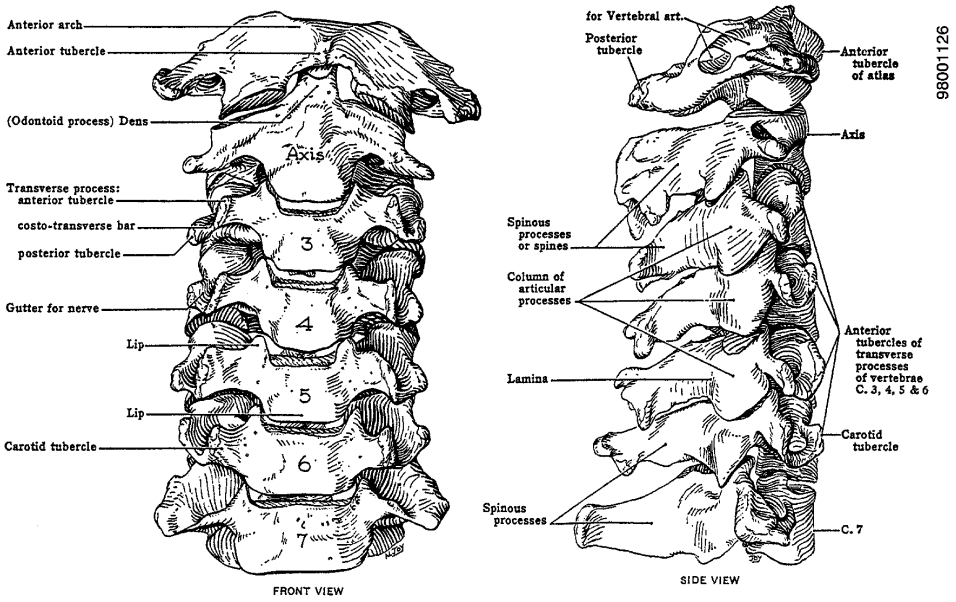

Figure 4-24.
Frontal and side view of the human cervical vertebral column (Reference 4-64).

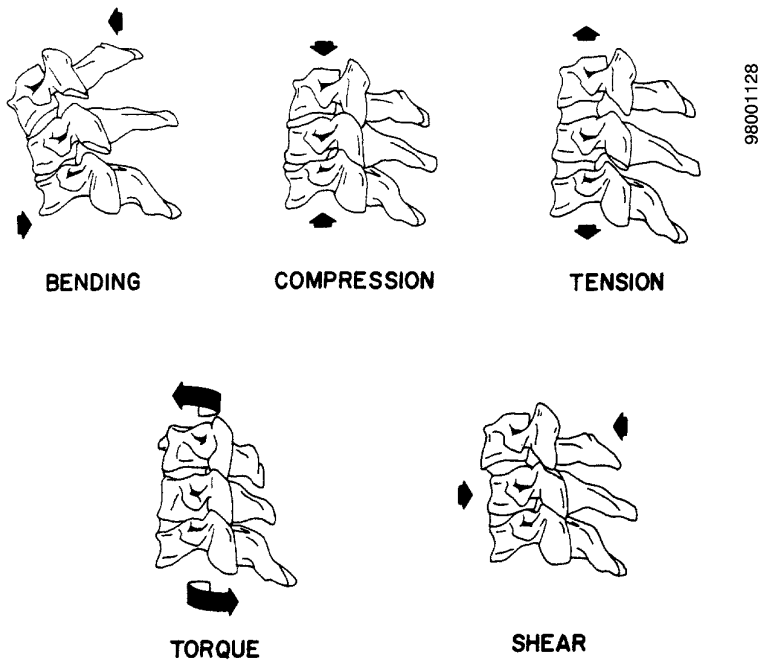

Figure 4-25.
Neck loading mechanisms (Reference 4-64).

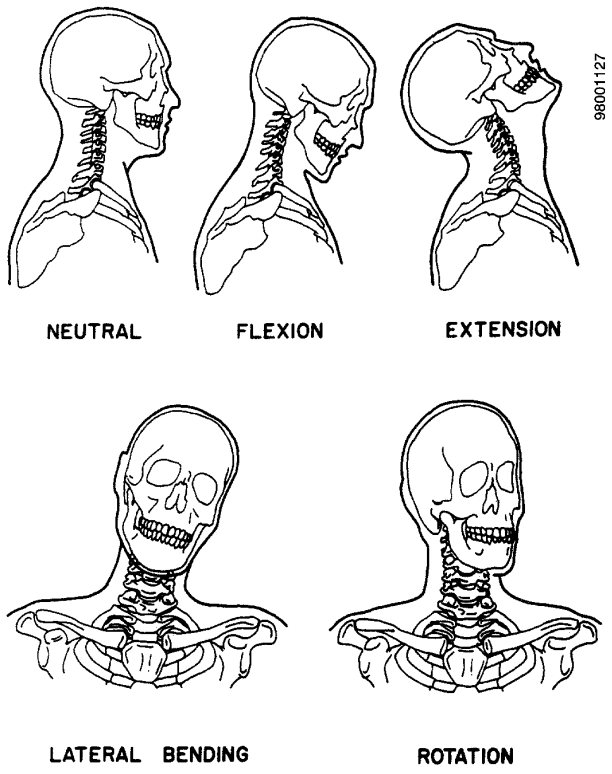

Figure 4-26.
Motion of the head/neck complex (Reference 4-64).

To evaluate human tolerance to injury, neck injury studies are conducted to measure and analyze the affects of various loading mechanisms on the neck. These loads are measured using ATD's, whole cadavers, individual spinal motion segments, and individual vertebrae. It is difficult to associate the cause of an injury with only one type of loading mechanism, since it is very common for injuries to result from a combination of loading conditions. The loading required to produce injury will vary substantially with the boundary conditions defined for the experiment, including the type of test specimen used, the initial positioning of the specimen, and the degree of fixation. In terms of the positioning of the specimen, a few degrees of variation can influence the difference between a flexion or extension injury. The following information describes the five loading mechanisms that have the potential to cause injury to the human neck.

Axial Compression

As a result of the complexity of the cervical spinal structure, purely compressive loading rarely occurs (Reference 4-64). However, many loading situations are considered to be predominantly compressive. In the upper cervical spine, multi-part fractures of the atlas originate from compressive forces. In the lower cervical spine, simple compressive fractures of the vertebral body occurring at the C4, C5, and C6 vertebrae are the most common sites of compressive injury. Ligamentous damage to the cervical spine is unlikely to occur under purely compressive loads

Compression-Flexion

The combination of a compressive load and a flexion bending moment results in increased compressive stresses in the anterior portion of the vertebral bodies and increased tension in the posterior portion (References 4-64 and 4-85). The high compressive forces typically cause failure of the anterior structures of the vertebral bodies. However, failure can also occur in the posterior portion of the vertebral bodies as a result of the high tensile stresses placed on the ligaments. Compression-flexion injuries of the spine include burst fractures, wedge compression fractures, hyperflexion sprains, unilateral and bilateral facet dislocations, "clay shoveler's" fractures, teardrop fractures, and soft tissue injuries.

Compression-Extension

The combination of a compressive load and an extension bending moment results in increased compressive stresses in the posterior portion of the vertebral bodies and increased tensile stresses in the anterior portion of the vertebral bodies (Reference 4-85). Compression-extension forces are believed to cause injuries throughout the entire cervical spine. The type of injuries produced are greatly dependent on the boundary conditions that are defined for the experiment. Fractures tend to occur in the spinous processes and in the vertebral bones surrounding the spinal canal. Rupturing of the anterior disc and anterior longitudinal ligament, horizontal vertebral body fractures, and "clay-shoveler's" fractures have been observed in experimental studies. In addition, "hangman's" fractures, which are traditionally associated with tension-extension mechanisms, have also been produced.

Axial Tension

Pure tensile loading is not a common neck loading mechanism (Reference 4-85). During motor vehicle accidents, rapid decelerative conditions produce inertial forces that act through the head's center of gravity, creating both shear and tensile loading of the neck. Ultimately, injury is caused by the loading of the ligamentous structures of the neck and is restricted to the upper

cervical spine. For example, this type of loading can generate occipitoatlantal distraction with unilateral or bilateral dislocation of the occipital condyles. This can produce ligamentous injuries without fracturing the hard tissue.

Tension-Extension

The combination of tension-extension loading is a common injury mechanism. Neck injuries resulting from tension-extension loading include "whiplash", "hangman's" fractures, horizontal fractures of the vertebral body, teardrop fractures, and structural injury to the anterior column of the spine (References 4-64 and 4-85). Large accelerations may injure the anterior longitudinal ligament and intervertebral disk or produce horizontal vertebral fractures. Tension-extension injuries typically occur via one of three methods (Reference 4-64):

1. Constraint of the head with continued forward motion of the torso. (diving accidents, falls, or unbelted occupant contacting windshield)
2. Abrupt forward acceleration of the torso producing inertial neck loading. ("whiplash")
3. Forceful loading below the chin directed in a posterosuperiorly direction (judicial hanging or air bag deployment at an out-of-position occupant).

Tension-Flexion

The combination of a tensile load and a flexion bending moment results in increased tensile stresses in the posterior portion of the vertebral bodies and increased compressive stresses in the anterior portion (Reference 4-85). Various experimental studies have suggested that tension-flexion loading produces injuries similar to compression-flexion loading, including bilateral facet dislocations, unilateral facet dislocations, and hyperextension sprains. These results indicate that the flexion bending moment is the primary factor generating the injuries.

Axial Rotation/Torsion

Torsional loading is thought to play a role in both upper and lower cervical spinal injuries (Reference 4-64). Injuries to the atlantoaxial joint, including rotary atlantoaxial dislocation with or without tearing of the alar ligaments, unilateral anterior and posterior subluxations, and bilateral anterior and posterior subluxations, are common to the upper cervical spine. These injuries may result from a combination of shear and torsional loading and typically include the dislocation of one or both of the surfaces of the atlas facets on the axis facet joint surface. In the lower cervical spine, the contribution of torsional loading to injuries is debatable. It has been demonstrated that the lower cervical spine is stronger in torsion that the atlantoaxial joint of the upper cervical spine, implying that torsional loading affects the lower cervical spine to a lesser degree. In addition, it is believed that torsional loading may produce unilateral facet dislocations in the lower cervical spine; however, this has not been demonstrated experimentally (Reference 4-85).

Fore-Aft (Horizontal) Shear, Lateral Shear, and Lateral Bending

Horizontal shear can produce anterior and posterior atlantoaxial subluxations resulting from transverse ligament failure or fracture of the odontoid process (Reference 4-64). These injuries can induce spinal cord impingement and make surgical repair procedures extremely challenging. Lateral shear and lateral bending are injury mechanisms that occur within the coronal plane of the body and are generally produced during side-impact collisions. Lateral shear loading produces nerve-root avulsion injuries and may also contribute to the type of odontoid fractures that occur from trauma. Forced lateral bending can generate radicular symptoms and bracheal plexus injuries. These loading mechanisms, in combination with other

loads, have been shown to produce hemorrhagic lesions in the C4-C5 and C6-C7 disc spaces of human cadavers. They can also initiate unilateral wedging and/or produce simple unilateral fractures of the cervical vertebrae (Reference 4-85).

4.3.6.2 Injury Tolerance

Numerous studies have been conducted to determine human tolerance levels for the cervical spine (Reference 4-85). Studies include the use of human volunteers, whole cadavers, isolated head and cervical spines, isolated cervical spine motion segments, animals, anthropomorphic test devices, and analytical techniques. However, several limitations exist which make it difficult to accurately define the injury tolerance criteria, including:

- Pure loading of the spine is rare.
- The observed motions and forces of the head do not necessarily reflect the motions or true injury mechanism of the cervical spine.
- Neck loading is strongly influenced by the inertial behavior of the head.
- Changes in the initial position of the spine, the end condition, and the eccentricity of the applied force have been shown to change the injury produced.
- Variation in the selection of test subjects, boundary conditions, restraint systems, and testing environments.

These limitations exist in both the automotive and aviation testing communities. However, the aviation industry has an additional limitation involving the selection of the ATDs used during testing. Presently, the aviation community uses the Hybrid II ATD, which lacks sufficient instrumentation and biofidelic characteristics in the neck region of the ATD body. Improved instrumentation and biofidelity initiated the design of the Hybrid III ATD, which is currently used by the automotive industry (Reference 4-86). The Hybrid III ATD features the Denton six-axis upper neck load cell for measurement of neck forces and moments during impact conditions. The Hybrid III ATD also possesses an articulated neck structure that is comparable to the human neck.

4.3.7 Spinal Injury Tolerance

Presently, the FAA specifies a single loading requirement for the spinal column during impact testing. FAR Part 23.563(c)(7) states that the “compression load measured between the pelvis and the lumbar spine of the ATD may not exceed 1,500 pounds” (Reference 4-76).

The human spinal column serves numerous functions in the human body. It is responsible for protecting the spinal cord, providing support and structure for the body, and enabling movement of the head, neck, and torso (Reference 4-64). The human spinal column is comprised of 24 individual vertebrate and 2 groupings of fused vertebrae. The 24 individual vertebrae create the flexible portion of the spine that is divided into 3 different sections: cervical (7 vertebrae), thoracic (12 vertebrate) and lumbar (5 vertebrae). The hard tissue vertebrae are connected by several different types of soft tissue, including ligaments, skeletal muscles, and intervertebral discs. The two fused groupings, the sacrum and coccyx, are situated beneath the lumbar vertebrae and form the rear wall of the pelvic girdle. The vertebral structures that form the sacrum and coccyx do not possess the same features as the individual vertebrae. For example, the fused vertebrae do not possess the posterior structures of the individual vertebrae. The anatomy of the spinal column is illustrated in Figure 4-27.

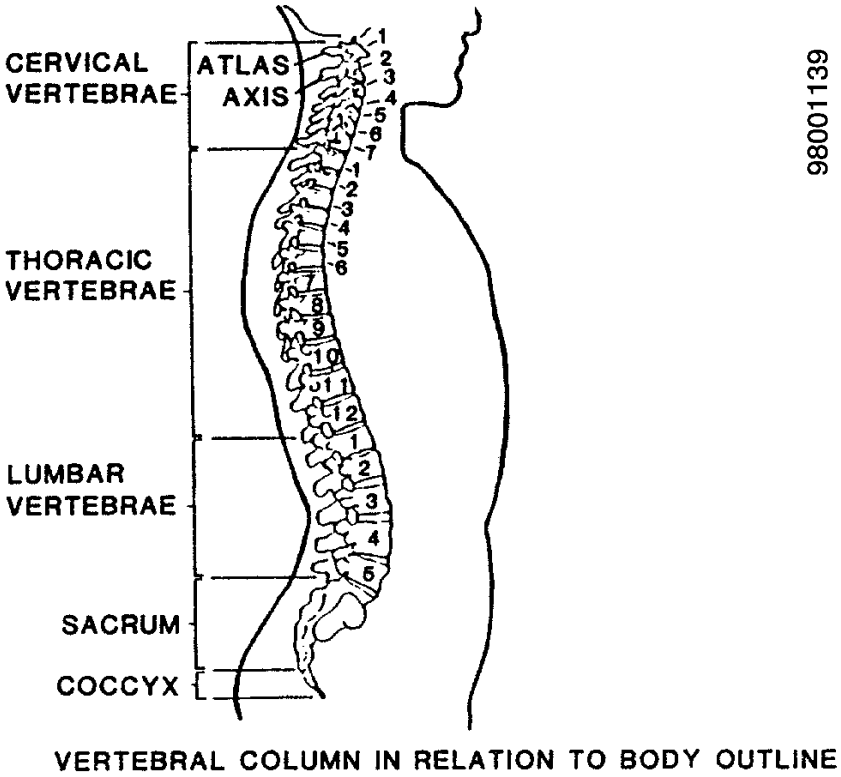

Figure 4-27.
Anatomy of the spinal column (Reference 4-2).

4.3.7.1 Injury Mechanisms

Injuries to the spinal column are categorized by the primary direction of loading (Reference 4-64). The five basic engineering descriptions of spinal loading (bending, compression, tension, torque, and shear) are shown in Figure 4-25 in Section 4.3.6.1. Spinal injuries can be attributed to combinations of these loading mechanisms.

To evaluate human tolerance to injury, studies are conducted to measure and analyze the affects of various loading mechanisms on the spine. The loading required to produce injury will vary substantially with the boundary conditions defined for the experiment, including the type of test specimen used, the initial positioning of the specimen, and the degree of fixation. In terms of the positioning of the specimen, a few degrees of variation can influence the difference between a flexion or extension injury. The following information describes the loading mechanisms that have the potential to cause injury to the human spinal column.

Axial Compression

Axial compressive forces generally produce fracture-type injuries to the vertebral bodies of the spinal column. In light aircraft and helicopter accidents, the most common sites of compressive injury are T10-L2 (Reference 4-87). In combined loading situations involving flexion and compression, common injuries include anterior wedge fractures and burst fractures (Reference 4-64). These injuries usually occur in the C5-T1 and T11-L12 regions (Reference 4-88).

Axial Tension

Pure tensile loading is not a common spinal loading mechanism (Reference 4-85). During motor vehicle accidents, rapid decelerative conditions produce inertial forces that act through the head's center of gravity, creating both shear and tensile loading of the cervical portion of the spine. Ultimately, injury is caused by the loading of the ligamentous structures of the neck and is restricted to the upper cervical spine. For example, this type of loading can generate occipitoatlantal distraction with unilateral or bilateral dislocation of the occipital condyles. This can produce ligamentous injuries without fracturing the hard tissue.

Axial Rotation/Torsion

The rotation of the spinal column about its longitudinal axis in combination with axial and/or shear loads can create several different hard tissue injuries of the spine (Reference 4-64). Injuries include lateral wedge fractures, uniform compression of the vertebral bodies, and fracture of the articular facets and lamina. These injuries have the potential to cause neurological deficit, including paraplegia. In addition, injuries to the intervertebral discs, joints, and ligaments of the spinal column often result from torsional loads (Reference 4-89).

Fore-Aft (Horizontal) Shear

Horizontal shear in combination with flexion and rotation of the spine can produce both unilateral and bilateral dislocations of the thoracolumbar vertebrae (Reference 4-64). In the cervical spine, horizontal shear loads can produce anterior and posterior atlantoaxial subluxations resulting from transverse ligament failure or fracture of the odontoid process. These injuries can induce spinal cord impingement and make surgical repair procedures extremely challenging.

Spinal Flexion

During flexion of the spinal column, the anterior portions of the spine endure compressive loads, while the posterior portions endure tensile loads (Reference 4-64). As mentioned previously, flexion of the spinal column in combination with other injury mechanisms can produce a variety of injuries to the vertebrae, including unilateral and bilateral dislocations, anterior wedge fractures, and burst fractures. "Chance" fractures are also related to the flexion of the spinal column. These fractures occur when the lumbar spine flexes over the lap belt, separating the posterior components of the vertebral bodies.

Spinal Extension

During extension of the spinal column, the anterior portions of the spine experience tensile loading, while the posterior portions experience compressive loading (Reference 4-64). Extension injuries tend to produce teardrop fractures in the cervical spine. They have also been associated with a loss of posterior vertebral height that, in turn, can cause injury to the articular facets, pedicles, and laminae of the vertebrae. In the thoracolumbar spine, injuries may include fractures to the posterior components of the vertebrae and distraction fractures of the vertebral bodies (Reference 4-90). During ejection from F/FB-118 aircraft, extension of the spinal column has ruptured the anterior longitudinal ligament in the thoracic spine (Reference 4-64).

4.3.7.2 Injury Tolerance

The quantity of reported spinal injury tolerance data is extremely limited. The spinal column is not injured as frequently as other body regions including the head and the thorax, and, therefore, it has not been studied to the same degree (Reference 4-64). In addition, several limitations exist in both the automotive and aviation research communities that make it difficult to accurately define injury tolerance criteria, including:

- Pure loading of the spinal column is rare; injuries typically result from a combination of loading mechanisms.
- The overall configuration of the spinal column plays a large role in defining the injury pattern.
- It is difficult to develop explicit injury criteria for the spinal column, since the failure of the spinal components includes both the hard and soft tissues.
- Neck loading is strongly influenced by the inertial behavior of the head.
- The observed motions and forces of the head do not necessarily reflect the motions or true injury mechanism of the cervical spine.
- Changes in the initial position of the spine, the end condition, and the eccentricity of the applied force have been shown to change the injury produced.
- Variation in the selection of test subjects, boundary conditions, restraint systems, and testing environments.

Presently, injury tolerance data is collected from instrumented human volunteers, whole cadavers, isolated head and cervical spines, isolated cervical spine motion segments, animals, and ATDs. In terms of the ATDs, the aviation community utilizes the Hybrid II ATD that is capable of measuring the compressive loads in the lumbar spine (Reference 4-86). The Hybrid II has a non-articulating pelvis and a straight spinal column, and can only be positioned in a reclined or seated position. The automotive industry uses a version of the Hybrid III ATD referred to as the “automotive" ATD. This particular ATD has a curved spinal column, but does not possess the instrumentation required to measure the lumbar loads in the spine. Similar to the Hybrid II, the automotive ATD can only be positioned in a reclined or seated position and has a non-articulating pelvis. The military uses another version of the Hybrid III ATD referred to as the "pedestrian" ATD. This ATD has an articulating pelvis, a straight spinal column, and is instrumented to measure the spinal compressive loads in the lumbar spine. In addition, the pedestrian ATD is not limited to a reclined or seated position, but instead has the ability to stand. As a result of the differences among these three types of ATDs, it is difficult to compare the collected data from the related impact tests that are conducted within these communities.

4.3.8 Upper-Extremity Injury Tolerance

In GA accidents, injuries to the upper extremity may result from contact with the aircraft interior and/or from flailing of the arm. The types of injuries sustained may include damage to both the hard and soft tissues of the arm. A study conducted by researchers from the Department of Emergency Medicine at Johns Hopkins University School of Medicine compared the autopsy data from aviation crashes that occurred in both 1980 and 1990. The data revealed that upper-extremity fractures comprised only 0.6 pct of the total injuries received by aircraft occupants during both 1980 and 1990 (Reference 4-91). In comparison with the injury tolerance of other body regions, this data suggests that the evaluation of upper-extremity injury tolerance may not be a current priority for the GA community.

Presently, with the exception of specific ejection ATDs, standard ATDs are not capable of measuring upper-extremity loading. However, an increase in upper-extremity injuries related to air bag deployments in automobile accidents has heightened interest in assessing upper-extremity injury. Recently, the Research Arm Injury Device (RAID) was introduced and is being used to examine the interaction between the upper extremities and automobile air bags. Prior to the development of the RAID, a limited number of research studies were conducted to investigate upper-extremity injury mechanisms and to develop human tolerance injury values for the arm (Reference 4-64). The human tolerance values for the hard tissue components of the arm that have been reported in the literature are listed in Table 4-4.

Table 4-4.
Upper-extremity bone tolerance values

Upper-Extremity Bone	Gender / Notes	Torque (N-m)	Bending (kN)	Average Max. Moment (N-m)	Long-Axis Compression (kN)
Clavicle	Male*	15	0.98	30	1.89
	Female*	10	0.60	17	1.24
Humerus	Male*	70	2.71	151	4.98
	Female*	55	1.71	85	3.61
Radius	Male*	22	1.20	48	3.28
	Female*	17	0.67	23	2.16
Radius	27 cm support**			35	
	14 cm support**			18	
	**		0.52		
Ulna	Male*	14	1.23	49	4.98
	Female*	11	0.81	28	3.61
Ulna	27 cm support**			42	
	14 cm support**			22	
	**		0.627		

* Messerer
** Yamada - Japanese male bones

4.3.9 Chest Impact Tolerance

In FAR Part 23.562(c)(6), the FAA has specified requirements for chest impact tolerance in terms of the loads exerted by the individual shoulder harness straps. For a single strap, the loads may not exceed 1,750 lb. If dual straps are used, the total strap loads may not exceed 2,000 lb.

In the automotive industry, injuries to the thorax typically result from interaction with the steering column, restraint system, instrument panel, or deploying air bag (Reference 4-64). Similar interactions with interior structures can also occur in GA accidents. To evaluate the potential for thoracic injury in frontal impacts, the automotive community utilizes Hybrid II and Hybrid III ATDs to examine the peak longitudinal spinal acceleration and maximum chest deflection experienced during impact. In lateral impacts, the Side Impact Dummy (SID) is used to record the peak lateral spinal acceleration. The following sections briefly describe the acquisition, analysis, and application of these measurements.

4.3.9.1 Acceleration Criterion

Peak spinal acceleration provides a general indication of the “overall severity of whole-body impact” (Reference 4-64) and is used to evaluate the potential for thoracic injury in the human body. This acceleration is measured using a triaxial accelerometer that is positioned at the center of gravity of the thoracic spine (Reference 4-86). Both the Hybrid II and Hybrid III ATDs

are capable of measuring this acceleration. For frontal motor vehicle collisions, the Code of Federal Regulations 571.208 (Reference 4-84) specifies that the peak spinal acceleration can not exceed 60 G during a period of 3 msec or longer. This data is displayed in Table 4-5. Use of the acceleration criterion is limited to predicting the severity of human skeletal injury (Reference 4-92). Note: All experiments discussed in Table 4-5 utilized human cadavers as test subjects, unless otherwise specified.

Table 4-5.
Frontal impact injury tolerances (Reference 4-64).

Tolerance Level	Injury Level	Reference
Force		
3.3 kN to sternum	Minor Injury	Patrick, et al. (1969)
8.8 kN to chest and shoulders	Minor Injury	Patrick, et al. (1969)
Acceleration		
60 G	3-msec limit for Hybrid II and III	FMVSS 208
Deflection		
58 mm	No rib fracture	Stalnaker and Mohan (1974)
76 mm	Limit for Hybrid III	FMVSS 208
Compression		
20 pct	Onset of rib fracture	Kroell, et al. (1971, 1974)
32 pct	Flail chest	Kroell, et al. (1971, 1974)
40 pct	Tolerance for rib cage stability	Viano (1978)
VC_{max}		
1.0 m/sec	25 pct probability of AIS >3 (anesthetized rabbits)	Viano and Lau (1985)
1.3 m/sec	50 pct probability of AIS >3 (anesthetized rabbits)	Viano and Lau (1985)

4.3.9.2 Compression Criterion

Another predictor of thoracic trauma is the magnitude of chest compression, or deflection, that occurs during the impact of the chest with an external object. The Hybrid III is the only ATD capable of measuring chest compression (Reference 4-93). The thoracic region of the Hybrid III is comprised of three components: spine, rib cage, and a removable chest jacket. Six steel ribs are attached to the rear portion of the welded steel spinal column. The inside surface of each rib is covered with a polyviscous damping material that helps to generate the appropriate chest response to blunt trauma. The removable chest jacket is composed of urethane and is used to distribute loads during frontal impact. Chest compression is measured using a chest deformation transducer located within the thoracic region of the Hybrid III ATD. The transducer is comprised of a potentiometer that is positioned on top of a bracket that extends over the lumbar spine. Input to the potentiometer travels from the sternum via a rod and sliding mechanism. The amount of compression is determined by recording the instantaneous displacement of the ATD's sternum relative to its thoracic spine. The Hybrid III chest structure is capable of recording deflections up to 90 mm in depth. As indicated in Table 4-5, FMVSS 208 specifies a maximum chest compression of 76 mm for the 50th-percentile Hybrid III ATD.

Kroell, et al., discovered that the degree of chest compression correlated well with the Abbreviated Injury Scale (AIS) (References 4-94 and 4-95). The following linear equation was developed to represent the relationship between chest compression and AIS:

$$AIS = -3.78 + 19.56C \quad (4)$$

The variable *C* represents the deformation of the chest divided by the chest depth. Research conducted by Viano demonstrated that an average maximum compression (C_{max}) of 40 pct can produce severe injuries to internal organs. To better protect these internal organs, Viano has proposed a C_{max} of 32 pct that will help to maintain sufficient rib cage stability.

In automotive accidents, compression of the chest typically results from interaction with the steering wheel, air bag, or shoulder belt. The load applied from the interaction with the steering wheel or air bag tends to produce a distributed deformation across the chest, whereas the load applied by the shoulder belt results in a localized chest deformation. Unfortunately, the majority of the chest compression tolerance data that is provided in the literature reflects only the effects of distributed loads. However, the GA community utilizes three-point restraint systems that may induce localized chest deformation, suggesting that localized chest deformation data will need to be collected to accurately evaluate the injury tolerance of the chest in aviation-related accidents.

4.3.9.3 Viscous Criterion (VC)

In order to define appropriate thoracic injury tolerance criteria, it is necessary to have a thorough understanding of the injury mechanisms that affect the soft tissues in this region. Within this region, injuries to the heart, lungs, and major vessels of the cardiovascular system can occur (Reference 4-64). The heart is subject to contusion and/or laceration resulting from deformation of the chest. High rates of chest loading can disrupt the electromechanical transduction pathways within the heart, inducing fibrillation or cardiac arrest. Within the lungs, high rates of chest loading can damage the alveoli capillary beds in the lung tissue. Fractured ribs can puncture the lung wall, initiating internal bleeding. Internal bleeding can also result from the rupturing of major blood vessels near the heart.

Soft-tissue injuries are dependent on both the degree and the rate of chest deflection (Reference 4-92). These properties are evaluated by a relationship developed by Lau and Viano called the Viscous Criterion. Lau and Viano define the Viscous Criterion as “any generic biomechanical index of injury potential for soft tissue defined by rate-sensitive torso compression” (Reference 4-92). The criterion is based on the viscous response, VC, which is determined by multiplying the velocity of chest deformation and the instantaneous chest compression. The maximum risk of soft tissue injury is defined by the peak viscous response, VC_{max}.

Research conducted by Lau and Viano has demonstrated that this criterion is a reliable indicator of soft tissue injury in certain regions of the body. As illustrated in Figure 4-28, the criterion operates at an optimal level for velocities of deformation between 3 to 30 m/s. As the velocity of deformation falls below 3 m/s, soft tissue injury can be evaluated strictly by the degree of compression. Within this range, crushing injuries are common. However, as the velocity of deformation reaches and exceeds 30 m/s, the rate of compression becomes the primary factor in determining the severity and type of soft tissue injury. Blast injuries are common to this range and initially occur to the lungs and other hollow, thoracic organs.

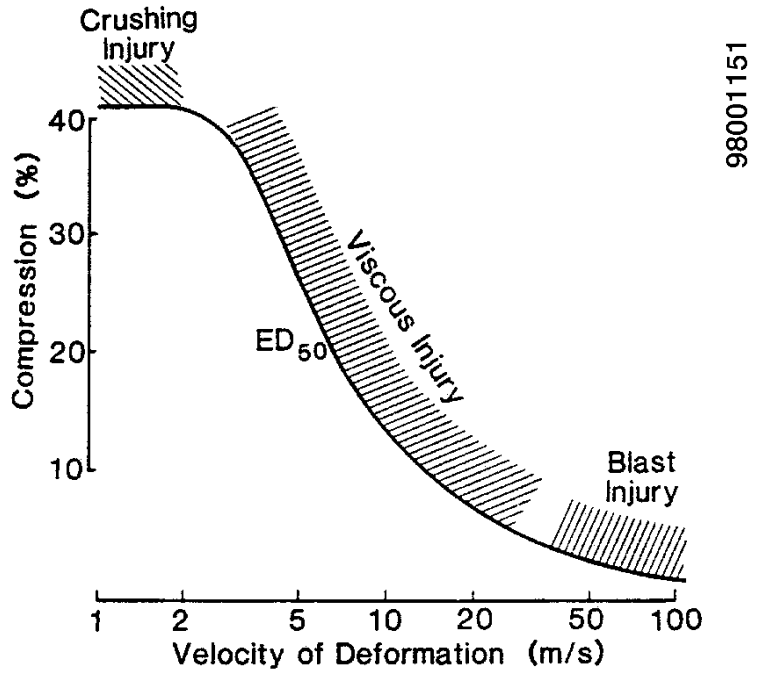

Figure 4-28.
Optimal range for application of the Viscous Criterion (Reference 4-92).

4.3.9.4 Thoracic Trauma Index (TTI)

In 1979, the SID was created to evaluate the potential for human injury during side-impact collisions (Reference 4-86). In the SID's thoracic region, injury potential is monitored by a measurement of the peak lateral spinal acceleration. An array of 12 accelerometers is used to record the response of the sternum, ribs, and thoracic spine during impact (Reference 4-64). The acceleration data acquired is evaluated using the Thoracic Trauma Index (TTI). This criterion is based on the age of the test subject, the peak lateral accelerations of either the 4th or 8th rib and the 12th thoracic vertebra, and the subject's mass (Reference 4-96). Specifically, the TTI is represented by the following expression:

$$TTI = \left(1.4 \times Age\right) + \tfrac{1}{2}\left(Rib_y + T12_y\right)\left(\frac{Mass}{Mass_{st}}\right) \qquad (5)$$

where: Rib_y = average acceleration of the 4th struck-side rib
$T12_y$ = average acceleration of the 12th thoracic vertebra acceleration
Mass = subject mass
$Mass_{st}$ = standard mass of 75 kg

For measurements recorded using the SID, the TTI expression is altered by the removal of the age factor and the mass ratio.

Investigations by Morgan, et al., have shown that the TTI is an accurate predictor of thoracic injury level resulting from a lateral impact (Reference 4-97). Table 4-6 displays TTI values for automotive side impacts. Note: All experiments discussed in Table 4-6 utilized human

cadavers as test subjects, unless otherwise specified. In terms of the use of the TTI in evaluating thoracic injuries in aviation crashes, current research projects are being conducted at the Civil Aerospace Medical Institute and Wichita State to investigate the accuracy of the TTI over non-impulse, longer term G loads.

Table 4-6.
Lateral impact injury tolerances (Reference 4-64)

Tolerance Level	Injury Level	Reference
Force		
7.4 kN (drop test)	AIS 0	Tarrierre, et al. (1979)
10.2 kN (drop test)	AIS 3	Tarrierre, et al. (1979)
5.5 kN (pendulum impact)	25-pct probability of AIS 4	Viano (1989)
Acceleration		
45.2 G $T8_Y$	25-pct probability of AIS 4	Viano (1989)
31.6 G $T12_Y$	25-pct probability of AIS 4	Viano (1989)
27.7 G Upper sternum-X	25-pct probability of AIS 4	Cavanaugh, et al. (1990)
TTI		
85 G	Max in SID for four-door cars	FMVSS214
90 G	Max in SID for two-door cars	FMVSS214
Compression to half thorax		
35 pct	AIS 3	Stalnaker, et al. (1979)
35 pct	AIS 3	Tarrierre, et al. (1979)
31 pct (includes arms)	25-pct probability of AIS 4	Cavanaugh, et al. (1990)
Compression to whole thorax		
38.4 pct	25-pct probability of AIS 4	Viano (1989)
VC_{max} to half thorax		
< 1.0 m/sec	AIS 0-2	Cavanaugh, et al. (1990) and unpublished data
>1.0 m/sec	AIS 4-5	
VC_{max} to whole thorax		
1.47 m/sec	25-pct probability of AIS 4	Viano (1989)

4.3.10 Abdominal Impact Tolerance

Presently, the FAA specifies the abdominal impact tolerance requirement in terms of the position of the lap belt during impact testing. FAR Part 23.563(c)(4) states that the "safety belt must remain on the ATD's pelvis during the impact" (Reference 4-76).

The abdomen of the human body is a large cavity located below the diaphragm and above the pelvic girdle. The abdominal cavity is filled with numerous organs, each of which respond differently to mechanical loading. Figure 4-29 illustrates the positioning of these organs within the abdominal cavity.

4.3.10.1 Influential Factors

There are several factors that influence the mechanical properties, injury mechanisms, and injury tolerances of the abdominal region (Reference 4-64). These factors can be described as being either external or internal to the abdominal cavity. External factors include:

- Rate of impact loading
- Impact force
- Energy input at impact
- Rapid deceleration of the occupant's body.

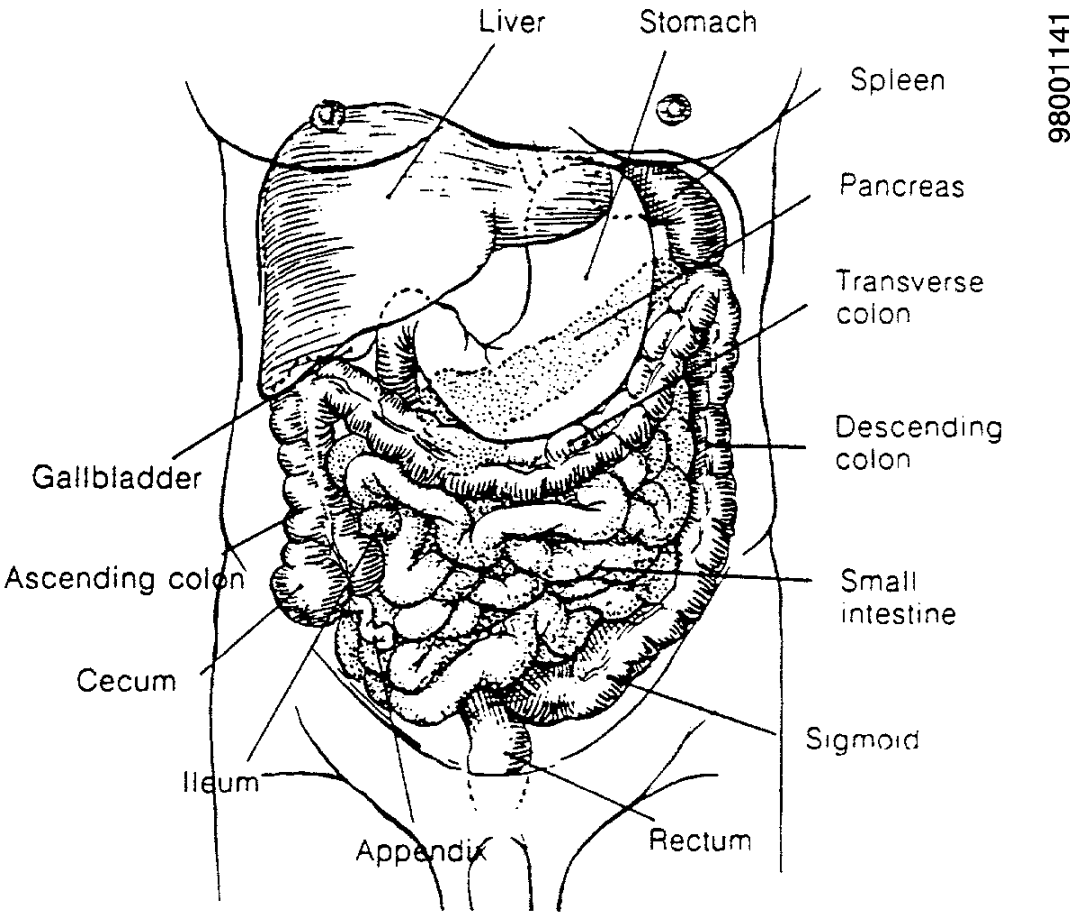

Figure 4-29.
Organs of the abdomen (Reference 4-64).

The internal factors that influence the mechanical characteristics exhibited by a particular abdominal organ include:

- Location of the organs within the cavity
- High mobility of the organs
- Gross density
- Age
- Pathological state.

The location of the organs in the abdomen dictates whether they will be injured by mechanical loading. Certain organs are positioned behind the lower rib cage and may receive more protection than other abdominal organs. Organ location becomes increasingly important in experiments that are conducted using animals as human surrogates. The organs of these animals tend to have a different geometry than human organs, and may be located in different positions within the abdominal cavity. This makes it challenging to generate worthwhile comparisons between animals and humans.

The organs of the abdomen are also highly mobile. Many of the organs are not rigidly fixed within the abdominal cavity, which allows the organs to change their position in response to changes in overall body posture and orientation (References 4-98 and 4-99). The peritoneum membrane that covers the organs and the inner cavity of the abdomen also creates a low-friction interface between the organs and the cavity walls that increases organ mobility (Reference 4-64). These properties alter the repeatability of injuries that are sustained under similar types of mechanical loading.

The gross density of the abdominal organs causes each individual organ to behave differently under mechanical loading. Abdominal organs can be separated into two different categories: solid organs and hollow organs. The liver and the spleen are examples of solid organs that are characterized by their fluid-filled vessels and dense composition. The stomach and intestines are examples of hollow organs. Hollow organs are less dense than the solid organs, as a result of the presence of a large cavity within the organ. In addition, the age and pathological state of the organs may also affect the organs' response to mechanical loading. These physical properties vary among the abdominal organs, making the force and injury analysis process extremely difficult.

4.3.10.2 Injury Mechanisms

Trauma to the abdomen may occur by penetration of objects into the abdomen or from blunt impact to the region. Injuries resulting from blunt impact are usually more difficult to diagnose. In addition, the mortality rate associated with blunt trauma to the abdomen is significantly higher than the rate associated with penetrating trauma (Reference 4-64). The following injury mechanisms have been associated with blunt trauma:

Compression

Compression injuries to the abdomen typically result from blunt impacts to the abdominal surface. During impact, the outer surface of the abdominal region deforms, pressing the superficial organs against other internal organs and surfaces. Several impact studies have demonstrated a relationship between maximum abdominal wall compression and abdominal injury severity (Reference 4-100). This relationship may be a function of the type of collision used to produce the injuries.

Wave Motion

Injuries to the abdominal region can occur to areas that are remote from the site of the blunt impact. These injuries may be attributed to stress and shear waves which propagate through the organs and tissues of the abdominal cavity (References 4-101 and 4-102). The magnitude of the wave is primarily defined by the velocity of deformation. For high-velocity deformations (>50 m/sec), the waves originate at the impact site and propagate through the abdominal tissues at the speed of sound. Injuries to the tissues occur between the boundaries of differing tissue types (Reference 4-64). Three different injury mechanisms have been suggested for high-velocity deformations including:

- Stress-wave-induced compression and re-expansion of the stressed abdominal wall
- Production of a pressure differential across the boundary
- "Spalling" – as the wave travels from a dense to a much-less-dense medium, energy is released.

In lower-velocity deformations (<15 m/sec), injuries occur from the propagation of a shear waves which move transversely through the abdominal tissues for a long duration of time. The three injury mechanisms proposed include:

- Differential motion of connected adjacent structures
- Strain at the attachment sites
- Collision of the viscera with stiffer structures.

Submarining

In the automotive industry, several studies have been conducted to examine the interaction of the abdominal region with the vehicle restraint system (Reference 4-64). Accident investigations and experimental studies have revealed that high lap belt loads can cause injuries to both the pelvic and abdominal region of the human body. These injuries generally result from misplacement of the restraint system and/or "submarining". The term "submarining" was introduced to describe the movement of the occupant's body with respect to the lap belt portion of a restraint system. Submarining occurs when the iliac crests of the pelvis slide below the lap belt, thereby loading the abdomen. Currently, the presence of submarining is detected by changes in lap belt loading; otherwise, must be observed visually. Improvements in restraint systems have helped to decrease the occurrence of submarining injuries when the lap belt is worn in the correct position. Specifically, the automotive industry has changed from a two-point restraint to a three-point restraint, while the military has changed from a four-point restraint to a five-point restraint.

Pressure

High rates of loading generate an increase of the internal fluid pressure of the abdomen (Reference 4-64). This increased pressure can produce viscous injuries including tensile or shear strains in the liver, tears at the pedicle or hilar regions of the spleen, or avulsion of the blood vessels in the abdominal region.

4.3.10.3 Injury Tolerance

In the aviation industry, studies were conducted by DeHaven and by Windquist, et al., to investigate abdominal injuries in light plane accidents. In a study conducted in 1944, DeHaven observed that the abdominal wall could resist an impact of approximately 2,200 lb (Reference 4-103). A second study, performed by Windquist, et al., in 1953, examined the injuries sustained from blunt abdominal trauma relative to objects within an aircraft cockpit (Reference 4-104). Results from the study indicated that the following forces were survivable: a force of 1,080 lb against a 10 $in.^2$ area, a force of 893 lb against a protruding pin, and a force of 750 lb through the abdominal belt.

Regarding the issue of submarining, Walfisch, et al., subjected 14 belted cadavers to a series of sled impacts (Reference 4-105). Initially, a lap belt load of 450 lb per side was recommended as the appropriate abdominal tolerance limit. This tolerance limit was later increased to an average lap belt tension of 790 lb per side, with a belt penetration of 1.5 in.

Presently, the aviation industry uses the Hybrid II ATD to evaluate the potential for injury during impact tests. In terms of abdominal injury, the Hybrid II ATD does not possess the instrumentation required to measure abdominal loads (Reference 4-86). In addition, the structure of the ATD abdominal region lacks biofidelic properties. To improve this process, researchers within the automotive industry are trying to develop quality ATD abdominal instrumentation and to enhance the biofidelity of the ATD abdominal structure.

4.3.11 Lower-Extremity Impact Tolerance

To date, the FAA has not specified any requirements for lower-extremity impact tolerance in FAR Part 23. However, in the design of a crashworthy aircraft, it is still important to understand the injury mechanisms that occur from impact to the lower extremities. It is also important to recognize the problems that can arise during egress from an aircraft when the occupant has sustained minor to serious lower-extremity injuries. Entrapment can occur if the occupant's injuries are so severe that he/she is unable to egress effectively.

In GA accidents, the types of injuries sustained by the lower extremities may include damage to both the hard and soft tissues. A study conducted by researchers from the Department of Emergency Medicine at Johns Hopkins University School of Medicine compared the autopsy data from aviation crashes that occurred in both 1980 and 1990 (Reference 4-91). The data revealed that lower-extremity fractures comprised 4.0 pct of the total injuries received by aircraft occupants during 1980 and 3.5 pct in 1990.

Injuries to the lower extremities depend on the type of impact sustained by the occupant (Reference 4-106). Fractures to the femur typically occur indirectly through the knee. In frontal-impact automotive accidents, loading of the femur occurs when the knee strikes the dashboard of the vehicle (Reference 4-64). This loading situation can also occur in aviation accidents when the knee impacts the instrument panel or the bulkhead of the plane's interior.

To investigate the injury tolerance of the femur, researchers in the automotive industry have conducted a variety of impact studies using Hybrid-III-type adult ATDs. From these studies, injury-assessment curves were developed to describe the axial compressive femur force as a function of the duration of loading (Reference 4-107). These curves are illustrated in Figure 4-30. If the value of the axial compressive femur load is above the time-dependent curve, distributed loads applied to the knee may cause fractures of the femur.

Figure 4-30 also describes the potential for fracture of the patella and pelvis as a result of distributed loads applied to the knee. These distributed loads can originate from direct contact with the vehicle or aircraft's interior (Reference 4-64). The patella can also be injured indirectly from contraction of the quadriceps muscle while in a sitting position with the knee partially flexed.

Other lower extremity injuries involve the tibia, fibula, and ankle. Fractures to the tibia and fibula typically occur from direct contact with the aircraft's interior. Ankle injuries, including hard tissue fractures and tearing of the soft tissues, are produced from pure vertical loading or combined loads resulting from supination or pronation and internal or external rotation of the ankle. Human tolerance values for the tibia and fibula are described in Table 4-7.

Presently, the aviation community uses the Hybrid II ATD to monitor the response of the lower extremities in impact tests. However, the Hybrid II is only instrumented to record the forces and moments of the lower femur (Reference 4-64). The automotive industry utilizes the Hybrid III ATD that contains more sophisticated lower-extremity instrumentation. The Hybrid III is capable of measuring both upper and lower femur forces and moments, knee position, knee-tibia displacement, knee-clevis forces, upper tibia moments, lower tibia forces and moments, and foot/ankle/toe forces and moments.

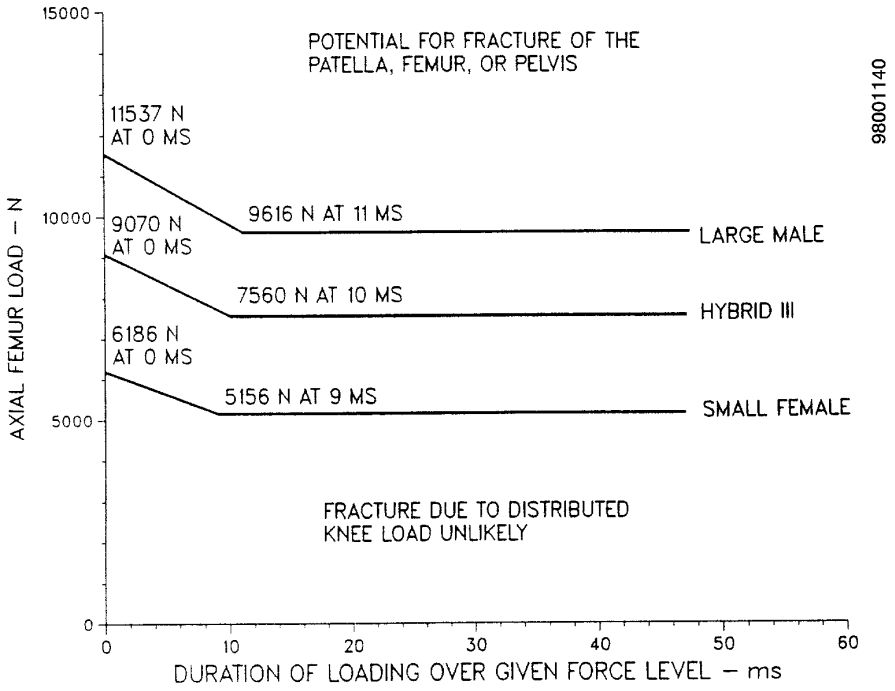

Figure 4-30.
Injury-assessment curves for axial compressive femur force measured with Hybrid III-type ATDs (Reference 4-107).

Table 4-7.
Strength of lower extremity bones (Reference 4-64)

Lower Extremity Bone	Gender	Torque (N-m)	Bending (kN)	Average Max. Moment (N-m)	Long-Axis Compression (kN)
Femur	Male	175	3.92	310	7.72
	Female	136	2.58	180	7.11
Tibia	Male	89	3.36	207	10.36
	Female	56	2.24	124	7.49
Fibula	Male	9	0.44	27	0.60
	Female	10	0.30	17	0.48

4.3.12 Injury Scales

The study of injury etiology requires the development and application of standard injury classification systems. In general, there are two types of scales used to categorize injuries: (1) scales which evaluate the physiological status of a patient before and during the treatment period for the injury, and (2) scales which describe the severity of an injury in terms of its anatomical location and specific wound type (Reference 4-108). The following scales represent the most popular classification systems within the injury assessment community.

4.3.12.1 Abbreviated Injury Scale

The Abbreviated Injury Scale (AIS), first published in 1971, was developed as a comprehensive system for rating injuries by type and severity (Reference 4-108). The goal was to create a system that would be acceptable to physicians, engineers, and researchers working in automotive crash investigation. Over the last decade, the AIS has evolved as the universal

system of choice for assessing impact injury severity. As the sophistication in injury assessment capabilities has improved, particularly among emergency room trauma specialists, the AIS has undergone several revisions. The latest revision was published in 1990.

As displayed in Table 4-8, the AIS classifies injuries by body region on a 7-point scale. The AIS numbers 1 - 6 indicate increases in injury severity ranging from minor to maximum injury severities. AIS number 9 represents those injury cases where trauma did occur, but no assessment information was provided to allow an AIS number to be assigned. The numbers in the AIS coding system do not indicate a relative weight. For example, AIS 2 is more severe than AIS 1, however, AIS 2 is not twice as severe as AIS 1. Additionally, two AIS 1 injuries are not equivalent to one AIS 2 injury. The AIS also divides the body into 9 major regions that provide a total of 1,320 injury descriptions. To determine the AIS number assigned to a particular injury, one would use the AIS dictionary to locate the specific body region and injury type in question.

Table 4-8.
Severity codes and corresponding descriptions for the AIS (Reference 4-108).

AIS No.	Severity Code
1	Minor
2	Moderate
3	Serious
4	Severe
5	Critical
6	Maximum Injury, Virtually Un-survivable
9	Unknown

4.3.12.2 Injury Severity Score

The Injury Severity Score (ISS) expands the AIS to consider the effects of injury to multiple body segments (Reference 4-109). The ISS defines six body regions: (1) head and neck, (2) face, (3) chest, (4) abdomen or pelvic contents, (5) extremities or pelvic girdle, and (6) external. As shown in Equation 6, the overall score is based on a mathematically derived code number determined from the highest AIS codes in each of the three most severely injured body regions.

$$ISS = (AIS_1)^2 + (AIS_2)^2 + (AIS_3)^2 \quad (6)$$

where: AIS_1 = Highest AIS anywhere in the body
AIS_2 = Highest AIS anywhere in the body except body region of AIS_1
AIS_3 = Highest AIS anywhere in the body except body region of AIS_1 or AIS_2

4.3.12.3 Injury Impairment Scale

The purpose of the Injury Impairment Scale (IIS) is to assess the level of impairment suffered as a result of the injury received by the victim (Reference 4-110). The IIS code numbers and their corresponding descriptions are provided in Table 4-9. Impairment is assigned in cases where whole-body dysfunction exists. The IIS is not used to assess the impairment of individual

body organs or body systems. When impairment levels are defined, they are based on the original injury sustained by the victim and are assessed one year following the occurrence of the injury.

Table 4-9.
Injury Impairment Scale (Reference 4-110)

IIS Code	Level of Impairment
0	No impairment, normal function
1	Impairment detectable, but does not limit normal function
2	Impairment level compatible with most, but not all, normal function
3	Impairment level compatible with some normal function
4	Impairment level significantly impedes some normal function
5	Impairment level precludes most useful function
6	Impairment level precludes any useful function

4.3.12.4 Glasgow Coma Scale

The Glasgow Coma Scale (GCS) is used to quickly and concisely quantify a complex head injury (Reference 4-111). The GCS provides a method for evaluating changes in the level of consciousness of a victim and is based on a functional assessment of eye opening, verbal response, and motor response. The observed function in each of these three categories is assigned a numerical value.. The numerical scores for the three assessment categories are added together to obtain a total score within a range from 3 (no response) to 15 (no impairment).

4.3.12.5 Concept of "Harm"

"Harm" is a measure of the economic cost associated with an injury. It is defined as the "sum of all injured people (fatalities and injured survivors), each weighted in proportion to the outcome, as represented by the cost of the person's most severe injury" (Reference 4-77). For example, in terms of cost, an AIS 5 injury has a higher cost than an AIS 6 injury. Overall, the concept of harm can be useful in identifying opportunities for reducing trauma-related injuries.

4.4 ANTHROPOMORPHIC TEST DEVICES (ATDS)

An anthropomorphic test device (ATD) is an instrumented mechanical device that is used to mimic the response of the human body under various loading and accelerative conditions. ATDs are commonly referred to as "crash test dummies" or "manikins". They can be designed to represent an entire human body or an individual body segment. Various ATDs have been created for the automotive industry, the aviation industry, and for various branches of the military. Initially, the primary function of the ATD was to represent the approximate size and weight of a human during dynamic loading of a test vehicle. Today, ATDs are also used to:

- Serve as a measurement device in the assessment of occupant injury protection in dynamic crash events
- Assist in the research, development, and certification of new or improved vehicles and safety systems
- Assist in the testing and certification of personal safety equipment (i.e., helmets, parachutes, flotation devices, etc.).